FREE WILL VS. DETERMINISM: RECONSTRUCTING THE MODEL FOR UNDERSTANDING SPACE-TIME DYNAMICS AND THE ROLE OF CONSCIOUSNESS WITHIN THE UNIVERSE

by

Lyndon Juden-Kelly

A thesis submitted in partial fulfillment
of the requirements for the degree of
Master of Arts (MA) in Human Development

The Faculty of Graduate Studies
Laurentian University
Sudbury, Ontario, Canada

THESIS DEFENCE COMMITTEE/COMITÉ DE SOUTENANCE DE THÈSE
Laurentian Université/Université Laurentienne
Faculty of Graduate Studies/Faculté des études supérieures

Title of Thesis
Titre de la thèse — FREE WILL VS. DETERMINISM: RECONSTRUCTING THE MODEL FOR UNDERSTANDING SPACE-TIME DYNAMICS AND THE ROLE OF CONSCIOUSNESS WITHIN THE UNIVERSE

Name of Candidate
Nom du candidat — Juden-Kelly, Lyndon

Degree
Diplôme — Master of Arts

Department/Program
Département/Programme — Interdisciplinary Health

Date of Defence
Date de la soutenance — April 9, 2015

APPROVED/APPROUVÉ

Thesis Examiners/Examinateurs de thèse:

Dr. Michael Persinger
(Supervisor/Directeur de thèse)

Dr. Robert Lafrenie
(Committee member/Membre du comité)

Dr. Cynthia Whissell
(Committee member/Membre du comité)

Dr. Stanley Krippner
(External Examiner/Examinateur externe)

Approved for the Faculty of Graduate Studies
Approuvé pour la Faculté des études supérieures
Dr. David Lesbarrères
M. David Lesbarrères
Acting Dean, Faculty of Graduate Studies
Doyen intérimaire, Faculté des études supérieures

ACCESSIBILITY CLAUSE AND PERMISSION TO USE

Abstract

The thrust of this thesis was to approach the historical question of whether or not “thought” or “mind” can affect physical processes from a different perspective. Alterations in generate random numbers from PN junction which are synapse-like interfaces mediating electron movement were assessed when people intended upon altering these fluctuations while being exposed to weak magnetic fields that could affect intention. The results indicated that specific physiological patterns of transcerebral magnetic fields interacted with intention to alter random fluctuation. Paired exposure of two random number devices at non-traditional distances to these patterned magnetic fields with changing angular velocities demonstrated clear evidence of classic excess correlation or “entanglement”. As the random variation drifted in one direction for one device the variation drifted in the other direction for the other device but only when the magnetic fields were operating. Quantitative electroencephalography (QEEG) correlates of the multiple subscales of a questionnaire by which “imaginative absorption” is inferred, indicated surprisingly strong associations between scores for specific subscales coupled to successful intention-related deviation of random numbers and low frequency power (theta-alpha range) within the right temporal lobe. However many other strong correlations were also observed. These results suggest that intention, an important traditional associate of “free will”, can affect random variations of electron-tunnelling processes but this coupling can be enhanced by externally originating pattern magnetic fields. These same fields when applied to two different spaces produce changes in random fluctuations that success excess correlation. One conclusion is that external forces that synchronize local spaces also occupied by brains could be a recondite determinant of the ultimate activity in electron movement in tissue whose correlative experience is the sense of “free will”.

Keywords

Consciousness; free will; intention; random numbers; physiologically patterned magnetic fields; QEEG; Mental absorption capacity.

Co-Authorship Statement

The following manuscript was prepared in collaboration with Dr. M. A. Persinger.

Acknowledgments

First and foremost I would like to thank Dr. Persinger for giving me the opportunity to study consciousness as a member of the Neuroscience Research Group (NRG). His mentorship has assisted and allowed me to identify and dissect some of the most complex problems challenging experts within the world of academia. I would also like to thank my other committee members; Dr. Whissell, and Dr. Lafrenie who have contributed to this very meaningful project. My NRG colleagues – and friends- must also be recognized insofar as many a discussion with these individuals has led to experimentation and analysis conducted within this document as well as within my Master's degree. My family deserves credit for my perceived success as well, as contributions from them have allowed me to continue my pursuit of higher education. In specific, I would like to thank my mother Lynda Kitchikeesic Juden, My father Andy Kelly, My aunts Sally and Leslie Juden as well as my grandpa David Juden. It is because of their unwavering support that I am able to continue attempting to blaze-trails through under explored avenues in the world of academia. I would also like to thank the people throughout my lifetime who have taken the time to listen to my ideas and who have provided insight and perspective. Finally I would like to thank all of the individuals who have doubted or given up on me, as I have used their scepticism, words, feelings, and actions as motivation to push forward with my intention and goals even when it felt as though the resistance was overly abundant.

Table of Contents

Table of Tables

Table of Figures

1 Chapter 1: Introduction

One of the assumptions of twenty-first century science is that the different increments of space and intervals of time that in large part define the traditional disciplines such as astronomy, chemistry, psychology, anthropology, physiology and physics are perspectives of the same Nature. The implicit inference of this approach is that there is a pattern of "connectivity" between these different levels of discourse because the phenomena that define them are various perspectives of the same "thing". Reductionism, the approach by which relationships between larger increments of space and time are transformed or fragmented into meaningful smaller increments of space or time is one contemporary approach. There is also parallelism which assumes that a stimulus that affects all levels of discourse which produce different manifestations could reveal the "transform function" or transposition of axes by which all levels of perception of Nature are related.

The separation of Nature into units and processes may be an artifact of human language or verbal behavior. However if this is veridical, then there are particles or their aggregates which are considered matter and there are processes which are considered discrete energies. The primary differences between them are space and time, respectively. To measure particles and matter, the amount of space is required. To measure energy or processes, time is required. The functions of matter are determined by their spatial structure. The functions of energy are determined by their temporal patterns.

The degree to which the energy or matter that describe a "thing" or a phenomenon are independent is likely to be a matter of perspective and the tools of measurement. The most fundamental component of the universe, that many consider the formative unit of reality, is the photon. It can be measured as a particle or as a wave. Whereas particles or mass required a medium through which they can interact and a clear "locality" for this interaction, energies can be capable of non-locality. Without any apparently intermediary, energies separated by substantial distances can exhibit excess correlation. Excess correlation means that a change in the locus of energy is associated with a systematic change in another locus of energy when random associations would be expected to occur.

In the famous depiction of de Broglie, a packet of energy or a pilot wave can exist as a wave field or as a particle. Every small particle and by implication large aggregates of particles in the universe is thus associated with a wave propagating through space (Aczel, 2002). What is still required is to understand and to experimentally demonstrate the conditions where one aggregate of particles and their energy waves can affect another aggregate of particles and their energies without any apparent intermediate locality.

Traditionally, human "thinking" or guided cognitive capacities towards an object with an intention or desired outcome has been considered an ephemeral state and often described although not defined as a "non-material" condition. However, modern quantitative electroencephalography (QEEG) has shown that the general classes of perceptions, ideations, and expressions are associated with coupled increases in energy within regions of the cerebrum that have been classically associated with these functions. In other words thought may be

considered “non-physical” or philosophically as the “mind.” However some energy that is strongly correlated in space-time with them can be measured.

The energies associated with cognition, which refer, to specific subjective processes attributed to thought, and those associated with the global state of these specific processes, that is, “the mind” are quite minute. Persinger (2010) showed that the action potential and even the resting membrane potential involve a discrete quantum of 10^{-20} Joules. A Joule is force over distance. This small amount of energy would be equivalent to the force between two electric charges separated by about 10 nm when applied over that distance. This is not a trivial energy as it is within the same order of magnitude as that required to stack a nucleotide base upon a RNA ribbon.

These magnitudes of energies are well within the ranges of those involved with the electron transfer that occurs within modern microelectronic devices such as the Random Event Generator (REG’s) hardware developed by the Princeton Engineering Anomalies Research Group (PEAR) which allow electrons to tunnel over substantial distance between two surfaces that allow either a 0 or 1 event to occur. Such digital sequences, when integrated over time, are the basis of information. In biological systems this information can be manifested as a base pair being added or not, potentially altering the ultimate protein composition. In electronic systems this information determines if either a 0 or a 1 is produced in a non-random order.

If both biological matter, such as the brain, and electronic (metal-crystal) matter rely upon discrete amounts of energy to operate, then the possibility exists that they could interact directly

and in a non-local manner if the conditions were optimal, insofar as a possible coupling is established and correlation is not considered causation. The exploration of this concept is the central thrust of this thesis. That is to say, measurable electromagnetic energy emitted from the brain during baseline conditions is typically associated with multiple repetitions per second or Hz, which is comparable to most electronic devices. It is assumed that if both involve these small energies and alterations in the sequence of these energies produce changes in thinking or deviations from random fluctuations, both should be affected by experimentally manipulated, appropriately patterned weak magnetic fields. Unlike random number generators that are fixed by structure and manufacturing codes, the dynamics of the human cerebrum will be more variable. Consequently, certain types of individuals or cognitive states, in this instance; capacity for "subjective" and "imagery" absorption, would be expected to increase the potential for interaction between cerebral and electronic systems as well as susceptibility to the influence of electromagnetic fields.

This thesis was designed to begin a different approach to the exploration of how the physical correlate or bases to thinking manifested as discrete amounts of energy can interact with electronic devices whose mechanisms define modern technology. Metaphorically this can be considered a study of "mind-matter" interactions, insofar as it is assumed that the agent by which alterations of matter manifest is the product of the focused measurable 'energies' emitted from the engaged mind. The term is traditional and does not imply necessarily that "the mind" is not matter. In fact implicitly it is more likely to suggest that the "mind" is energy and hence another form of "energy"-matter interactions.

1.1 The Issue of Mind-Matter Interactions

Mind-Matter Interaction (MMI) is one of the most intriguing complexities challenging physicists, philosophers, religious enthusiasts and mathematicians since the late 19th century wherein reports of séance-room sessions claimed to produce extraordinary movements of objects (Crookes et al., 1885). Classical mechanics describes a universe in a structured, mechanistic, and predetermined manner whereas quantum physics and critical approaches from consciousness research concerned with such issues, reveal an interactive environment wherein thought and action have subtle and/or an enormous impacts on the outcome of present, future, and even past circumstance (Braud, 2000).

Decades of MMI research wherein individuals actively intend upon the outcome of random events have uncovered evidence for consciousness-related anomalies in random physical systems (Radin & Nelson, 1989) due to the fact that research focused on whether or not deviations from physical randomness are due to human agent intention (Atmanspacher, 1989). Take for example, the varying number of methods and procedures already used to measure MMI or extra sensory perception which may very well have led to the distribution of results obtained over the years, through the systematic biases of the device in question as many different tools have been implemented including Random Event Generators (Dunne & Jahn, 1992), Random Number Generators (Bierman, 1996), Random Mechanical Cascade devices (Dunne et al., 1988), dice rolling (Smith, 1942), coin flipping (Spekkens & Rudolph, 2002) , and card guessing (Wiseman & Greening, 2002) just to name a few. In fact, the matter in which randomness is computed even varies amongst the different device used, the methods include, radioactive decay (Vincent, 1970;

Maddocks et al., 1972), electron tunnelling (Caswell et al., 2013), and thermal noise (Jun & Kocher, 1999).

To further the problem of obtaining true objectivity, and as in the case of cognitive dissonance, it is apparent within the literature that experimenters who actively belief in Psi-phenomenon – also known as 'sheep' - are more likely to obtain results that supported their hypothesis wherein skeptics – referred to as goats - were more likely to support the null, or obtain results in the negative direction away from expected. In fact, is has been argued that Psi results can be influenced by the person who generates the targets in hit/miss circumstance (West & Fisk, 1953) or by the individual who first checks the data or 'collapses the wave function' (Feather & Brier, 1968). Despite the wide range of available methods and tools to employ, and pre-experimental belief, another dominating feature in the literature of Psi research is a term coined the 'file drawer effect'.

The file drawer effect is not exclusive to this field insofar as it implies conducting research but not reporting the results. This reality is evident – or perhaps not so – in the literature within both sheep and goat populations. Sheep would employ this strategy to put insignificant results in the file-drawer and publish only those results which support their hypothesis, whereas goats would practice the file drawer effect to hide significant results and publish only those which are insignificant or are in line with chance expectations. Despite this friction amongst the world of academia, the results from numerous meta-analyses on the subject have indicated that human intention/proximity does have an effect on random physical systems (Bosch et al., 2006; Honorton, 1989; Utts, 1991).

This effect, quantal in nature, may be due to the fact that molecular pathways could be epiphenomenal transports of quanta with increments in the order of 10^{-20}J. This discrete value is associated with action potentials, intersynaptic events, the biophysical bases of membrane potentials, the number of action potentials per cell from magnetic energy potential, and the interionic distances around membranes (Persinger, 2010).

In order to confirm or deny the literature on the potential role of humans to be the mechanism by which significant alterations in random physical systems manifest as measured by REG's – one might deem it necessary to create a model in which; (1) there is an establishment of the effect of human intention upon random physical systems, wherein deviations from chance expectations are observed, and the facilitation of this effect could be enhanced or inhibited through the appropriate experimental conditions, (2) the quantification of subjective experience is documented in which human traits –not states- could be used as a predictive tool of Mind Matter Interaction, and (3) it could be demonstrated that non-local random events as produced by random number generators share 'excess correlation', or cease random computation and output 'events' in relation to each other once entangled through the appropriate equipment and technologies. Such an approach would encourage the exploration of less accepted practices and would also suggest successful outcomes from techniques such as healing intention defined as; the act of holding a benevolent desire for another human being to achieve or sustain a state of health, or more generally, a state which is enhanced (Radin et al., 2004).

2 Chapter 2: Electromagnetic Field Effects of Intentional Thinking Upon Random Number Generators: "The Energy (Mind)-Matter Interaction

2.1 Introduction

Human consciousness (Rose, 2006) can be considered a complex electromagnetic matrix that is entangled with the matter occupying an apparently constrained volume (McFadden, 2002; 2007) - being the human brain. It has been assumed through calculation that human thought may be able to affect the universe through subtle energies associated with the action potential with energies in the order of 10^{-20}J - which also matches the magnitude associated with electrical forces between ions on the neuronal membrane's surface (Persinger et al., 2008). Decades of research have suggested that human proximity can affect the dynamics of certain processes that strongly depend on "random" processes (Radin et al., 2006).

It has already been experimentally demonstrated that complex cognitive processes associated with "intention" or focused cerebral thinking towards an outcome can be described by physiochemical parameters and that the magnitudes of energies associated with these processes are within the range by which interactions or modulations from gravitational forces applied across the cellular membrane and width might occur (Caswell et al., 2013). In fact, this effect which elicits significant results in binary outcome, has been affected through the experimental application of specific temporally patterned magnetic fields applied to the whole body with an intensity of 400nT (Caswell et al., 2014), wherein the reversal of intention effects upon the operation of a REG was observed.

The conclusion of intention or 'free-will' as described by physiochemical parameters is of

critical importance insofar as measurements by a photomultiplier at distances of 15 cm from the head demonstrated significant increases in biophoton energies along the right side but not the left when subjects imagined white light in dark environments. The increased power density of ~ 3 x $10^{-11}W/m^3$ did not occur when the same subjects thought about mundane experiences. These results support Bokkon's hypothesis that visual imagery is strongly correlated with the release of biophotons and may be the actual experience of organized matrices of photons (Dotta & Persinger 2011). This suggests that our thoughts may not only interact with the environment but may also add to, dictate, or determine what is observed and experienced from the perspective of the observer.

If this is the case then previous research indicates that there might be a means to adequately quantify the power and intensity of human intention through the application of the appropriate technologies and through the correct identification of relevant subjective experiences which may define the bell-curve within successful Psychokinesis (PK) attempts. The present study was created to explore the possibility of further enhancing or inhibiting intended thinking processes directed towards a proximal Random Event Generator which produces "events" through electron tunnelling. Subjective experience questionnaires were also administered to quantify the effects of absorption and its correlates on PK performance.

2.2 Methods

An experimental procedure was designed to facilitate deviations away from chance expectations within the output of a Random Event Generator (REG) which is a device created and

manufactured by the Princeton Engineering Anomalies Research (PEAR) Group which computes randomness based off of electron tunneling procedures within two Esaki diodes within the apparatus. The REG software allows for the collection of a number of statistical variables in order to measure the distribution of randomness computed over a specific amount of time, these variables include; mean number of 1's computed over a given period, a z-score (which indicates distance from chance expectations), Standard Deviation, Max z-score, and Min z-score (values which indicate the boundary conditions of randomness). The design included 9 conditions during Human Intention or EM-field exposure directly applied to the REG (no human intention; background testing). The conditions lasted five minutes in duration each and commenced in the following order; pre-treatment, Lindagene, Thomas 1, Burst-X 1, Thomas 2, Burst-X 2, Thomas 3, Burst-X 3, post-treatment. The terms "Lindagene", Thomas, and Burst-X refer to the three different patterns of magnetic fields that were generated across the subject's temporal lobes or across the REG device. The shapes of Thomas pulse and Burst-X configurations have been published elsewhere but can be found in the Appendices of this document, Lindagene is a combination of these field configurations and others.

The pre and post treatment conditions followed the same procedure as field conditions requiring the participant to intend upon the REG results, with the exception that no fields were applied. The Lindagene condition acted as the priming field and depending on odd or even days of testing or odd or even subjects tested. The Thomas exposure and Burst-X exposure would be switched in the presentation order, following either an A-B-A-B-A-B (odd participant number [human] or day of testing [background]) sequence or B-A-B-A-B-A (even participant number [human] or day of testing [background]) template.

The weak fields are equivalent in intensity to that of man-made ambient fields in which we are constantly immersed (1 – 5 tesla). They were applied through small solenoids (an energized coil of insulated wire which produces a magnetic field within the coil) within containers that are placed (in human conditions) on each side of the head at the level of the temporal lobes. Delay between points and point duration was altered from 1,1 ms to 3,3 ms depending on odd or even day of testing or subject tested. The numbers refer to the point durations (in milliseconds) of the numbers that composed the pattern. For example 1 refers to 1 ms point durations while 3 refers to 3 ms point durations.

During all conditions the participant (N=15) was asked to intend on the output generated from the REG. They were asked to influence the random walking line generated by quantum tunneling processes within the device through the process of 'intended' or active thinking. Participants were shown and explained how the device operates before testing. However biofeedback from the machine was not given as participants sat quietly in a Faraday chamber within the consciousness lab at Laurentian University during the procedure. To keep participants engaged, they were asked at the completion of each condition whether or not they thought the line deviated up or down, and whether or not they thought the deviation was significant or insignificant.

The REG was placed 1 meter in front and to the left of the individual who sat comfortably in an arm chair. To determine background, the solenoids were placed 10 cm's to the left and the right of the REG, in the same location where human testing occurred but with no participant present, the Faraday chamber was closed and lights were turned off. Several REG variables were

collected during each condition to discern if differences occurred between them, namely z-scores (computed from the distribution of Random events associated with electron tunneling procedures generated within the device during the condition; mean=100+/-), min/max z-scores (which denote the boundary conditions of deviations away from the mean), min/max z-score locations within output (demonstrates wherein the REG output the greatest deviations occurred). Means and standard deviations were calculated.

2.3 Results

Multiple regression analysis within SPSS indicated that the z-scores obtained from the REG's output during the first Thomas exposure and the pre-field conditions were able to predict z-scores during the post field condition. Z-scores from the 1st Thomas conditions explained 31% of the variance in post-field z-scores [η^2=30.6, F(1,16)=7.05, p=.02, SEE=.87], while z-scores during the pre-field condition explained an additional 29% of the variance when a second model within multiple regression was created (max steps 4)[η^2=60.2, F(2,15)=11.36, p=<.01, SEE=.68].

Table 2.1 Multiple regression coefficients: post-treatment z-scores predicted by 1st Thomas exposure and pre-treatment z-scores

Variable		B	Std. Error	Beta	t
Model 1	(Constant)	.08	.21		.40
	1st Thomas Exposure z-scores	.49	.19	.55	* 2.66
Model 2	(Constant)	.12	.16		.71
	1st Thomas exposure z-scores	.54	.15	.60	**3.69
	Pre-treatment z-scores	.50	.15	.55	**3.34

***p<.05, **p<.001**

When the analysis was performed on the first half of the dataset (including background and human results), the z-scores during the 1st Thomas condition still entered the equation and explained 60.7% of the variance in post-field z-scores [η^2=60.7, F(1,6)=9.28, p=.02, SEE=.58] (Table-2.2), indicating that the 1st Thomas exposure (5 minutes) explained a significant amount of variance in the presence and absence of a subject.

Table 2.2 Multiple regression coefficients: post-treatment z-scores (1st half of dataset) predicted by 1st Thomas exposure z-scores

Variable	B	Std. Error	Beta	T
Model 1 (Constant)	-.28	.24		-1.17
1st Thomas Exposure z-scores	.67	.22	.78	*3.05

***p<.05, **p<.001**

When the analysis was performed on the second half of the dataset (only human cases), the z-scores during the 3rd Thomas condition entered the equation and accommodated for 50.5% of the variance in post-field condition z-scores [η^2=50.5, F(1,8)=8.17, p=.02, SEE=.87](Table-2.3.).

Table 2.3 Multiple regression coefficients: post-treatment z-scores (2nd half of dataset) predicted by 3rd Thomas exposure z-scores

Variable	B	Std. Error	Beta	T
Model 1 (Constant)	.01	.29		.04
3rd Thomas Exposure z-scores	.96	.34	.71	*2.86

***p<.05, **p<.001**

ΔPK-signature was a variable computed to discern the change in REG output after EM-field exposure. This was accomplished in both human and background conditions by taking post-

field z-scores and subtracting the z-scores from the pre-field condition (Post-Pre), even if background conditions do not necessarily display a 'PK-signature'. Correlational analysis indicated this computed variable was positively correlated with z-scores during the 1st Thomas condition [$r^2(18)=.56$, $p=<.01$] (Figure-2.1.).

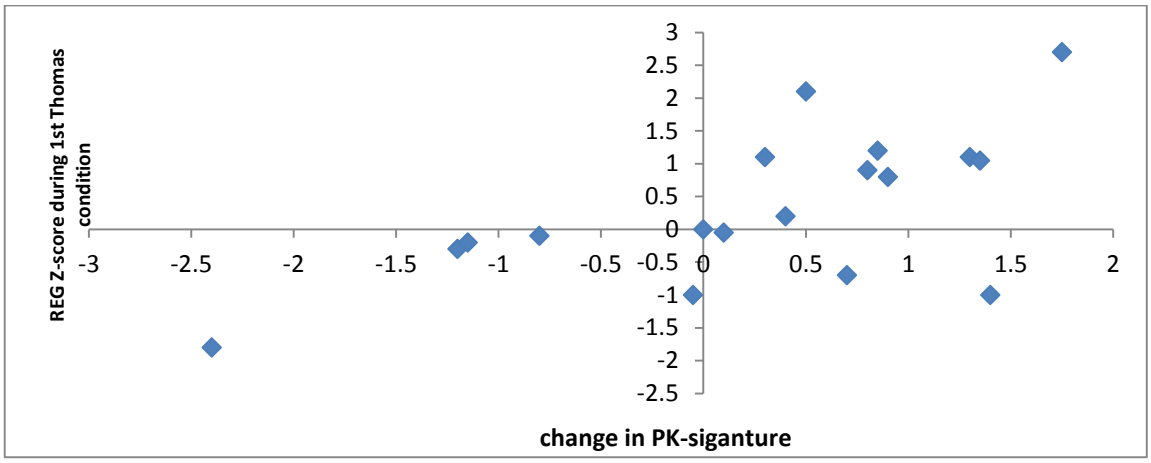

Figure 2.1 Significant correlation between Δ PK signature (Δ z-scores; post-treatment z-scores – pre-treatment z-scores) and REG Z-scores during the 1st Thomas treatment.

Δ PK-signature was also found to be significantly correlated with z-scores during the 3rd Thomas condition [rho (18) =.49] (Figure-2.2.).

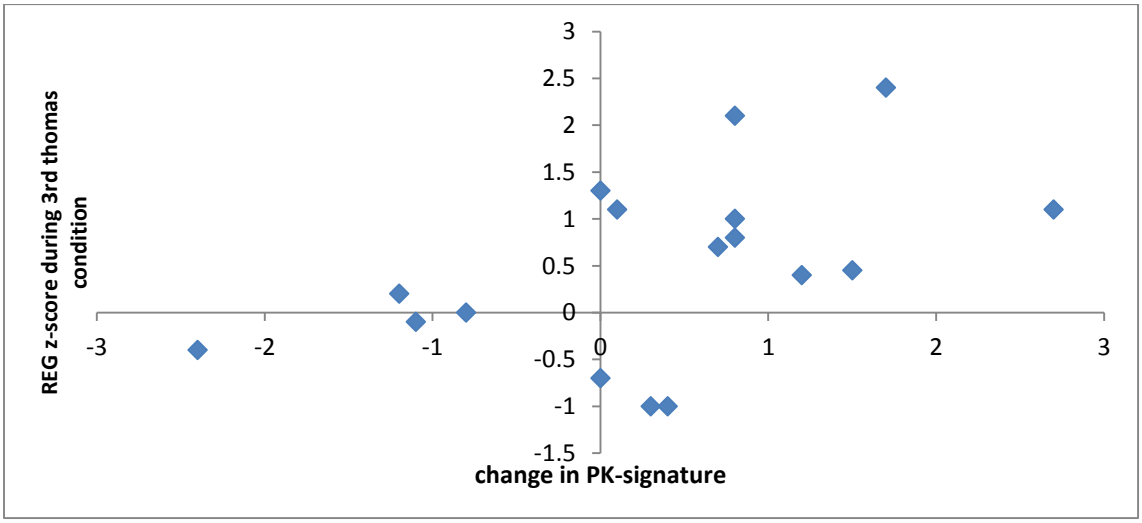

Figure 2.2 Significant correlation between Δ PK signature (Δ z-scores; post-treatment z-scores – pre-treatment z-scores) and REG Z-scores during the 3rd Thomas condition.

When multiple regression analysis was performed in order to predict Δ PK-signature z-scores within the whole dataset including human and background testing, the z-scores from the 1st Thomas condition explained a significant amount of variance within these values [η^2=33.3, F(1,20)=9.99, p=<.01, SEE=.89]. The model was strengthened by the predictive properties of z-scores during the 3rd Thomas condition [η^2=48.6, F(2,19)=8.98, p=<.01, SEE=.80] and z-scores during the 3rd Burst-X condition [η^2=60.2, F(3,18)=9.08, p=<.01, SEE=.73]. When this same analysis was performed on just background conditions, the 1st Thomas exposure accommodated a significant amount of variance in ΔPK-signature z-scores [η^2=71.5, F(1,5)=12.56, p=<.02, SEE=.52]. When multiple regression analysis was performed on just human conditions in order to predict PK-signature z-scores, the 1st Thomas condition explained a significant amount of variance [η^2=41.2, F(1,13)=9.09, p=.01, SEE=.88]. The effect was strengthened by the 3rd Thomas condition [η^2=63.4, F(2,12)=10.40, p=<.01, SEE=.73] (Table-2.4.).

Table 2.4 Results of multiple regression analysis: predicting ΔPK-signature by field treatment within entire dataset, background, and human testing conditions

Analysis	**Predictors of ΔPK-signature**	**F-statement**
Entire dataset	Thomas 1	[η^2=33.3, F(1,20)=9.99, p>.01, SEE=.89]
	Thomas 1 & Thomas 3	[η^2=48.6, F(2,19)=8.98, p>.01, SEE=.80]
	Thomas 1 & Thomas 3 & Burst-X 3	[η^2=60.2, F(3,18)=9.08, p>.01, SEE=.73]
Background	Thomas 1	[η^2=71.5, F(1,5)=12.56, p>.02, SEE=.52]
Human	Thomas 1	[η^2=41.2, F(1,13)=9.09, p=.01, SEE=.88]
	Thomas 1 & Thomas 3	[η^2=63.4, F(2,12)=10.40, p>.01, SEE=.73]

The multiple regression coefficients from the analyses (max steps 4) above are displayed below in Table 2.5.

Table 2.5 Multiple Regression coefficients: Predicting ΔPK-signature by field treatment within entire dataset, background, and human testing conditions

Analysis & Variable	B	Std. Error	Beta	T
Entire dataset results				
Model 1 (Constant)	-.*02*	.19		-.09
Thomas 1	.58	.18	.58	*3.16
Model 2 (Constant)	-.17	.19		-.90
Thomas 1	.53	.17	.53	3.18
Thomas 3	.44	.19	.39	2.38
Model 3 (Constant)	-.25	.17		-1.47
Thomas 1	.*53*	.15	.54	3.57
Thomas 3	.*57*	.18	.51	3.22
Burst-X 3	-.*33*	.14	-.36	-2.29
Non-human Results				
Model 1 (Constant)	-.*77*	.23		*-3.36
Thomas 1	.79	.22	.85	*3.55
Human Results				
Model 1 (Constant)	.*28*	.23		1.22
Thomas 1	.64	.21	.64	*3.02
Model 2 (Constant)	.09	.20		.43
Thomas 1	.65	.17	.66	*3.76
Thomas 3	.51	.19	.47	*2.70
***p<.05, **p<.001**				

When average z-scores were computed for all 3 Burst-X conditions and then entered into a one-way analysis by human testing conditions (background/human), significance was observed [$F(1,22)=4.82$, $p=<.04$, $\eta^2=.18$] with background conditions deviating away from chance expectations specifically in the up direction. The human conditions did not significantly deviate away from chance expectations. However they significantly deviated from background conditions (Figure-2.3), suggesting that a significant deviation away from chance expectation was elicited when the Burst-X fields were applied directly to the REG device, but not when the fields were applied to humans during 'active thinking' directed towards the device.

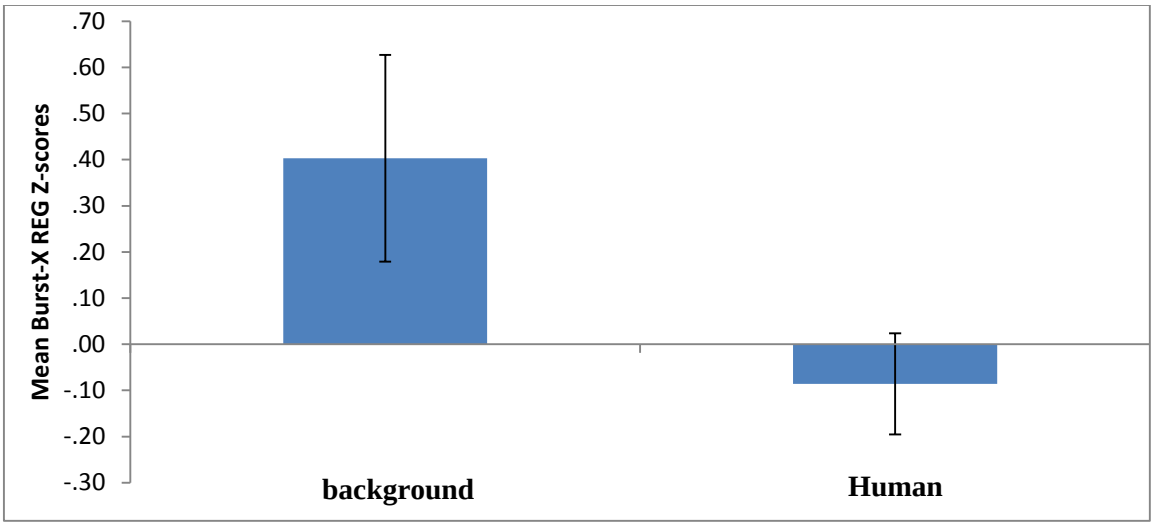

Figure 2.3 REG Z-scores during all Burst-X treatments by background and human testing conditions

With regard to standard deviation, when average values were computed for all nine conditions (pre/post baselines and field conditions) and then entered into a one-way analysis by human (background/human), significance was observed [$F(1,22)=5.09$, $p=.03$, $\eta^2=.19$] (Figure-2.4.).

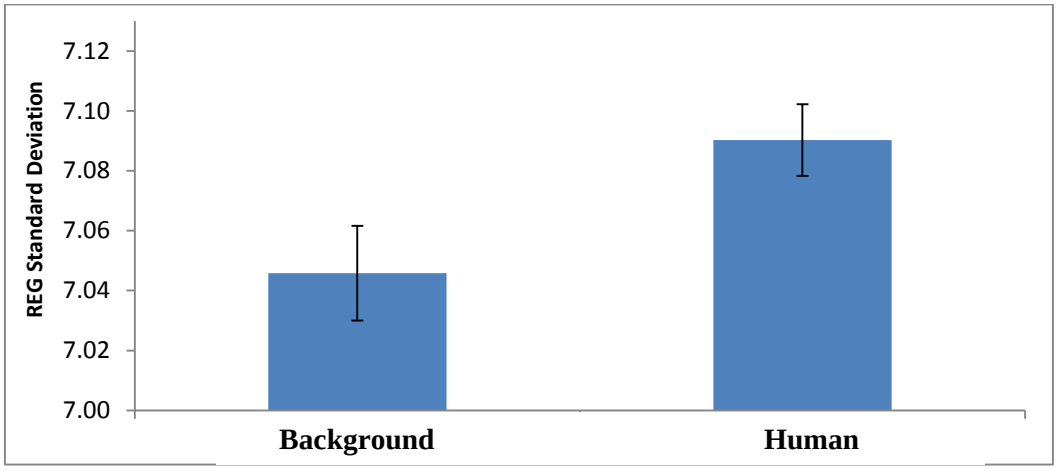

Figure 2.4 REG Standard deviation values during the entire paradigm (9 conditions) by background and human testing conditions

When averages were computed for standard deviation values during only (EM) field conditions one-way analysis of variance by human (background/human) was found to be significant [$F(1,22)=8.29$, $p=<.01$, $\eta^2=.27$] (Figure-2.5.).

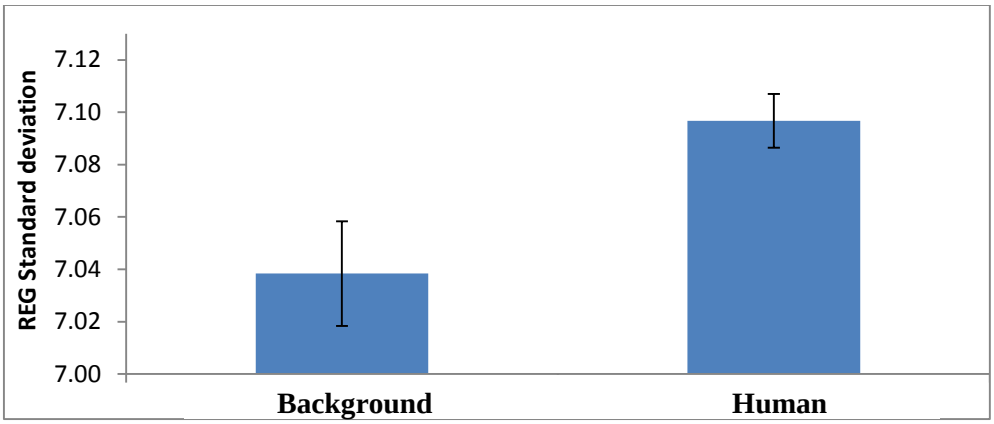

Figure 2.5 REG standard deviation values during field treatments (7 conditions) by background and human testing conditions

When averages were computed for standard deviation values during all three Thomas conditions and then entered into a one-way analysis by human (background/human), significance was observed [$F(1,22)=5.28$, $p=.03$, $\eta^2=.19$] (Figures 2.6).

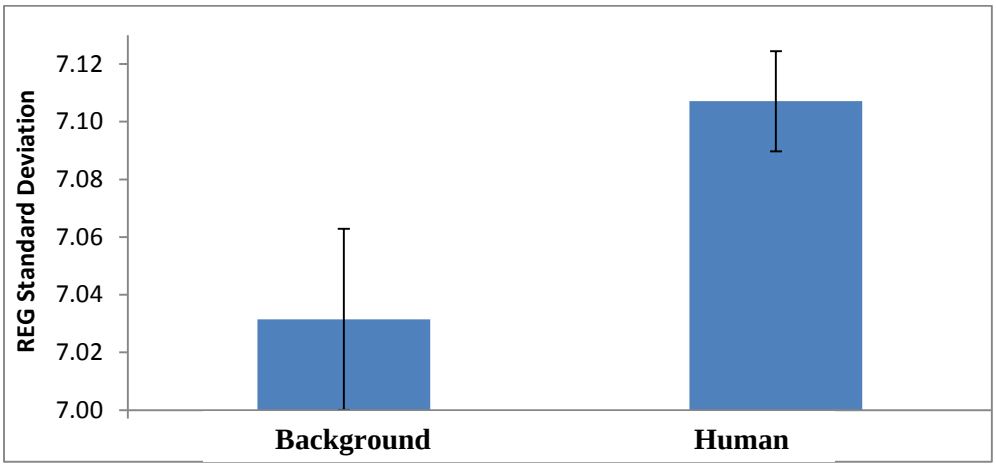

Figure 2.6 REG standard deviation values during Thomas treatments (3 conditions) by background and human testing conditions

When standard deviation values from each of the nine conditions included in the study were entered into a multiple regression analysis in order to predict human interaction (background/human) significance was observed [$\eta^2=.19$, $F(1,20)=4.81$, $p=.04$, $SEE=.44$]. The standard deviation values during the Lindagene condition explained a significant amount of the variance in human interaction (Table-2.6.).

Table 2.6 Multiple regression coefficients; human proximity/intention predicted by standard deviation values within the primer field (Lindagene) condition

Variable	B	Std. Error	beta	T
Model 1 (Constant)	-8.82	4.34		-2.04
SD values during Lindagene condition	1.35	.613	.44	*2.19

***p<.05**

REG means and standard deviations during each field condition for human and background testing utilizing both 1,1 and 3,3 field parameters can be observed in Figures 2.7-2.8 which demonstrates that standard deviation values for background testing during 3,3 field parameters deviated from all other testing procedures within the condition in question during the 1st Burst-X and 3rd Thomas conditions (figure-2.8).

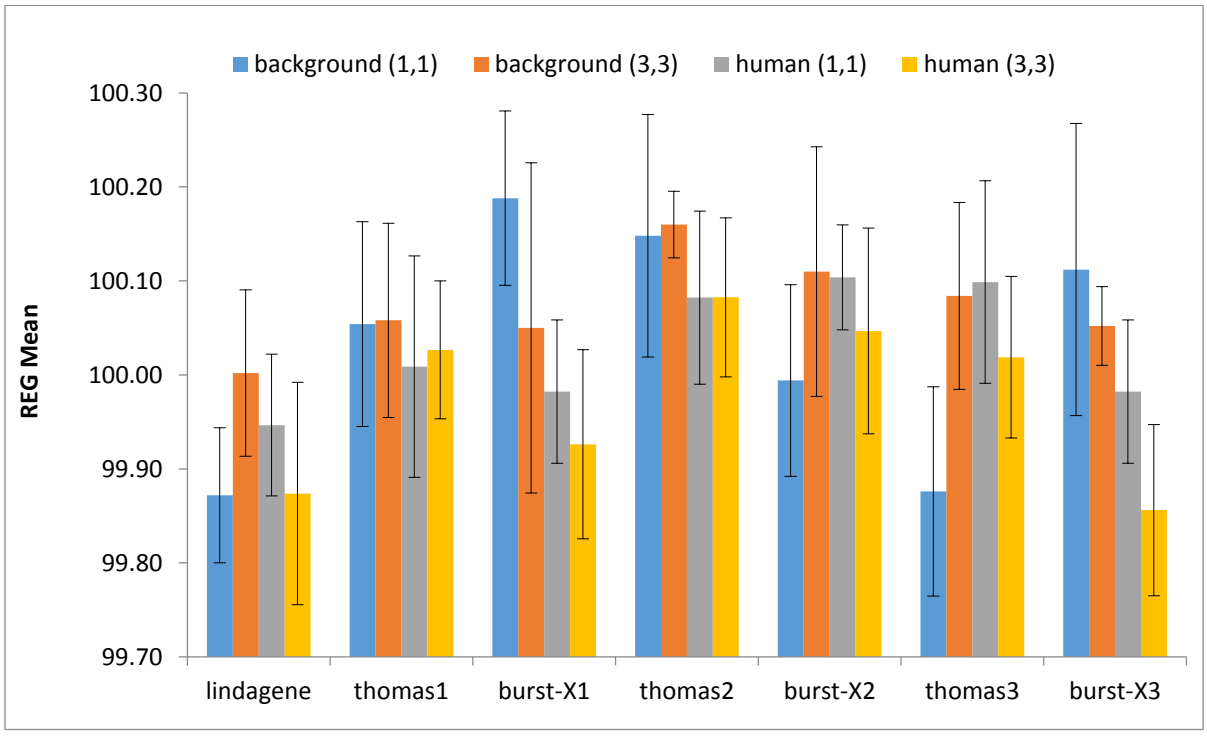

Figure 2.7 REG means (average # of 1 bits/200) during field treatments for human and background testing conditions with 1,1 and 3,3 field parameters

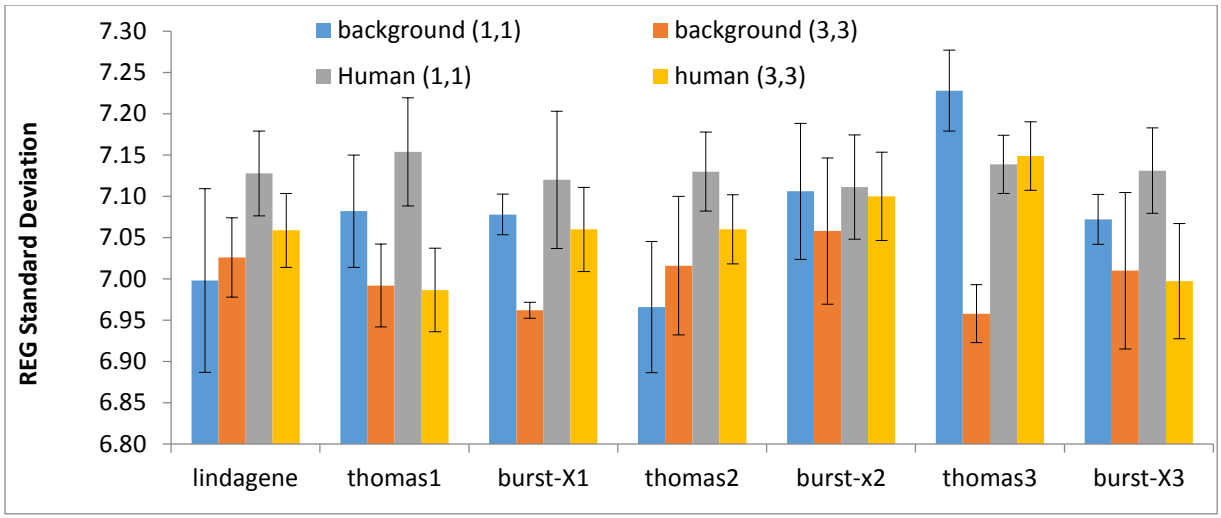

Figure 2.8 REG standard deviation values during field treatments for human and background testing conditions with 1,1 and 3,3 field parameter

Max and min z-score location within the output was measured during each condition for human and background testing for 1,1 ms and 3,3 ms field parameters. The results can be observed in Figures 2.10-2.11 and demonstrated that only max z-score location during human testing conditions in the 3rd burst-X condition with 3,3 field parameters deviated from all other testing procedures during that condition. Max values were achieved more quickly in this condition then in all other testing methods.

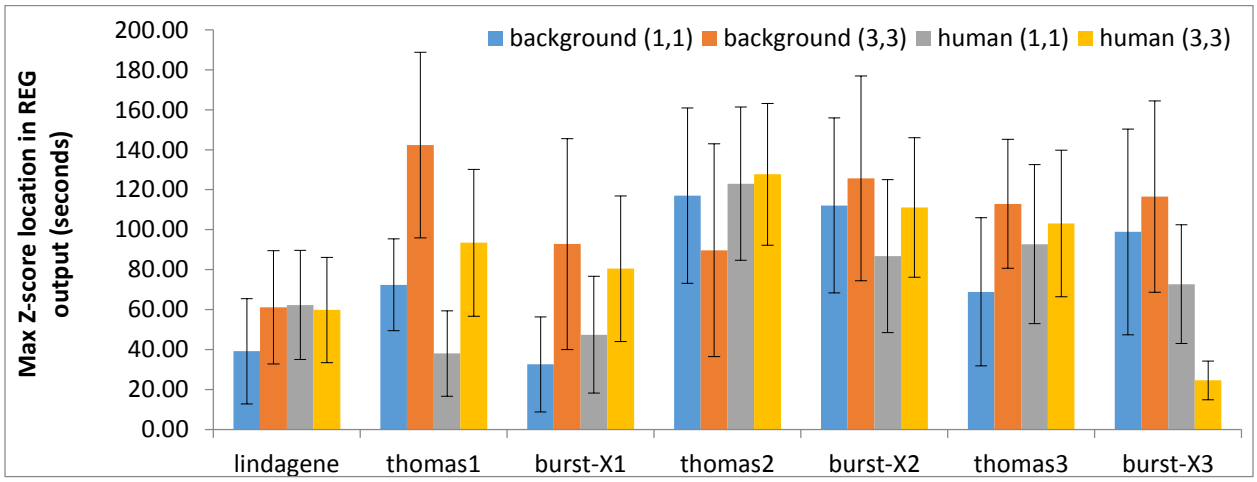

Figure 2.9 Time within REG output where Max Z-score value was achieved by field conditions for human and background testing conditions with 1,1 and 3,3 field parameters

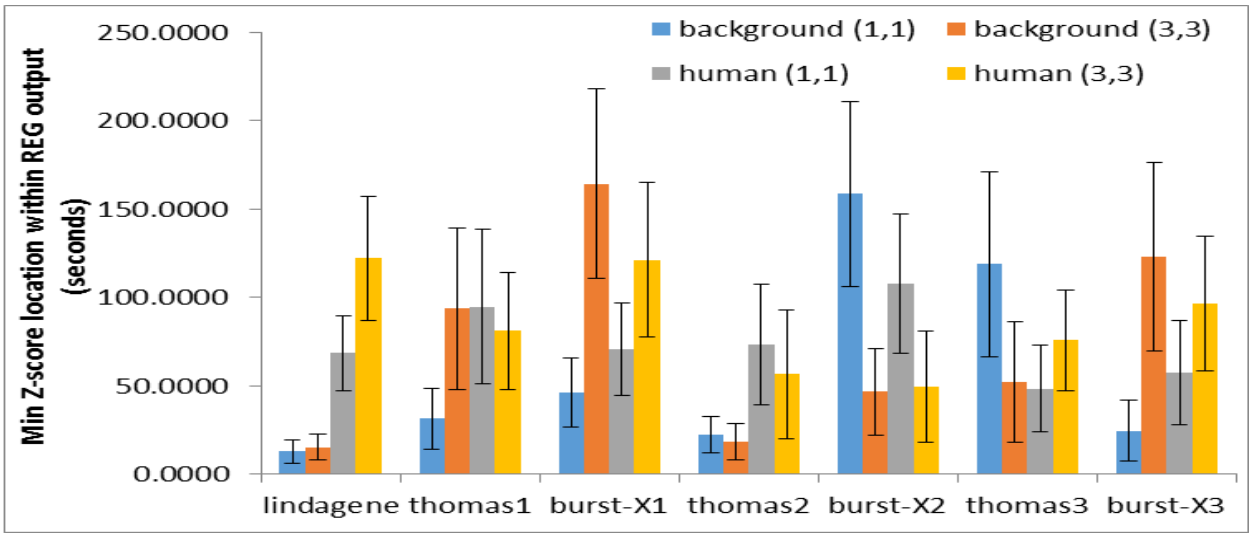

Figure 2.10 Time within REG output where Min z-score value was achieved by field conditions for human and background testing conditions with 1,1 and 3,3 field parameters

2.2.1 Spectral Analysis

Spectral analysis computed on 30 minutes of REG data during the lindagene condition during and absent of human intention revealed the variance explained in the REG output up to the Nyquist Limit. The results are shown in Figures 2.12-2.13.

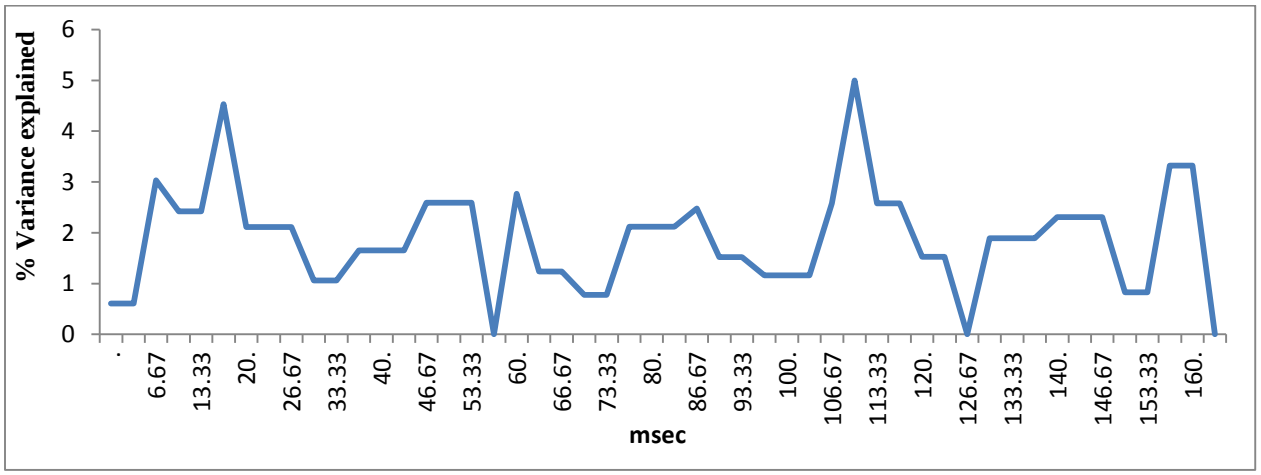

Figure 2.11 Spectral Analysis: Variance explained in REG output by t (msec) within 30 minutes of the primer field treatment (Lindagene) during human testing conditions

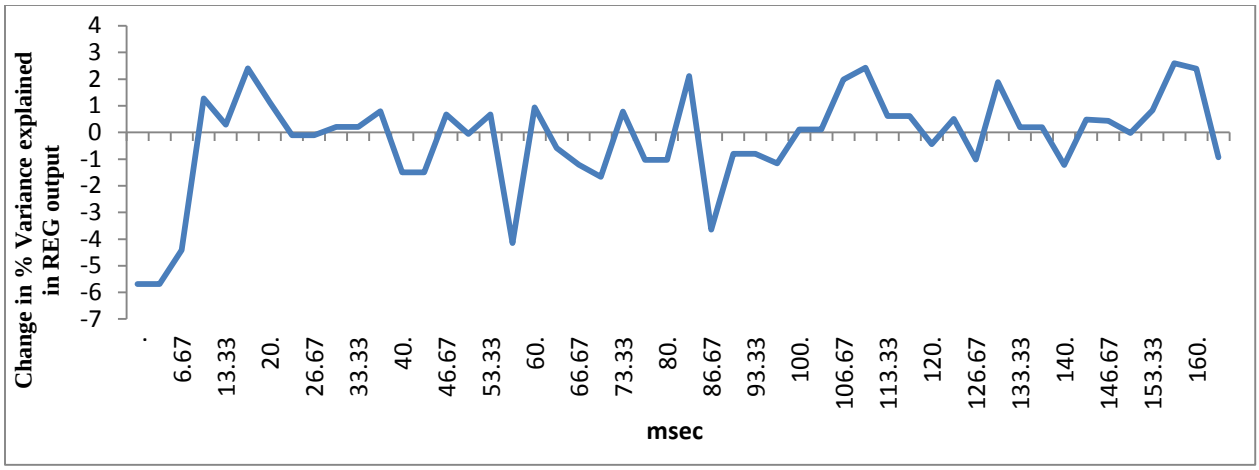

Figure 2.12 Spectral Analysis: change in variance explained in REG output by t (msec) within the primer field treatment (Lindagene); Human testing minus background testing conditions

The latter figure is derived from an analysis which subtracted the variance explained within 30 minutes of spectral analyzed primer field application applied directly to the REG during background testing (Figure-2.13) subtracted from 30 minutes of the Lindagene condition during human testing.

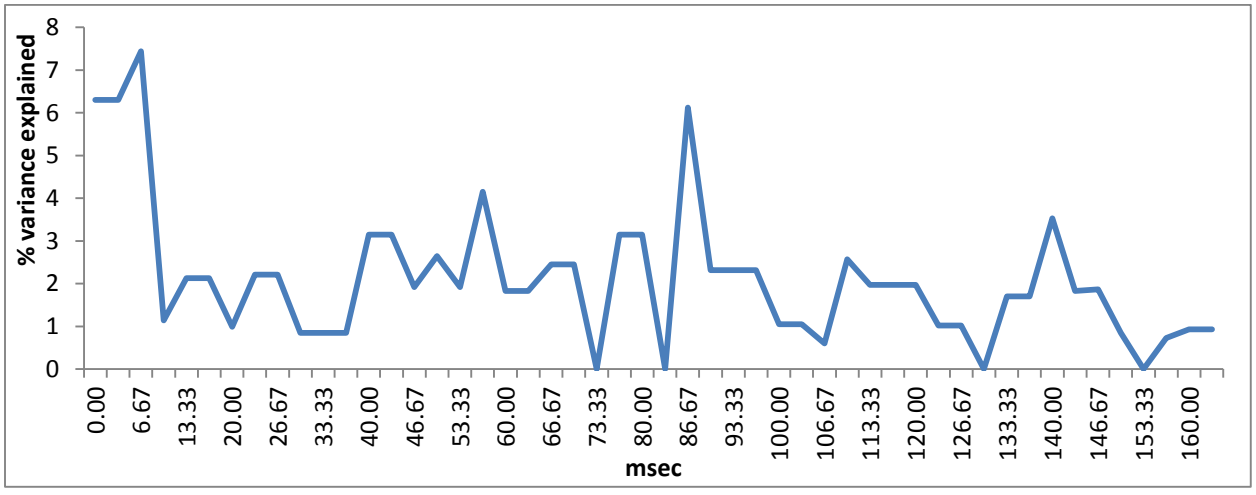

Figure 2.13 Spectral Analysis: Variance explained in REG output by t(msec) within the primer field treatment (Lindagene); background testing conditions

The variance explained during 30 minutes of true baseline from the REG with no field application or human proximity or intention can be observed in Figure-2.14

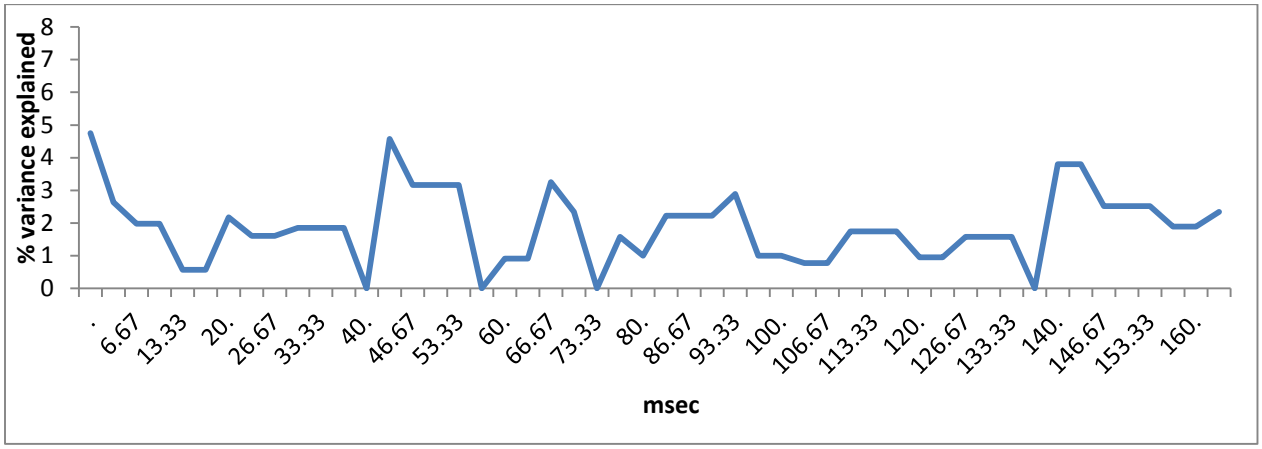

Figure 2.14 Spectral Analysis: Variance explained in REG output by t(msec) within Pre-treatment during background testing conditions

The change in variance explained when true baseline values were subtracted from 30 minutes of spectral analyzed data from the Lindagene condition during background testing conditions in either case can be observed in Figure-2.15.

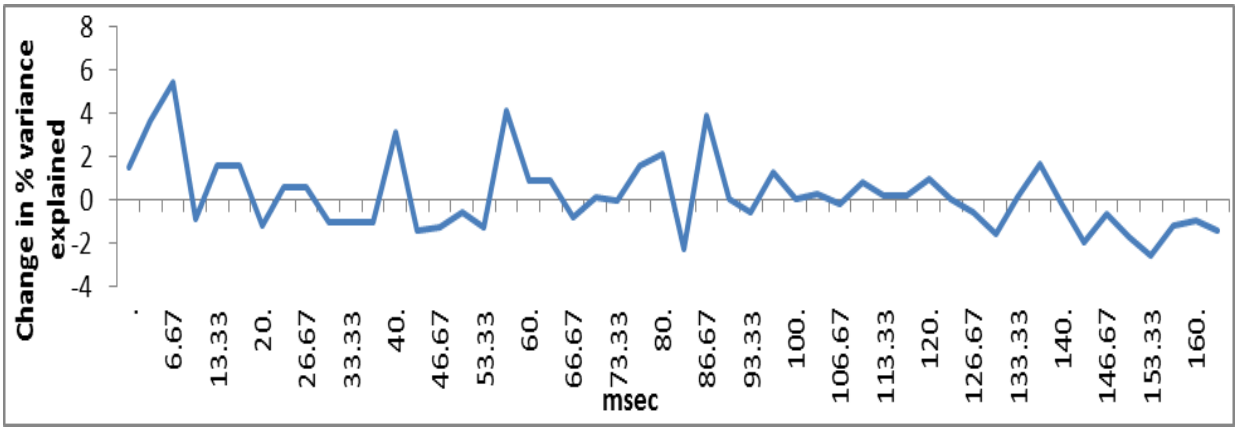

Figure 2.15 Spectral Analysis: Δ Variance explained in REG output by t(msec); 30 minutes of the primer field treatment (Lindagene) – 30 minutes of Baseline during background testing conditions

2.3.1 Remote Behavioral Guessing

After each condition (1pre/post field, 7 field conditions; Thomas 1, Burst-X1, Thomas 2, Burst-X 2, Thomas 3, Burst-X 3) participants were asked whether or not they thought the random walking line generated by the REG output during intention went up or down, and whether or not they thought the output was significant or not (random walking line being inside or outside parabola's after the 5 minute condition). This task should be considered rather difficult given that no biofeedback was given during the intention task. However given the nature of the Remote Behavioral Guessing (RBG) procedure, participants had two 50% chance opportunities (1 for direction, 1 for significance; each scored as .5 for a total score out of 1) of obtaining a correct score (1 correct guess=.5, 2 correct guess=1).

When these RBG measures were graphed over each condition, the results can be observed in Figure-2.16.

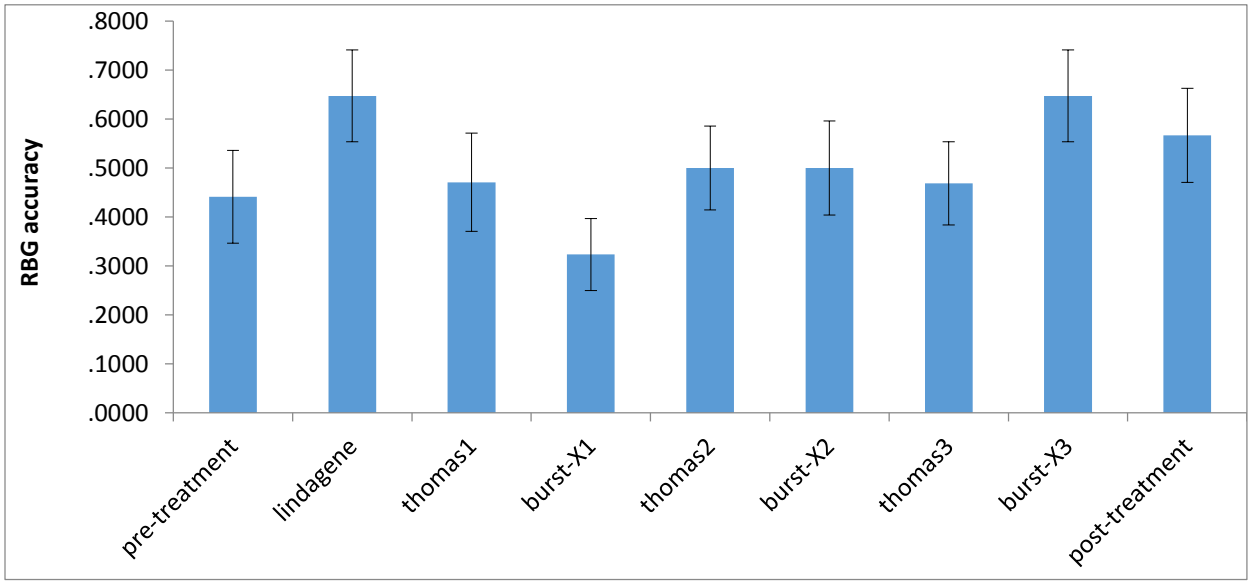

Figure 2.16 Remote Behavioral Guessing: accuracy by all human testing conditions

Even though order effects were controlled during the procedure, the data can be arranged such that the X axis is representative of field exposure time. The visual representation of which can be observed in Figure-2.17.

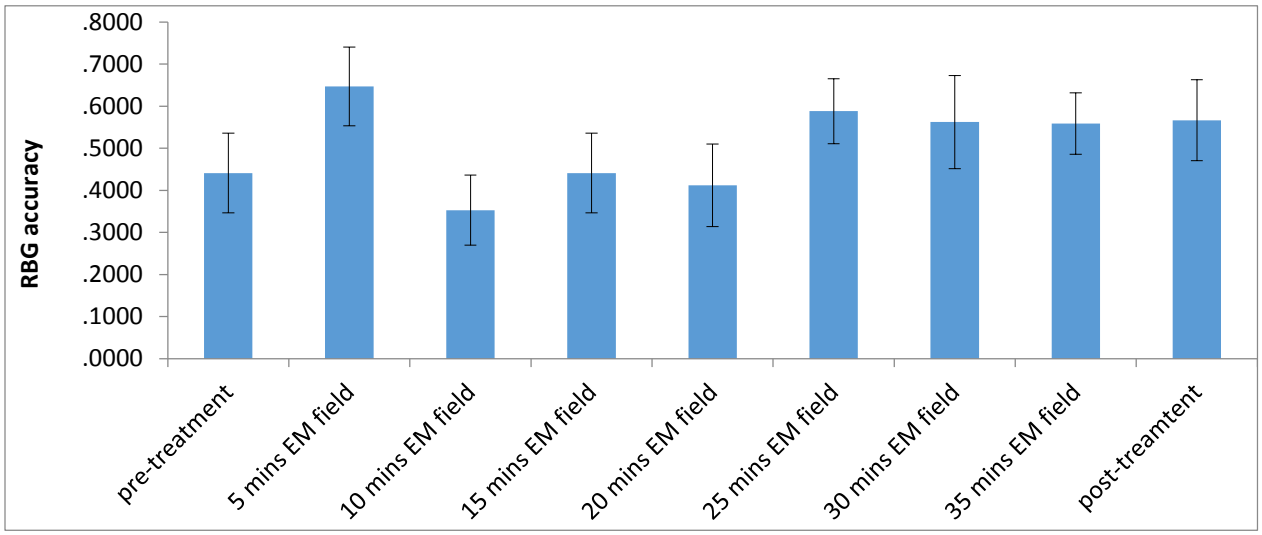

Figure 2.17 Remote behavioural guessing: accuracy by t of field treatment exposure within all human testing conditions

These measures were segmented into 1,1 and 3,3 configurations over each *condition*. The results can be observed in Figure-2.18 & 2.19 respectively.

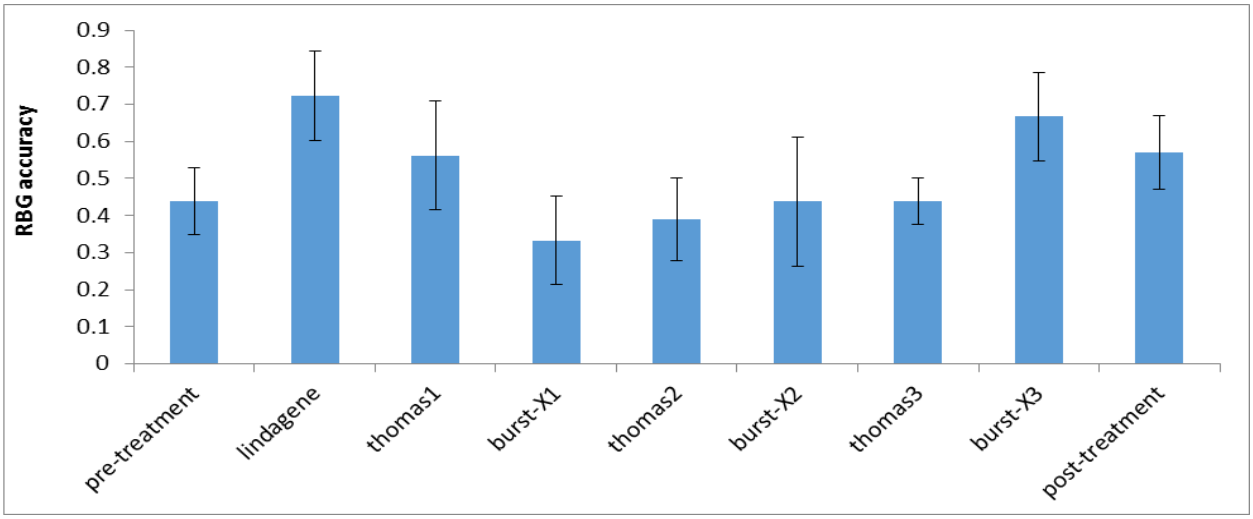

Figure 2.18 Remote behavioural guessing: accuracy by condition for 1,1 field parameters within all human testing conditions

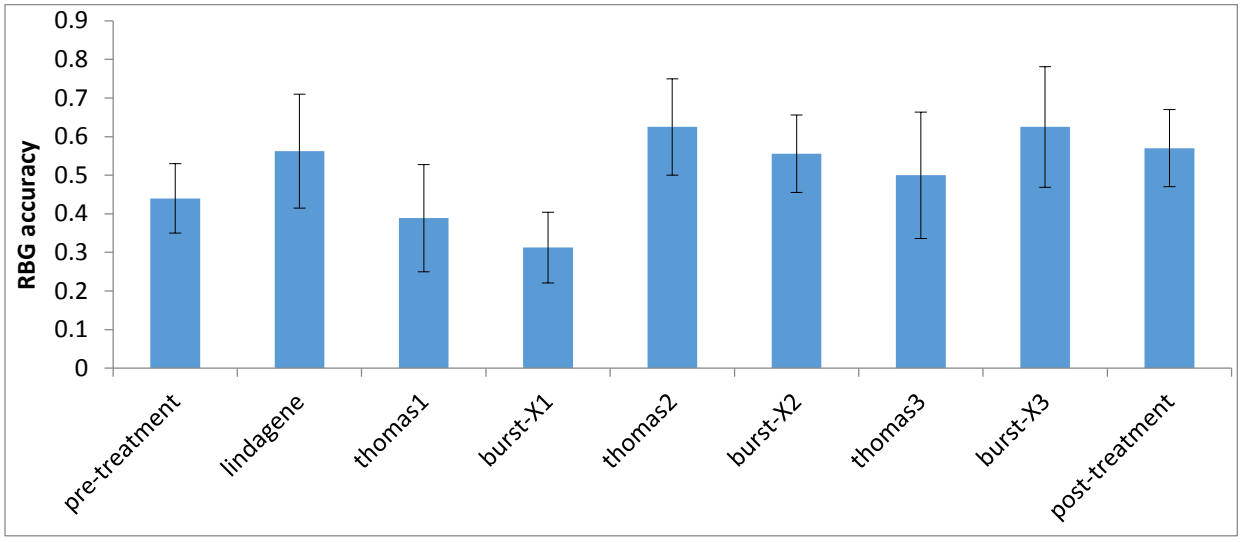

Figure 2.19 Remote behavioural guessing: accuracy by condition for 3,3 field parameters within all human testing conditions

Non-parametric Chi-square analysis found that RBG scores during the 1st Burst-X condition were significantly deviated from expected values [$X^2(2) = 6.12$, $p<.05$](Table-2.7).

Table 2.7 Remote Behavioural Guessing: accuracy during the first Burst-X condition within human testing conditions

	Observed N	Expected N	Residual
.00	7	5.7	1.3
.50	9	5.7	3.3
1.00	1	5.7	-4.7
Total	17		

When RBG scores were entered into the database ignoring counterbalancing efforts for Thomas and Burst-X in the A1-B1-A2-B2-A3-B3 format, chi-square analysis revealed that RBG scores in the 7th field condition representing B3 in the procedure and 30-35 minutes of field exposure including both Burst-X & Thomas Pulse were found to be significantly deviated from chance expectations [$X^2(2) = 7.88$, $p<.02$] (Table-2.8).

Table 2.8 Remote Behavioural Guessing: accuracy during field condition 7; 30-35 minutes into field treatment procedure (B3;Burst-X & Thomas)

RBG accuracy	Observed N	Expected N	Residual
.00	2	5.7	-3.7
.50	11	5.7	5.3
1.00	4	5.7	-1.7
Total	17		

2.3.2 Tellegen Absorption Scale

Tellegen Absorption Scale (TAS) scores from the participants included in the paradigm were entered into multiple regression analysis in order to predict Remote Behavioral Guessing (RBG) accuracy during the pre-treatment condition. The results can be observed in Table-2.9

Table 2.9 Multiple Regression results: predicting Remote Behavioural Guessing Accuracy during pre-treatment with Tellegen Absorption Scale scores

Predictor of RBG accuracy during Pre-treatment Condition	**F-statement**
Content cluster 4 (Can summon vivid and suggestive images)	[η^2=.49, F(1,15)=14.29, p=.002, SEE=.29]
Content Cluster 6 (Can become absorbed in own thought)	[η^2=.66, F(2,14)=13.47, p=.001, SEE=.24]
Content Cluster 2 (Responsive to inductive stimuli)	[η^2=.75, F(3,13)=13.04, p=.002, SEE=.29]

One-way analysis of variance revealed the relevant TAS*RBG accuracy relationship as can be observed in figures 2.20-2.21.

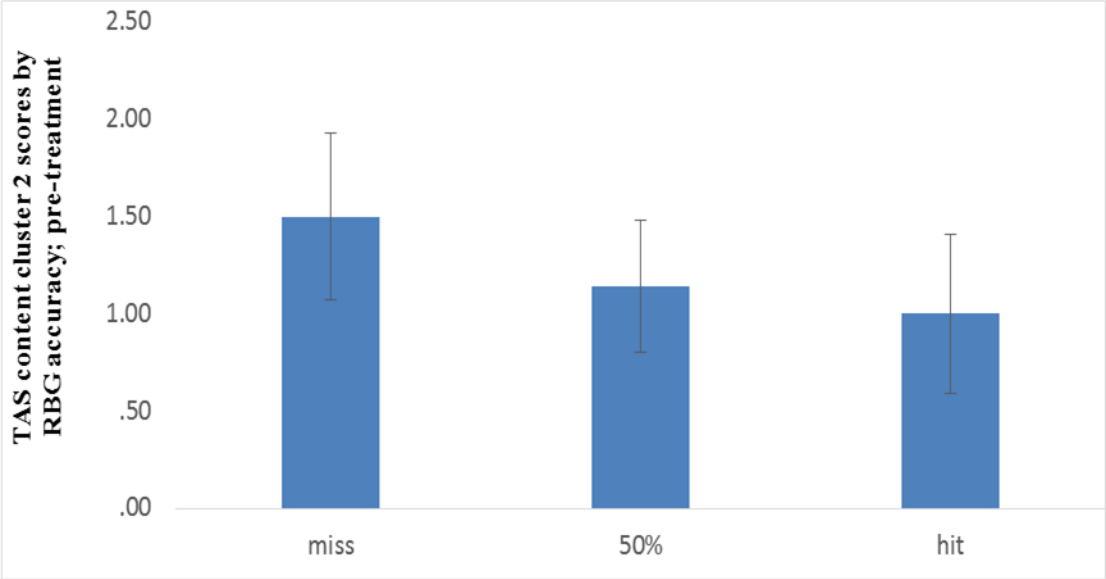

Figure 2.20 Tellegen Absorption Scale: content cluster 2 (responsive to inductive stimuli) scores (/5) by Remote Behavioural Guessing Accuracy during pre-treatment human testing conditions

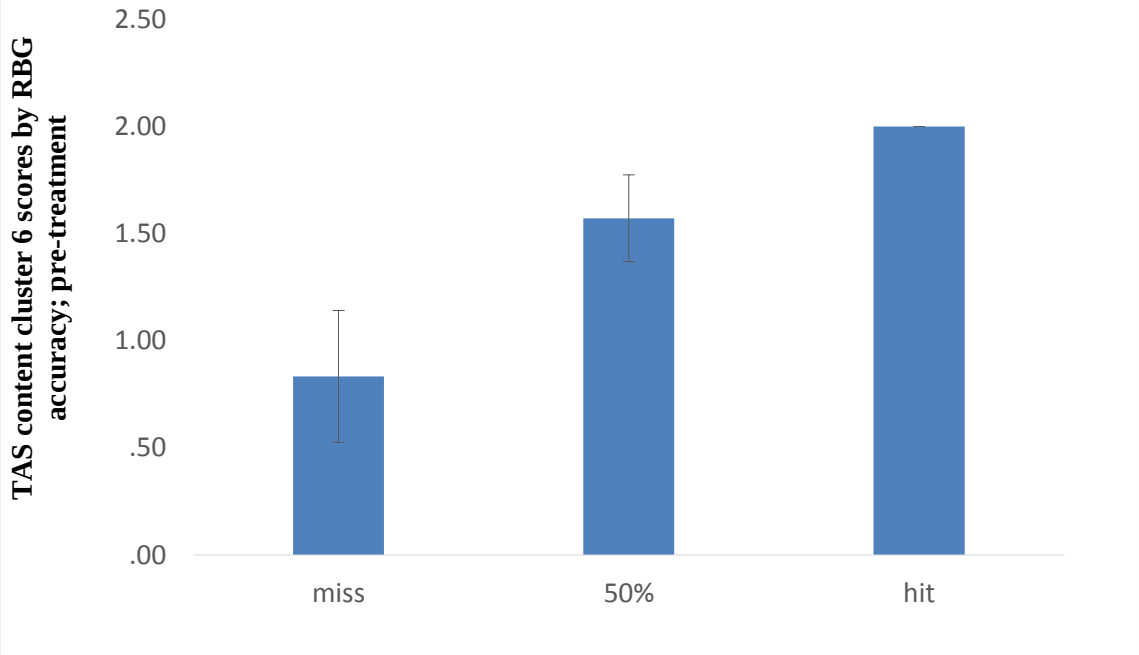

Figure 2.21 Tellegen Absorption Scale: content cluster 6 (Can become absorbed in own thoughts and imaginings) scores (/2) by Remote Behavioral Guessing Accuracy during pre-treatment

Analysis also indicated that Factor cluster 5 (Vivid reminiscence) [η^2=.39, $F_{(1,13)}$=8.24, p<.02,

SEE=.30] and Content cluster 5 (Has "crossmodal" experience) [η^2=.70, F(2,12)=14.27, p=.001, SEE=.22] entered the model to predict post-treatment RBG accuracy. *Post hoc* analysis indicated that participants who had a 'miss' scored significantly higher on factor 5 then participants who had a 'hit' in RBG accuracy during the post-treatment condition.

The Δ no-field RBG accuracy was computed (post-treatment RBG accuracy – pre-treatment RBG accuracy), and then entered into multiple regression analysis as the dependent variable along with TAS scores and field condition RBG scores. The results can be observed in Table-2.11.

Table 2.10 Multiple regression results; predicting Δ no-field RBG accuracy with Tellegen Absorption Scale scores and significant field condition Remote Behavioural Guessing accuracy

Model	**Predictor of Δ no-field RBG accuracy**	**F-statement**
1	TAS Factor 5 (Vivid Reminiscence)	[η^2=.72, $F_{(1,12)}$=30.77, p<.001, SEE=.33]
2	TAS Content cluster 7 (Can vividly re-experience the past)	[η^2=.83, $F_{(2,11)}$=25.93, p<.001, SEE=.27]
3	RBG scores during 1st Burst-X treatment	[η^2 =.89, $F_{(3,10)}$=27.0, p<.001, SEE=.22]
4	RBG scores during 1st Thomas Pulse treatment	[η^2 =.93, $F_{(4,9)}$ =30.64, p<.001, SEE=.19]

One-way analysis of variance revealed the relationship between the TAS Factor 5, content cluster 7 scores and Δ no-field RBG accuracy. This pattern is shown in Figures 2.25-2.26.

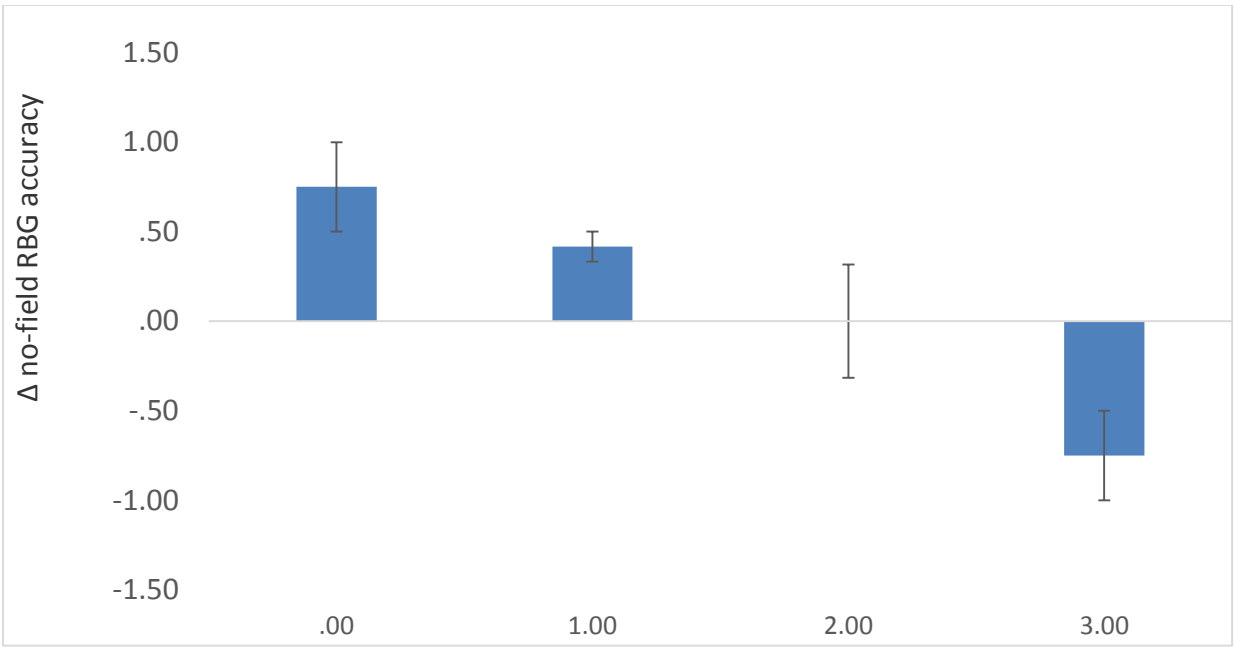

Figure 2.22 Remote Behavioural Guessing: Δ No-field accuracy (post-treatment – pre-treatment) by Tellegen Absorption Scale factor 5 (Vivid reminiscence) scores (/3)

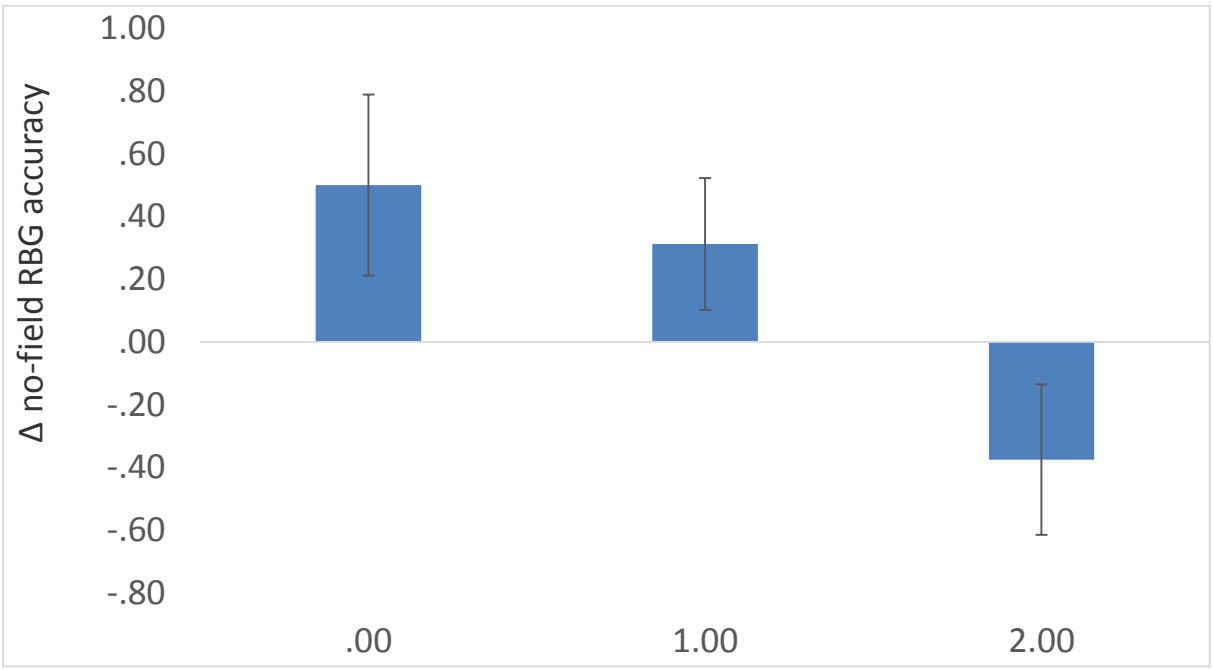

Figure 2.23 Remote Behavioural Guessing: Δ No-field accuracy by Tellegen Absorption Scale content cluster 7 (Can vividly re-experience the past) scores (/2)

2.4 Discussion:

The results of this particular experimental design indicated that focused cerebral activity from human operators directed towards random physical processes computed from electron tunneling computations within a Random Event Generator produced significant deviations from chance expectations within the device. These results support the meta-analysis conducted in Psi literature (Bosch et al., 2006; Utts, 1991;Honorton & Ferrari, 1989; Radin & Nelson, 2003; Storm, 2006; Jahn et al., 1997). This effect was not observed during baseline REG output in the absence of human intention and proximity.

It is suggested that specific electromagnetic field configurations employed within the study significantly altered the REG output when applied to both humans during intention conditions and the device directly without a human operator. The intricate relationship between Psi execution (eliciting results), Psi ability (predicting results) and the trait of absorption is interesting. Accuracy within the RBG measure, which required participants to make an attempt at predicting their intention success on the REG output with no live feedback provided, showed differences across field conditions and could be predicted by particular Tellegen Absorption Scale (TAS) scales and subscales.

The absorption related scales which served as a favorable Psi predisposition included: Content cluster 6: Can become absorbed in own thoughts and imaginings and Content cluster 4: Can summon vivid and suggestive images. Disadvantageous Psi traits included Factor 5: Vivid Reminiscence and Content cluster 5: Can vividly re-experience the past. These absorption related results suggest that successful PK ability, MMI or Consciousness Correlated Collapse is most

effectively executed by energies (Content cluster 4) that shared variance with the capacity to be absorbed in one's own thoughts and imaginings. However, it is deterred by traits that call upon the past (Factor 5; Content cluster 5). These findings support the model of free will over determinism given the appropriate energies for successful mind matter intervention and the expression of favorable absorption related subjective experiences.

3 Chapter 3: Testing the Construct Validity of the Tellegen Absorption Scale

3.1 Introduction

The Tellegen Absorption scale (TAS) is 1 of the scales on the Multidimensional Personality Questionnaire (MPQ) and measures the *trait* of absorption. This is one of the most frequently studied correlates of hypnotisability or "openness to absorbing and self-altering experiences" (Tellegen & Atkinson, 1974). Clinical application of the TAS has demonstrated that high scorers with regard to absorption are at risk for several disorders including post chemotherapy treatment nausea (Zacharie et al., 2007), morbid obesity (Wickramasekera, 1995), nonorganic chest pain (Saxon & Wickramasekera, 1994), anticipatory nausea and vomiting (Chalis & Stam, 1992), nightmares (Belicki & Belicki, 1986), and bulimia nervosa (Pettinati et al., 1985).

Absorption as a risk of stress related disorders may be due to the fact physiological activation of the hypothalamic-pituitary-adrenal-axis has been observed after the perception of a stressor, which results in neuroendocrine and immune changes as well as general homeostatic dysfunction (Flor &Turk, 1989; Wickramasekera, 2000). With this in mind, it has been reported that high absorbers have been observed to amplify even minimal unpleasant sensations in their bodies (Menzies et al., 2008). High absorbers have also been found to attend too much to physiological responses to stressors, sometimes in negative ways (Flor &Turk, 1989; Neff et al., 1983; Shea et al., 1993; Wickramasekera, 1988; Wickramasekera, 2000; Wickramasekera, 2003; Wickramasekera et al., 1996). These findings encouraged researchers to conclude that absorption is a predisposing factor to stress-related physical symptoms which may lead to chronic psychophysiological disorders (Roche & McConkey, 1990; Wickramasekera, 2003).

Absorption in-and-of-itself has been identified as a disposition for having episodes of "total" attention that fully engages ones representational resources, with a heightened sense of reality granted for the intentional object of interest. Absorption also includes imperviousness to distracting events, as well as an altered sense of reality in general, including an emphatically altered sense of self. The *trait* of Absorption has been labelled as central to understanding the nature of subjective experience as well as to aspects of cognition and behavior. The *trait* of absorption is to a disposition as the *state* of absorption is to experience. Absorption - in and of itself - involves a readiness for affective engagement and is measured on the TAS by the Absorption Ability Index (AAI).

3.1.1 Absorption ability index

The Absorption Ability Index (AAI) is a subset of 29 absorption related questions on the TAS which can be further organized into 6 factors (Tellegen, 1992) and 9 content clusters (Tellegen, 1982) and are also a part of either subscale: sentient or prone to altered and imaginative states (PTIS).

3.1.2 Sentient

Sentient is the 1st TAS subscale and is composed of 11 absorption related questions which measure TAS factors: Factor 1, Responsiveness to engaging stimuli and Factor 2, Synesthesia. Both are reported to have a narrowing consciousness with an external focus. There are several content clusters including: Content cluster 1, Is Responsive to Engaging Stimuli (IRTES), Content cluster 2" Is Responsive to Inductive Stimuli (IRTIS) and Content cluster 5: Has "crossmodal" experiences (e.g., synaesthesia).

3.1.3 Prone To altered and Imaginative States

Prone to Imaginative and altered states (PTIS) is the 2nd subscale on the Tellegen Absorption Scale (TAS) and is composed of 18 absorption related questions. TAS factors within PTIS measurement include: (Factor 3) Enhanced cognition, (Factor 4) Oblivious/dissociative involvement, (Factor 5) Vivid reminiscence, and (Factor 6) Enhanced awareness. Content clusters within the PTIS measurement include; (Cluster 2) Is Responsive to "inductive" stimuli, (Cluster 3) Often thinks in images, (Cluster 4) Can summon vivid and suggestive images, (Cluster 6) Can become absorbed in own thoughts and imaginings, (Cluster 7) Can vividly re-experience the past, (Cluster 8) Has episodes of expanded awareness, and (Cluster 9) Experiences altered states of consciousness.

3.1.4 Responsiveness to Engaging Stimuli/ Is Responsive to Engaging Stimuli

Responsiveness to engaging stimuli (IRTES) is the 1st factor on the TAS and consists of the same questions as the 1st content cluster labelled as 'Is responsive to engaging stimuli' (IRTES). Questions included within the IRTES factor and content cluster are included within the TAS subscale 'Sentient' and measure traits that are believed to have a narrowing consciousness with an external focus and are presented in Table-3.1.

Table 3.1 Responsiveness to Engaging Stimuli (IRTES) Tellegen Absorption Scale questions

Q2: I can be greatly moved by eloquent or poetic language
Q6: I like to watch cloud shapes change in the sky
Q15: The crackle and flames of a wood fire stimulate my imagination
Q23: I often take delight in small things (like five-pointed star shape that appears when you cut an apple across the core or the colors in soap bubbles
Q34: I can be deeply moved by a sunset

3.1.5 Synesthesia

Synesthesia (S) is the 2nd Factor from analyses conducted by Dr. Tellegen with regard to the TAS and has been reported as a trait with a narrowing of consciousness with an external focus

(Tellegen, 1992). Synesthesia is part of the TAS subscale 'Sentient' and is quantified by questions (Table-3.2) which also measure several content clusters including: Content cluster 2, 'Is responsive to Inductive Stimuli' and Content cluster 5, 'Has "crossmodal" experiences.

Table 3.2 Synesthesia (S) Tellegen Absorption Scale questions

Q10: Textures – such as wool, sand, wood – sometimes remind me of colors or music
Q17: Different colors have distinctive and special meanings for me
Q26: Some of my most vivid memories are called up by scents and smells
Q27: Some music reminds me of pictures or changing color patterns
Q30: The sound of a voice can be so fascinating to me that I can just go on listening to it
Q33: I find that different odors have distinctive colors

3.1.6 Enhanced cognition

Enhanced cognition (EC) is the 3rd factor and is said to have an expansion of consciousness with an external focus. EC is a part of the TAS subscale; Prone to imaginative and altered states. Questions that relate to the factor of Enhanced cognition (Table-3.3) also measure several content clusters including; (Content cluster 3) Often thinks in images, (Content cluster 4) Can summon vivid and suggestive images, (Content cluster 8) and Has episodes of expanded (e.g., ESP-like) awareness.

Table 3.3 Enhanced Cognition (EC) Tellegen Absorption Scale questions

Q13: If I wish I can imagine that my body is so heavy that I could not move it if I wanted to
Q14: I often somehow sense the presence of another person before I actually see or hear her/him
Q22: My thoughts often don't occur as words but as visual images
Q28: I often know what someone is going to say before he or she says it
Q29: I often have "physical memories"; for example, after I have been swimming I may feel as if I am in the water
Q31: At times I somehow feel the presence of someone who is not physically there
Q32: sometimes thoughts and images come to me without the slightest effort on my part.

3.1.7 Oblivious/dissociative Involvement

Oblivious/dissociative involvement (ODI) is the 4th TAS factor and is said to portray a narrowing focus with an internal consciousness (Tellegen, 1992). This factor is part of the prone to

imaginary and altered states TAS subscale and is quantified by questions (Table-3.4) which also measure several content clusters (Tellegen, 1982) including. They include Content cluster 2: Is responsive to "inductive" stimuli, Content cluster 6): Can become absorbed in own thoughts and imaginings, and Content cluster 9: Experiences altered states of consciousness.

Table 3.4 Oblivious/Dissociative Involvement (ODI) Tellegen Absorption Scale questions

Q3: While watching a movie, a TV show, or a play, I may become so involved that I may forget about myself and my surrounding and experience the story as if it were real and as if I were taking part in it
Q7: If I wish, I can imagine (or daydream) some things so vividly that they hold my attention as a good movie or story does
Q16: It is sometimes possible for me to be completely immersed in nature or in art and to feel as if my whole state of consciousness has somehow been temporarily altered
Q18: I am able to wander off in my thoughts while doing a routine task and actually forget that I am doing the task, and then find a few minutes later that I have completed it
Q21: while acting in a play I think I could really feel the emotions of the character and "become" her/him for the time being, forgetting both myself and the audience

3.1.8 Vivid Reminiscence

Vivid reminiscence (VR) is the 5th factor on the TAS and is reported to have an expanding consciousness with an internal focus (Tellegen, 1992).VR is part of the prone to altered and imaginative states subscale on the TAS and is composed of questions (Table-3.5) which also measure TAS Content Clusters 4: Can summon vivid and suggestive images and 7: Can vividly re-experience the past.

Table 3.5 Vivid Reminiscence (VR) Tellegen Absorption Scale questions

Q1: Sometimes I feel and experience things as I did when I was a child
Q4: If I stare at a picture and then look away from it, I can sometimes "see" an image of the picture almost as if I were still looking at it
Q19: I can sometimes recollect certain past experiences in my life with such clarity and vividness that it is like living them again or almost so

3.1.9 Enhanced Awareness

Enhanced awareness (EA) is the 6th TAS factor and is reported to have an expanding consciousness with an external focus (Tellegen, 1992) and is a component of the Prone to altered

and imaginative states subscale. EA is composed of questions (Table-3.6) which also measure the TAS content cluster; Experiences altered states of consciousness.

Table 3.6 Enhanced Awareness (EA) Tellegen Absorption Scale questions

Q5: Sometimes I feel as if my mind could envelope the whole world
Q9: I sometimes "step outside" my usual self and experience an entirely different state of being
Q11: Sometimes I experience things as if they were doubly real

3.1.10 Is Responsive to Engaging Stimuli

The cluster "is responsive to engaging stimuli" is measured by the same questions which quantify responsiveness to engaging stimuli.

3.1.11 Is responsive to inductive Stimuli

Is responsive to inductive stimuli (IRTIS) is the 2nd content cluster on the TAS and is a part of both TAS subscales; Sentient and Prone to altered and imaginative states. IRTIS is composed of questions (Table-3.7) which also measure TAS factors including: (factor 2) Synesthesia and (factor 4) factor Oblivious/dissociative involvement.

Table 3.7 Is Responsive To Inductive Stimuli (IRTIS) Tellegen Absorption Scale questions

Q3: While watching a movie, A TV show, or a play, I may become so involved that I may forget about myself and my surroundings and experience the story as if it were real and as if I were taking part in it
Q21: While acting in a play I think I could really feel the emotions of the character and "become" her/him for the time being, forgetting both myself and the audience
Q30: The sound of a voice can be so fascinating to me that I just go on listening to it

3.1.12 Often Thinks In Images

Often thinks in images (OTII), the 3rd content cluster on the TAS, is a component of the PTIS TAS subscale and is quantified by questions (Table-3.8) which also measure the TAS factor EC.

Table 3.8 Often Thinks In Images (OTII) Tellegen Aborption Scale questions

Q22: My thoughts often don't occur as words but as visual images
Q32: Sometimes thought and images come to me without the slightest effort on my part

3.1.13 Can Summon Vivid and Suggestive Images

Can summon vivid and suggestive images (CSVSI), the 4th content cluster and a component of the PTIS TAS subscale, is measured by questions (Table-3.9) which alsorepresent TAS factors EC and VR.

Table 3.9 Can Summon Vivid and Suggestive Images (CSVSI) Tellegen Absorption Scale questions

Q4: If I stare at a picture and then look away from it, I can sometimes "see" an image of the picture as if I were staring at it
Q13: If I wish, I can Imagine that my body is so heavy that I could not move it if I wanted to
Q29: I often have "physical memories"; for Example, after I have been swimming I may feel as if I am still in the water

3.1.14 Has "Crossmodal" Experiences (e.g., Synesthesia)

Has "crossmodal" experiences (HCE), the 5th content cluster and a component of the Sentient TAS subscale, is measured by questions (Table-3.10) included within the S TAS factor.

Table 3.10 Has "Crossmodal" Experiences (HCE) Tellegen Absorption Scale questions

Q10: Textures – such as wool, sand, wood – sometimes remind me of colors or music
Q17: Different colors have distinctive and special meanings for me
Q26: Some of my most vivid memories are called up by scents and smells
Q27: Some music reminds me of pictures or changing color patterns
Q33: I find that different odors have distinctive colors

3.1.15 Can Become Absorbed in Own Though and Imaginings

Can become absorbed in own thoughts and imaginings (BOATI), the 6th content cluster and a PTIS component, is measured by questions (Table-3.11) included within the ODI factor.

Table 3.11 Can Become Absorbed in Own Thoughts and Imaginings (BOATI) Tellegen Absorption Scale Questions

Q7: If I wish, I can imagine (or daydream) some things so vividly that they hold my attention as a good movie or story does
Q18: I am able to wander off in my thoughts while doing a routine task and actually forget that I am doing the task, and then find a few minutes later that I have completed it

3.1.16 Can Vividly Re-experience the Past

Can vividly re-experience the past (VRP), a component of the PTIS subscale and the 7th content cluster, is quantified by a couple of questions (Table-3.12) which also measure the TAS factor VR.

Table 3.12 Can Vividly Re-experience the Past (VRP) Tellegen Absorption Scale questions

Q1: Sometimes I feel and experience things as I did when I was a child
Q19: I can sometimes recollect certain past experiences in my life with such clarity and vividness that it is like living them again or almost so

3.1.17 Has Episodes of Expanded (e.g., ESP-like) Awareness

Has episodes of expanded awareness (EEA), the 8th content cluster and a portion of the PTIS subscale, shares measurement (Table-3.13) on the TAS with factor 3 EC.

Table 3.13 Has episodes of Expanded Awareness (EEA) Tellegen Absorption Scale questions

Q14: I often somehow sense the presence of another person before I actually see or hear her/him
Q28: I often know what someone is going to say before he or she says it
Q31: At times I somehow feel the presence of someone who is not physically there

3.1.18 Experiences Altered States of Consciousness

Experiences altered states of consciousness (EASC) is the 9th and final TAS content cluster and is a measurement of the PTIS subscale. It is measured by several questions (Table-3.14) which also measure factors ODI and EA.

Table 3.14 Experiences Altered States of Consciousness (EASC) Tellegen Absorption Scale questions

Q5: Sometimes I feel as if my mind could envelope the whole world
Q9: I sometimes “step outside” my usual self and experience an entirely different state of being
Q11: Sometimes I experience things as if they were doubly real
Q16: It is sometimes possible for me to be completely immersed in nature or in art and to feel as if my whole state of consciousness has somehow been temporarily altered

3.2 Methods

Over the course of 4 years, TAS scores had been collected after approved protocols from 91 members within the Laurentian Community. There were 3 separate experiments with the following populations; Study 1- N=15, Study 2 – N=17, and Study 3 – N=61.

3.2.1 Study 1

This study included the collection of TAS scores from the Neuroscience Research Group at Laurentian University (N=15). These scores were entered into a database with baseline quantitative Electroencephalographic (QEEG) recordings from days, weeks, and months prior to the completion of the TAS questionnaire. The QEEG profiles were used to predict TAS scores within multiple regression analysis within SPSS.

3.2.2 Study 2

This study is a subset of 2013 Clinical Neuroscience undergraduates who volunteered for a study which included the application of Electromagnetic (EM) field application and a procedure which required the participant to actively intend upon the output of a Random Event Generator (REG) - created by Princeton Engineering Anomalies Research Group (PEAR) in a procedure which included nine 5 minute conditions which proceeded in the following order; pre-treatment, Lindagene, Thomas 1, Burst-X 1, Thomas 2, Burst-X 2, Thomas 3, Burst-X 3, post-treatment. The pre and post treatment conditions followed the same procedure as field conditions requiring the participant to intend upon the REG results, with the exception that no fields were applied.

The Lindagene condition acted as the priming field, and depending on odd or even day of testing or odd or even subject tested. The Thomas exposure and Burst-X exposure was switched in the presentation order that followed an A-B-A-B-A-B sequence or B-A-B-A-B-A template. The weak fields (about 1 microTesla or 10 mG) which are equivalent in intensity to that of ambient fields in which we are frequently immersed were applied through small solenoids (an energized coil of insulated wire which produces a magnetic field within the coil) within containers that are placed (in human conditions) on each side of the head at the level of the temporal lobes. Delay between points and point duration were altered from 1,1 ms to 3,3 ms depending on odd or even day of testing or subject tested. During all conditions the participants (N=15) were asked to intend on the output generated from the REG. Specifically they were asked to influence the random walking line generated by quantum tunneling processes within the device through the process of intended thinking.

The device was shown to the participants and its operation was explained. However "biofeedback" from the machine was not given as participants sat quietly in a Faraday chamber within the consciousness lab at Laurentian University during the procedure. To keep participants engaged, they were asked at the completion of each condition whether or not they thought the line deviated up or down and whether or not they thought the deviation was significant or insignificant. The REG was placed 1 meter in front and to the left of the individual as he or she sat in a comfortable arm chair. During non-human testing the solenoids were placed 10 cm (to simulate the width of the human brain) the left and the right of the REG, in the same location where human testing occurred. The Faraday chamber was closed and lights were turned off. Several REG variables were collected during each condition, namely; z-score, min/max z-score

average, min/max z-score location within output, mean, and standard deviation.

3.2.3 Study 3

This study measured the influence of intention of 61 participants on a Live Feedback Random Number Generator (RNG). Intention effects were inferred by the performance on the Live Feedback RNG. Hits and misses were scored according to the participants enveloped bit containing either a 1 or a 0. All participants were exposed to weak complex magnetic field patterns known to facilitate learning and reduce depression (Baker-Price & Persinger, 2003). Participants were subject to various levels of a frustration task and assigned to one of 5 treatments: Control (no intent), neutral (intent), novice meditation, negative arousal, or positive arousal. The profile of mood states (POMS) brief was administered prior to and after treatment to measure the subjective effect of treatment.

3.3 Results

One-way analysis of variance (ANOVA) demonstrated that there were significant differences between the 3 studies with regard to TAS factor 3 EC [$F(2,88)=3.49$, $p=.035$, $\eta^2=.07$]. *Post-hoc* analysis indicated that NRG members scored significantly higher for this factor then did the members in the other 2 studies (Figure-3.1). When the TAS scores were entered into multiple regression analysis in order to predict study, significance was observed with EC and ODI entering as predictors [$F(2,88)=5.36$, $p=.006$, $\eta^2=.11$, SEE=.70] yielding the following equation:

predstudy= -.136*(Enhanced cognition) + .113*(Oblivious/Dissociative involvement) + 2.687.

Table 3.15 Tellegen Absorption Scale variables and visual Representations

Variable	Representation	Variable	Representation
Tas	Absorption ability index	Con1	Responsive to engaging stimuli
Sent	Sentient	Con2	responsive to inductive stimuli
Ptis	Proneness to imaginative and altered states	Con3	often think in images
Fac1	Responsive to engaging stimuli	Con4	can summon vivid and suggestive images
Fac2	Synaesthesia	Con5	has "crossmodal" experience
Fac3	enhanced cognition	Con6	Can become absorbed in own thoughts & images
Fac4	Oblivious/Dissociative Involvement	Con7	can vividly re-experience the past
Fac5	Vivid reminiscence	Con8	has episodes of expanded awareness
Fac6	Enhanced awareness	Con9	experiences altered states of consciousness

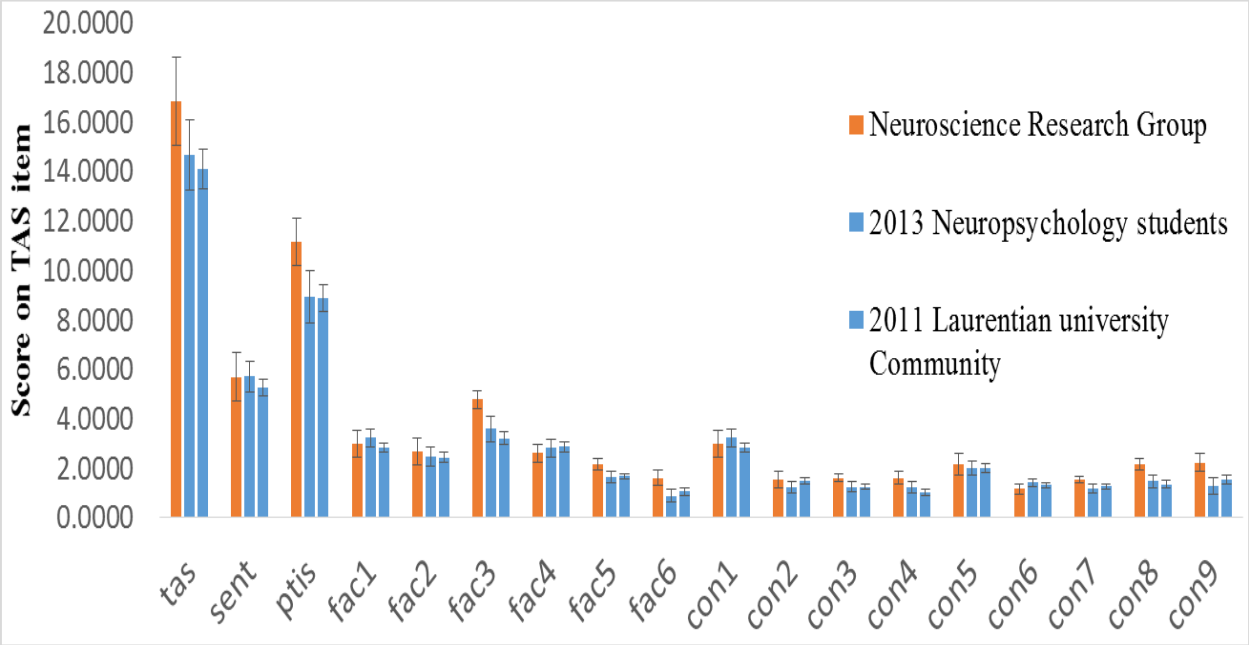

Figure 3.1 Tellegen Absorption Scale: scores by population; (1) 2014 Neuroscience Research Group Members, (2) 2013 Neuropsychology students, (3) 2011 Laurentian University community members

3.3.1 TAS Results from study 1

QEEG frequencies (Delta, Theta, Alpha1, Alpha2, Beta1, Beta2, Beta3, Gamma1, Gamma2) from all sensors (19 channel; fp1, fp2, f7, f3, fz, f4, f8, t3, c3, cz, c4, t4, t5, p3, pz, p4, t6, o1, and o2) along with other QEEG measures (#/ and % of GFP peaks for microstates A-D, # of times of appearance and duration of microstates A-D, and left/right parahippocampal activity) were simultaneously entered into multiple regression analysis (Max-steps 4) within SPSS in order to predict the scores of each TAS scale and subscale. The results can be observed in Table-3.16

Table 3.16 Main Quantitative Electroencephalography predictors (Max steps 4) of each Tellegen Absorption Scale (TAS scale and subscale

Variable & Activation	**F Statement**
Absorption ability index	
Decrease in beta2 within pz sensor	$F(1,13)=10.1$, $p<.01$, $\eta^2=.44$, SEE=4.92
Increase in delta within f8 sensor	$F(2,12)=14.23$, $p<.01$, $\eta^2=.70$, SEE=3.72
Increase in beta2 within c3 sensor	$F(3,11)=24.67$, $p<.01$, $\eta^2=.87$, SEE=2.57
Decrease in alpha1 within f8 sensor	$F(4,10)=27.72$, $p<.01$, $\eta^2=.92$, SEE=2.15
Sentience	
Decrease in beta2 within p3 sensor	$F(1,13)=8.22$, $p=.01$, $\eta^2=.39$, SEE=2.62
Increase in alpha2 within fp1 sensor	$F(2,12)=14.48$, $p<.01$, $\eta^2=.71$, SEE=1.89
Prone to imaginative and altered states	
Decrease in beta2 within pz sensor	$F(1,13)=6.5$, $p<.03$, $\eta^2=.33$, SEE=3.21
Increase in delta within f8 sensor	$F(2,12)=7.34$, $p<.01$, $\eta^2=.55$, SEE=2.74

Increase in gamma2 within t3 sensor	$F(3,11)=13.06$, $p<.01$, $\eta^2=.78$, SEE=2.00
Increase in the duration of microstate B	$F(4,10)=16.44$, $p<.01$, $\eta^2=.87$, SEE=1.63
Responsive to Engaging stimuli	
Decrease in beta2 within pz sensor	$F(1,13)=9.37$, $p<.01$, $\eta^2=.42$, SEE=1.46
Increase in alpha2 within c3 sensor	$F(2,12)=12.40$, $p<.01$, $\eta^2=.67$, SEE=1.14
Synesthesia	
Decrease in theta within t3 sensor	$F(1,13)=8.07$, $p=.01$, $\eta^2=.38$, SEE=1.44
Increase in beta2 within right parahippocampus	$F(2,12)=15.97$, $p<.01$, $\eta^2=.73$, SEE=1.00
Increase in gamma1 within o1 sensor	$F(3,11)=22.19$, $p<.01$, $\eta^2=.86$, SEE=.75
Increase in delta within fp2 sensor	$F(4,10)=26.51$, $p<.01$, $\eta^2=.91$, SEE=.61
Enhanced cognition	
Increase in delta within f8 sensor	$F(1,13)=11.73$, $p<.01$, $\eta^2=.47$, SEE=1.17
Decrease in alpha2 within o2 sensor	$F(2,12)=11.28$, $p<.01$, $\eta^2=.65$, SEE=.99
Decrease in # of gfp peaks for class A	$F(3,11)=15.47$, $p<.01$, $\eta^2=.81$, SEE=.76
Increase in delta within the left parahippocampus	$F(4,10)=19.92$, $p<.01$, $\eta^2=.89$, SEE=61
Oblivious/Dissociative involvement	
Decrease in beta2 within pz sensor	$F(1,13)=10.51$, $p<.01$, $\eta^2=.45$, SEE=1.07
Vivid Reminiscence	
Increase in gamma2 within t3 sensor	$F(1,13)=11.02$, $p<.01$, $\eta^2=.46$, SEE=.65
Decrease in gamma2 within fp1 sensor	$F(2,12)=11.06$, $p<.01$, $\eta^2=.65$, SEE=.54
Increase in beta2 within right parahippocampus	$F(3,11)=11.74$, $p<.01$, $\eta^2=.76$, SEE=.46

Enhanced awareness	
Decrease in beta2 within o2 sensor	$F(1,13)=5.54$, $p<.04$, $\eta^2=.30$, SEE=.98
Increase in beta1 within t3 sensor	$F(2,12)=6.94$, $p=.01$, $\eta^2=.54$, SEE=.83
Decrease in delta within o1 sensor	$F(3,11)=8.25$, $p<.01$, $\eta^2=.69$, SEE=.70
Decrease in beta3 within left parahippocampus	$F(4,10)=9.97$, $p<.01$, $\eta^2=.80$, SEE=.80
Responsive to engaging stimuli	
Decrease in beta2 within pz sensor	$F(1,13)=9.37$, $p<.01$, $\eta^2=.42$, SEE=1.46
Increase in alpha2 within c3 sensor	$F(2,12)=12.40$, $p<.01$, $\eta^2=.67$, SEE=1.14
Is responsive to inductive stimuli	
Decrease in beta2 within pz sensor	$F(1,13)=11.48$, $p<.01$, $\eta^2=.47$, SEE=.89
Increase in beta3 within c3 sensor	$F(2,12)=17.14$, $p<.01$, $\eta^2=.74$, SEE=.65
Often thinks in images	
Increase in delta within f8 sensor	$F(1,13)=16.35$, $p<.01$, $\eta^2=.56$, SEE=.44
Decrease in gamma2 within fp1 sensor	$F(2,12)=17.13$, $p<.01$, $\eta^2=.74$, SEE=.35
Increase in alpha2 within right parahippocampus	$F(3,11)=29.38$, $p<.01$, $\eta^2=.89$, SEE=.24
Decrease in duration of microstate B	$F(4,10)=43.53$, $p<.01$, $\eta^2=.95$, SEE=.18
Can summon vivid and suggestive images	(No variables loaded)
Has crossmodal experience	
Increase in delta within f8 sensor	$F(1,13)=10.65$, $p<.01$, $\eta^2=.45$, SEE=1.13
Increase in the # of times that microstate D appeared	$F(2,12)=18.22$, $p<.01$, $\eta^2=.75$, SEE=.79

Decrease in theta within p4 sensor	$F(3,11)=22.19$, $p<.01$, $\eta^2=.86$, SEE=.62
Increase in delta within o1 sensor	$F(4,10)=28.02$, $p<.01$, $\eta^2=.92$, SEE=.50
Can become absorbed in own thoughts and Imaginings	
Decrease in beta1 within o1 sensor	$F(1,13)=5.11$, $p<.05$, $\eta^2=.28$, SEE=.59
Increase in alpha2 within t6 sensor	$F(2,12)=12.26$, $p<.01$, $\eta^2=..67$, SEE=.42
Increase in delta within left parahippocampus	$F(3,11)=12.47$, $p<.01$, $\eta^2=.77$, SEE=.36
Can vividly re-experience the past	
Increase in gamma2 within t3 sensor	$F(1,13)=11.22$, $p<.01$, $\eta^2=.46$, SEE=.55
Increase in delta within t6 sensor	$F(2,12)=16.70$, $p<.01$, $\eta^2=.74$, SEE=.40
Decrease in theta within t3 sensor	$F(3,11)=24.70$, $p<.01$, $\eta^2=.87$, SEE=.29
Has episodes of expanded (ESP-like) awareness	
Decrease in # of gfp peaks for class A	$F(1,13)=4.78$, $p<.05$, $\eta^2=.27$, SEE=.78
Increase in gamma1 within t6 sensor	$F(2,12)=6.65$, $p<.02$, $\eta^2=.53$, SEE=.66
Decrease in beta2 within p3 sensor	$F(3,11)=11.29$, $p<.01$, $\eta^2=.76$, SEE=.49
Decrease in gamma1 within f7 sensor	$F(4,10)=15.40$, $p<.01$, $\eta^2=.86$, SEE=.39
Experiences altered states of consciousness	
Decrease in beta2 within o2 sensor	$F(1,13)=7.59$, $p<.02$, $\eta^2=.37$, SEE=1.20
Increase in alpha2 within t3 sensor	$F(2,12)=12.09$, $p<.01$, $\eta^2=.67$, SEE=.91
Increase in gamma2 within o2 sensor	$F(3,11)=25.40$, $p<.01$, $\eta^2=.87$, SEE=.58
Increase in alpha1 within fp1 sensor	$F(4,10)=39.99$, $p<.01$, $\eta^2=.94$, SEE=.42

The partial regression plots from these main QEEG predictors for each TAS scale and subscale are presented below in Figures 3.2-3.51.

3.3.2 Absorption ability Index Partial plots

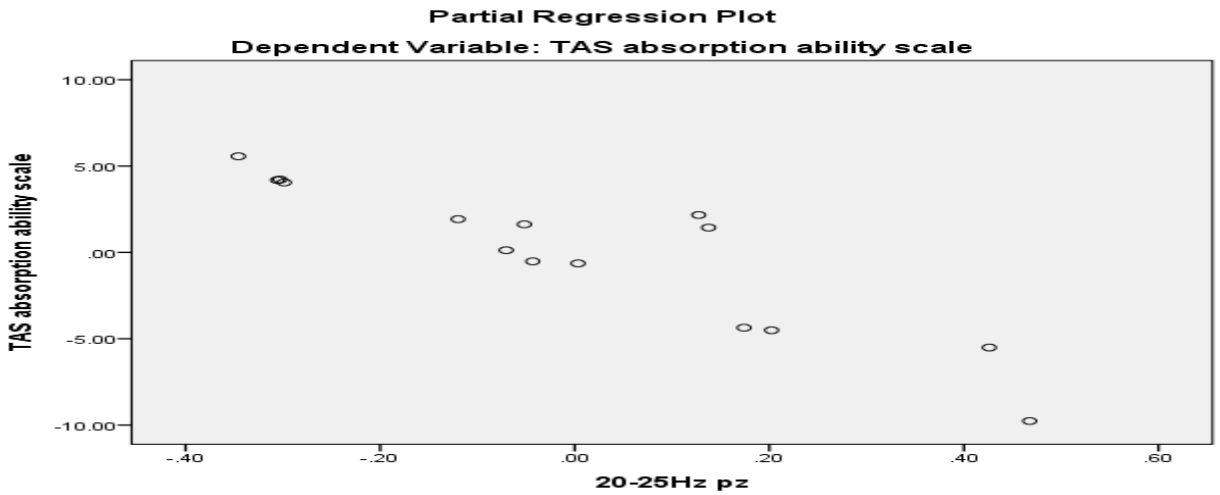

Figure 3.2 Absorption Ability Index: 1st quantitative electroencephalographic partial plot; decrease in 20-25Hz activity in pz sensor

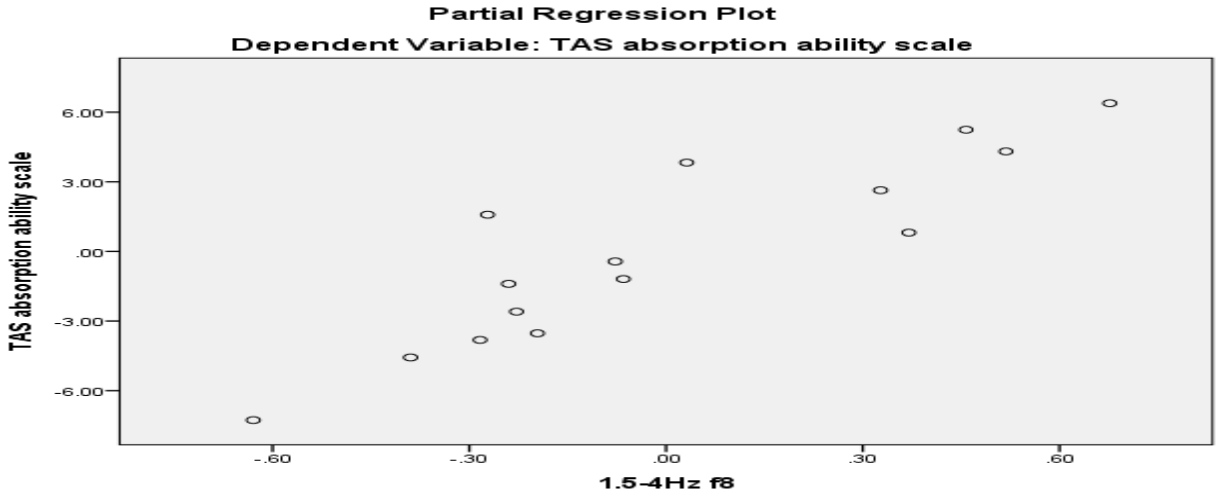

Figure 3.3 Absorption Ability Index: 2nd Quantitative Electroencephalographic partial plot; Increase in 1.5-4Hz activity in f8 sensor

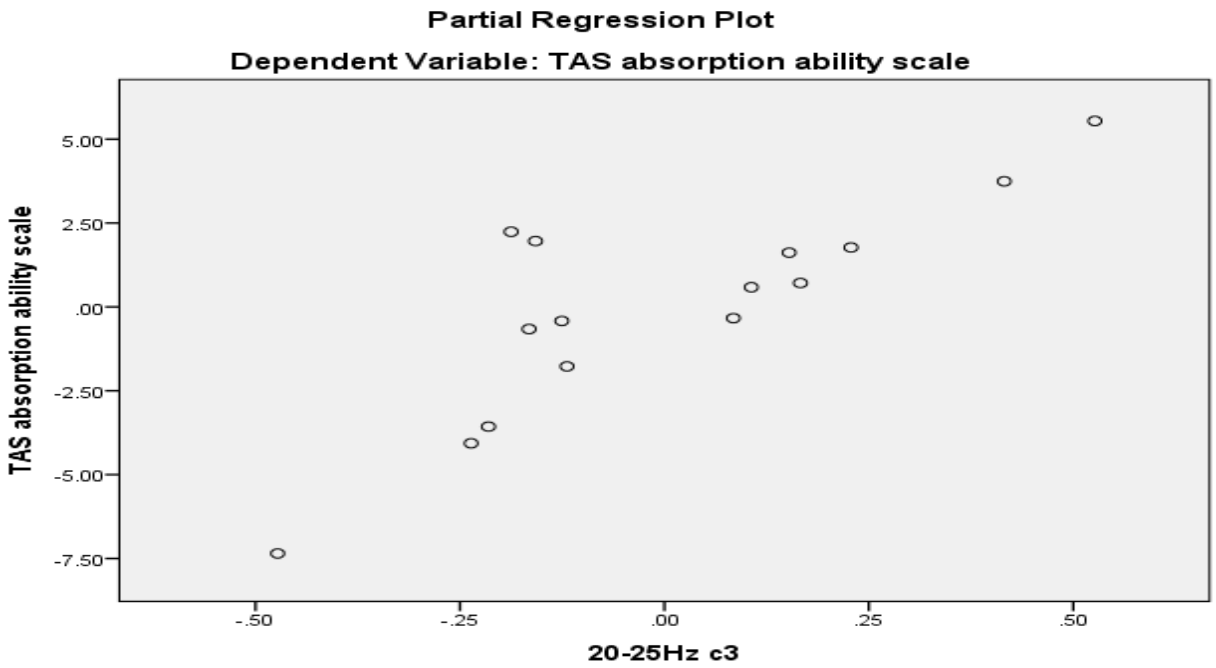

Figure 3.4 Absorption Ability Index: 3rd Quantitative Electroencephalographic partial plot; Increase in 20-25Hz activity in c3 sensor

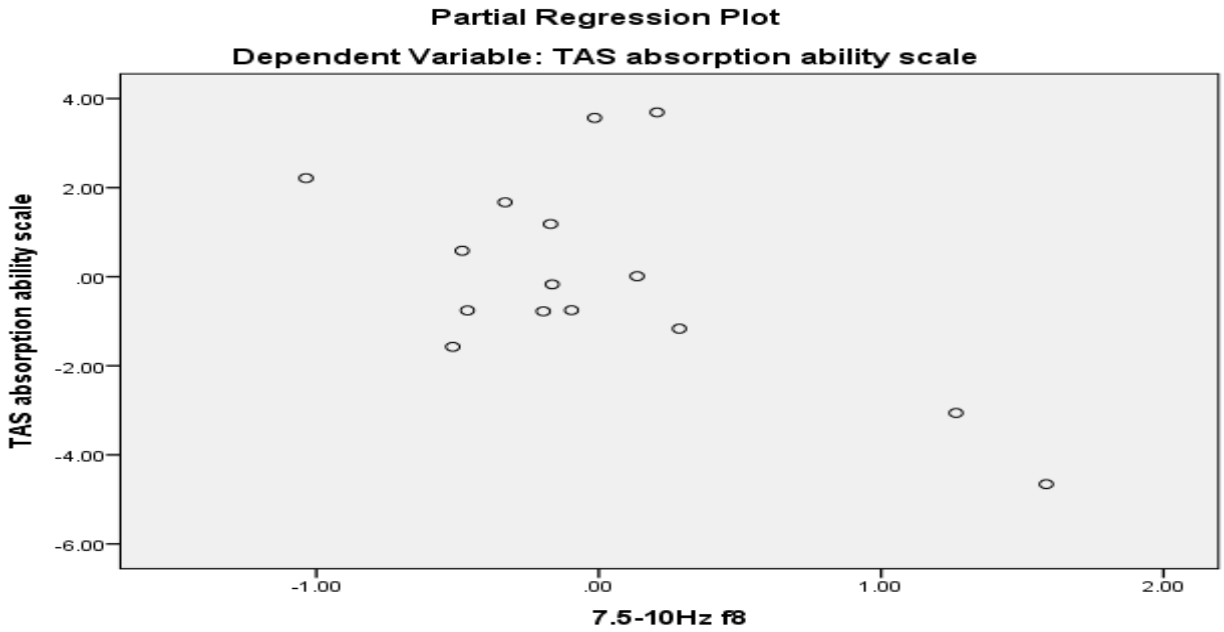

Figure 3.5 Absorption Ability index: 4th Quantitative Electroencephalographic partial plot; decrease in 7.5-10Hz activity in f8 sensor

3.3.3 Sentient Partial plots

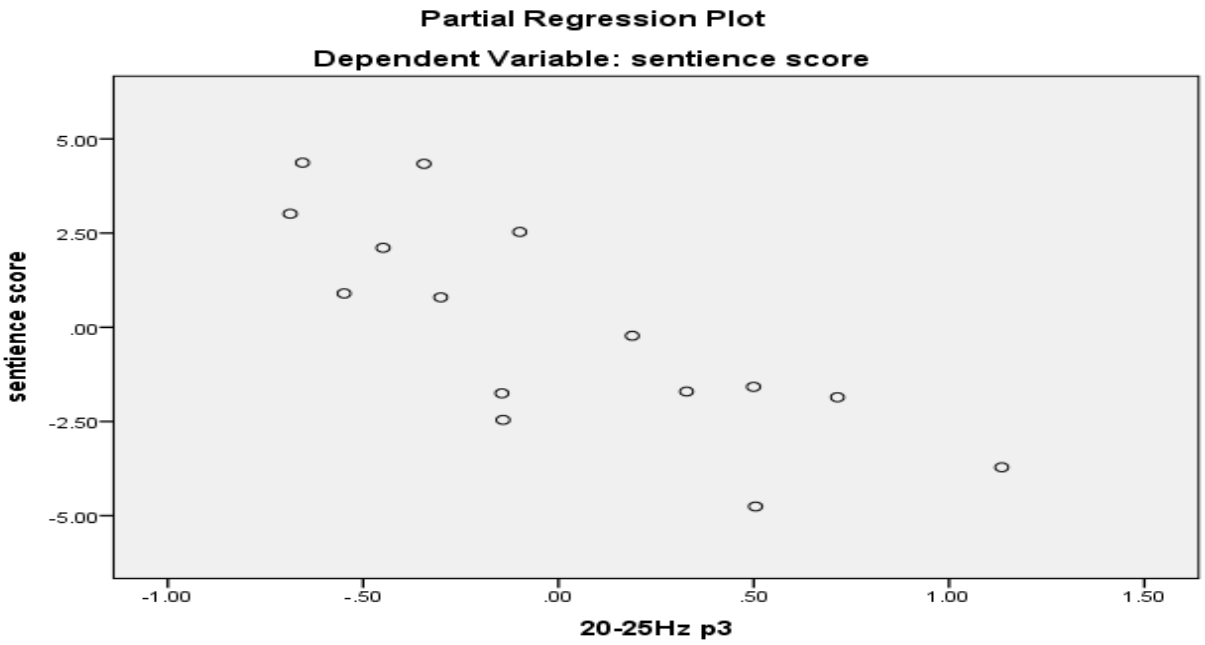

Figure 3.6 Sentient: 1st Quantitative Electroencephalographic partial plot; Decrease in 20-25Hz activity in p3 sensor

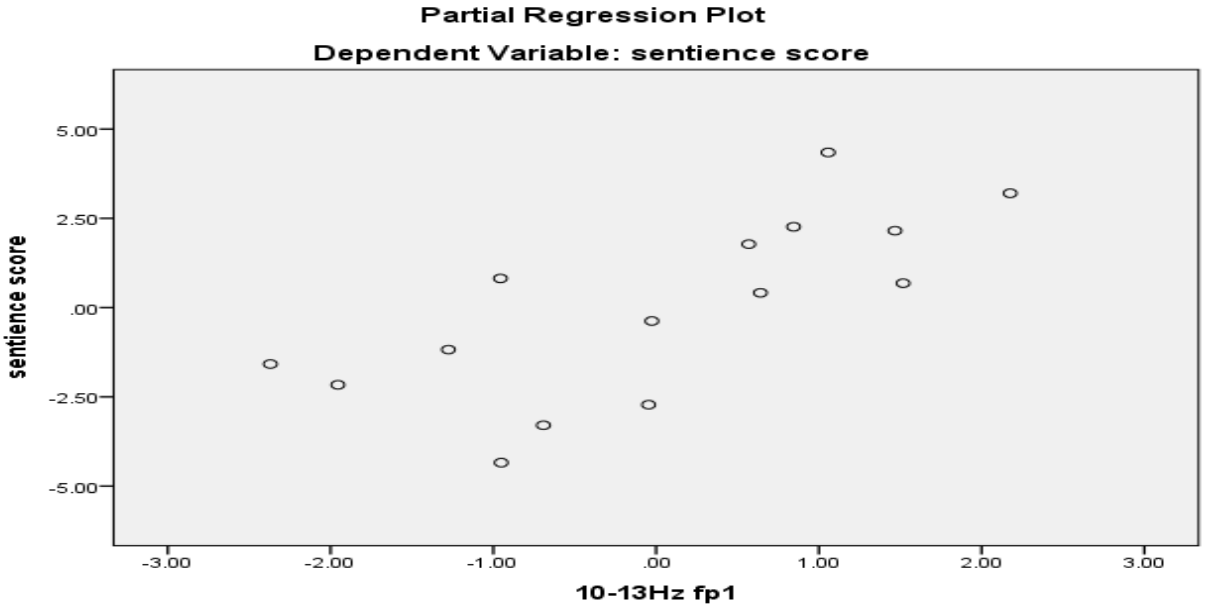

Figure 3.7 Sentient 2nd Quantitative Electroencephalographic partial plot; Increase in 10-13Hz activity in fp1 sensor

3.3.4 Proneness To Altered and Imaginary States Partial Plots

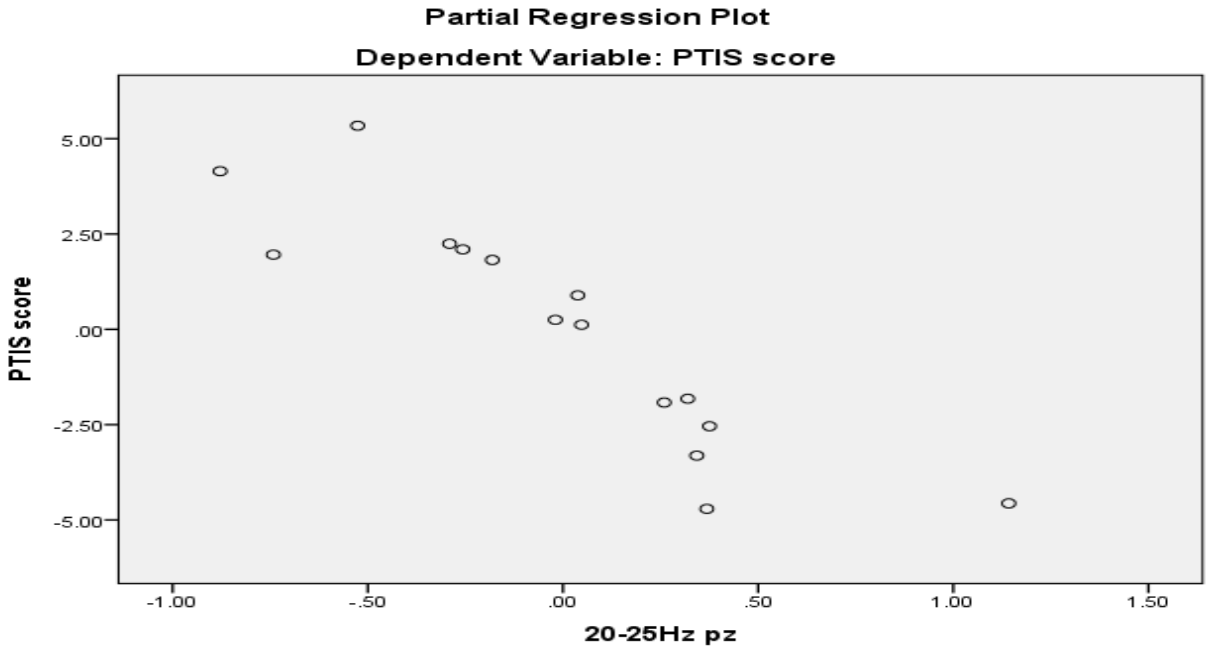

Figure 3.8 Prone to Imaginative and Altered States: 1st Quantitative Electroencephalographic partial plot; decrease in 20-25Hz activity in pz sensor

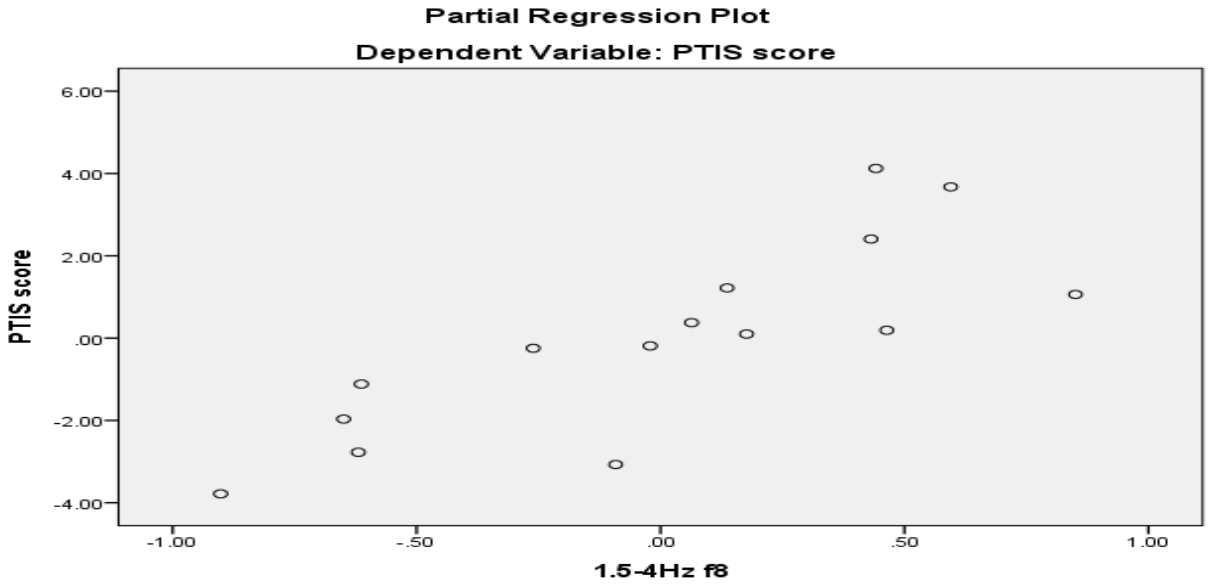

Figure 3.9 Prone to Imaginative and Altered States: 2nd Quantitative Electroencephalographic partial plot: increase in 1.5-4Hz activity in f8 sensor

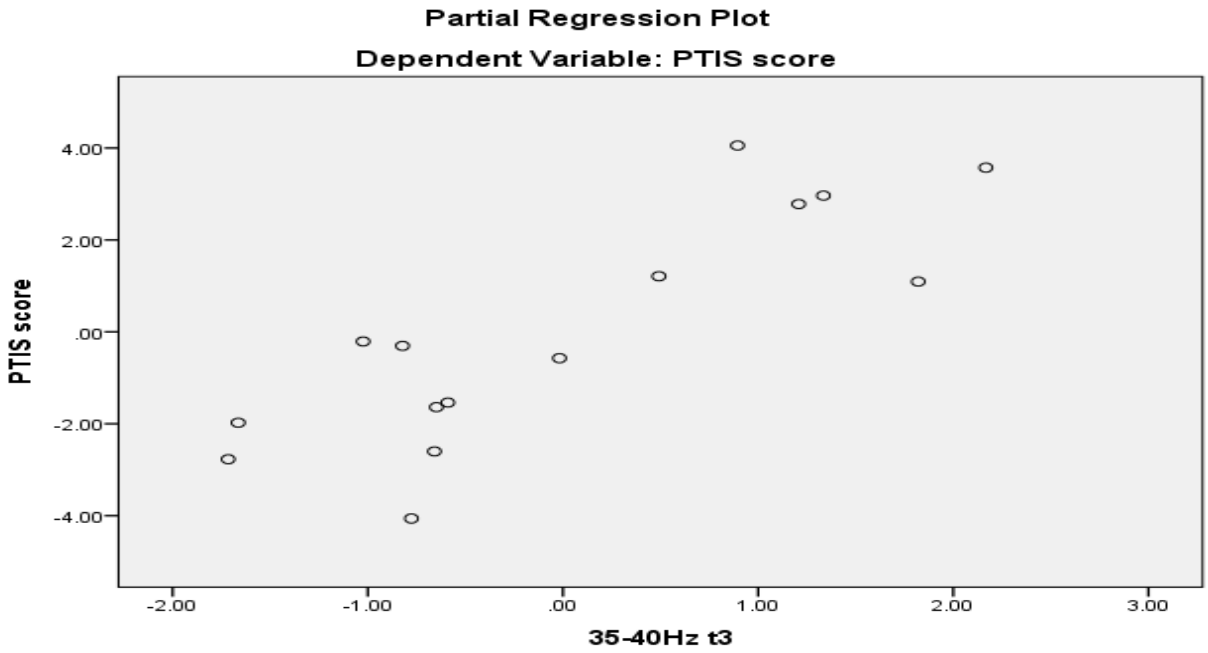

Figure 3.10 Prone to imaginative and Altered States: 3rd partial plot; increase in 35-40Hz activity in t3 sensor

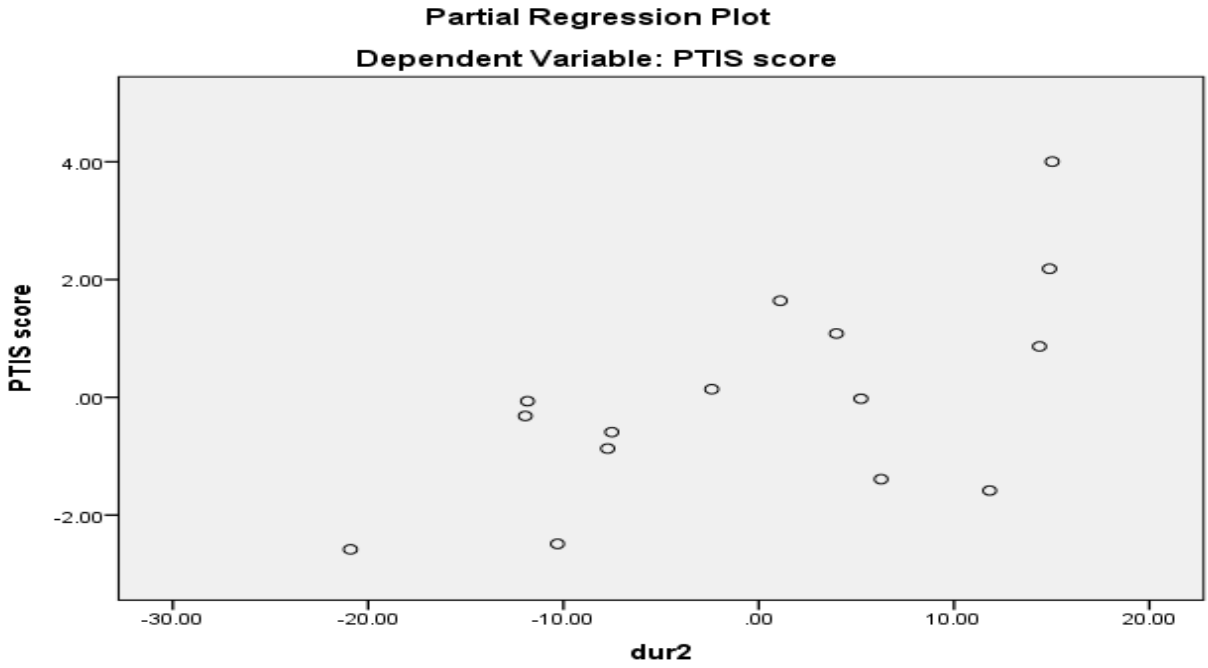

Figure 3.11 Prone to Imaginative and Altered States: 4th Quantitative Electroencephalographic partial plot: increase in the duration of microstate B

3.3.5 Factor 1: Responsive to Engaging Stimuli Partial Plots

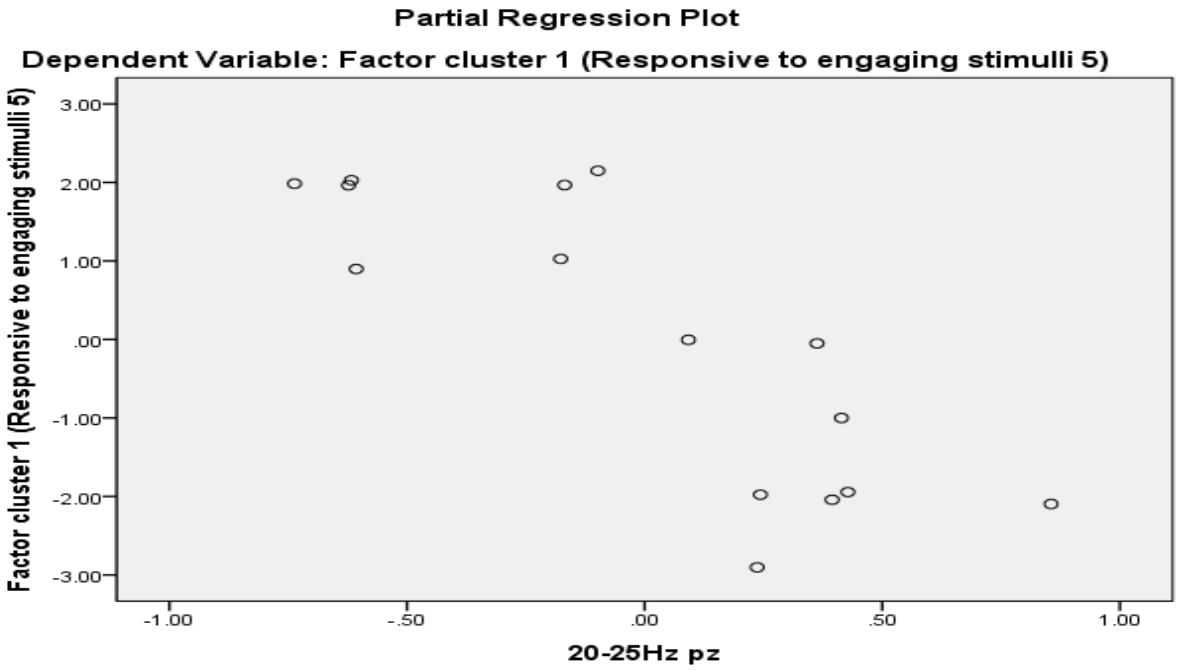

Figure 3.12 Responsive to Engaging Stimuli: 1st Quantitative Electroencephalographic partial plot: Decrease in 20-25Hz activity in the pz sensor

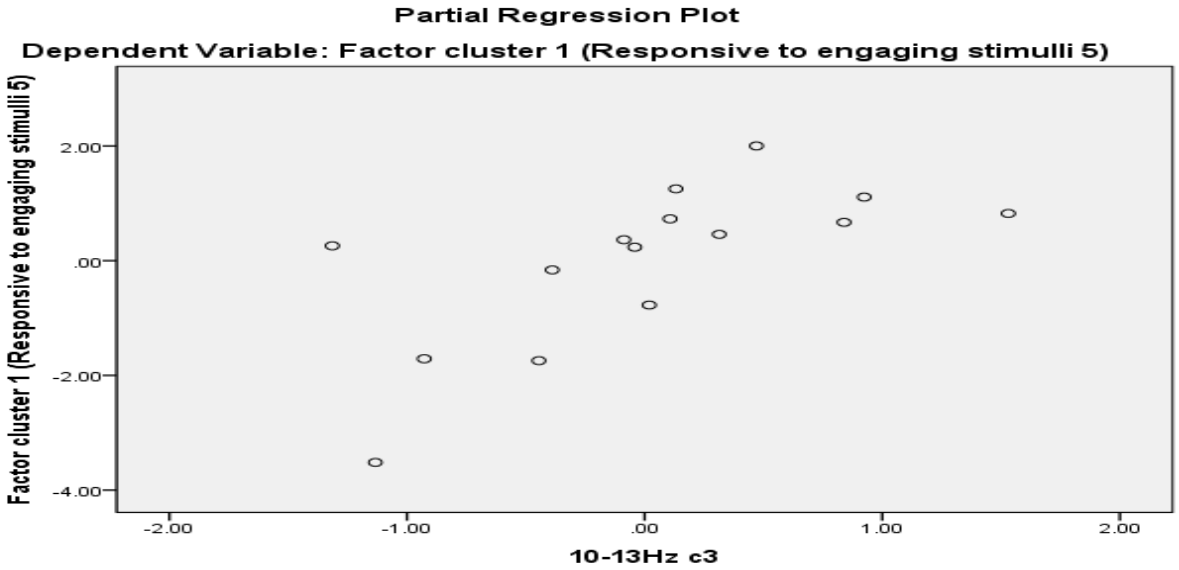

Figure 3.13 Responsive to Engaging Stimuli: 2nd Quantitative Electroencephalographic partial plot: increase in 10-13Hz activity in the c3 sensor

3.3.6 Factor 2: Synesthesia Partial Plots

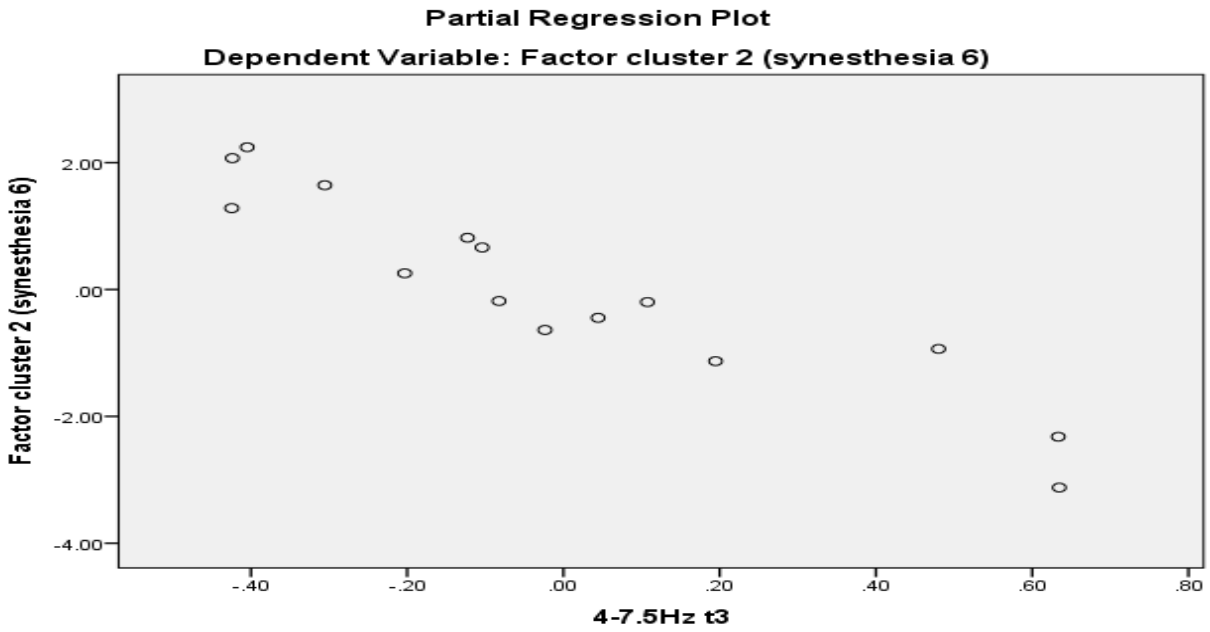

Figure 3.14 Synesthesia: 1st Quantitative Electroencephalographic partial plot; decrease in 4-7.5Hz activity in the t3 sensor

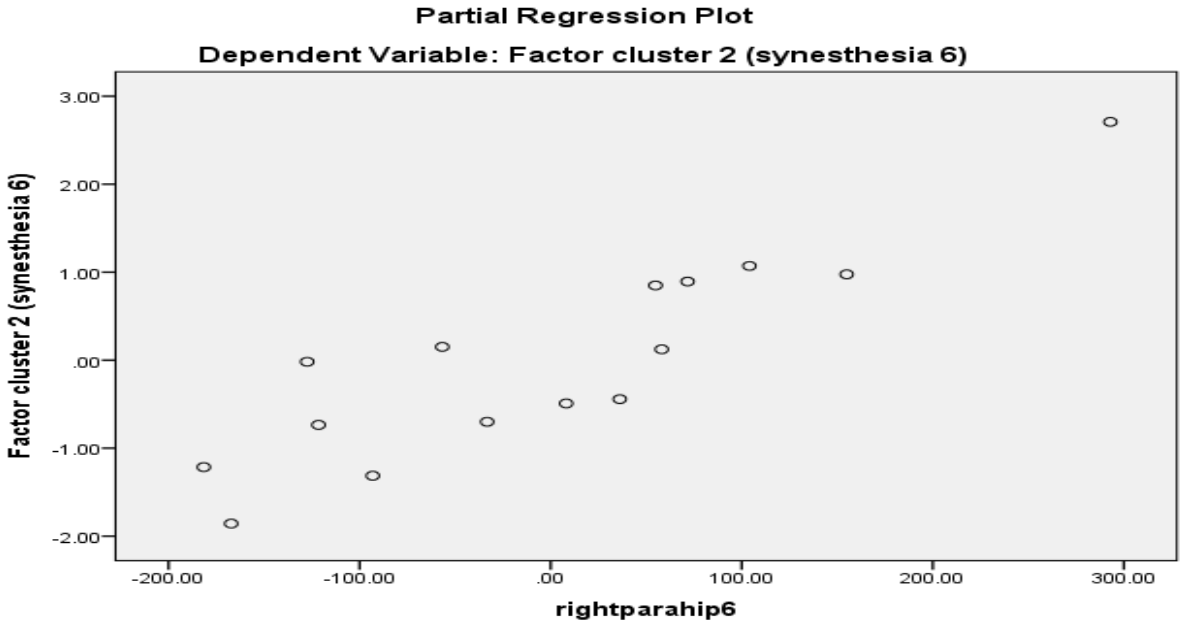

Figure 3.15 Synesthesia: 2nd Quantitative Electroencephalographic partial plot; increase in 20-25Hz activity in the right parahippocampus

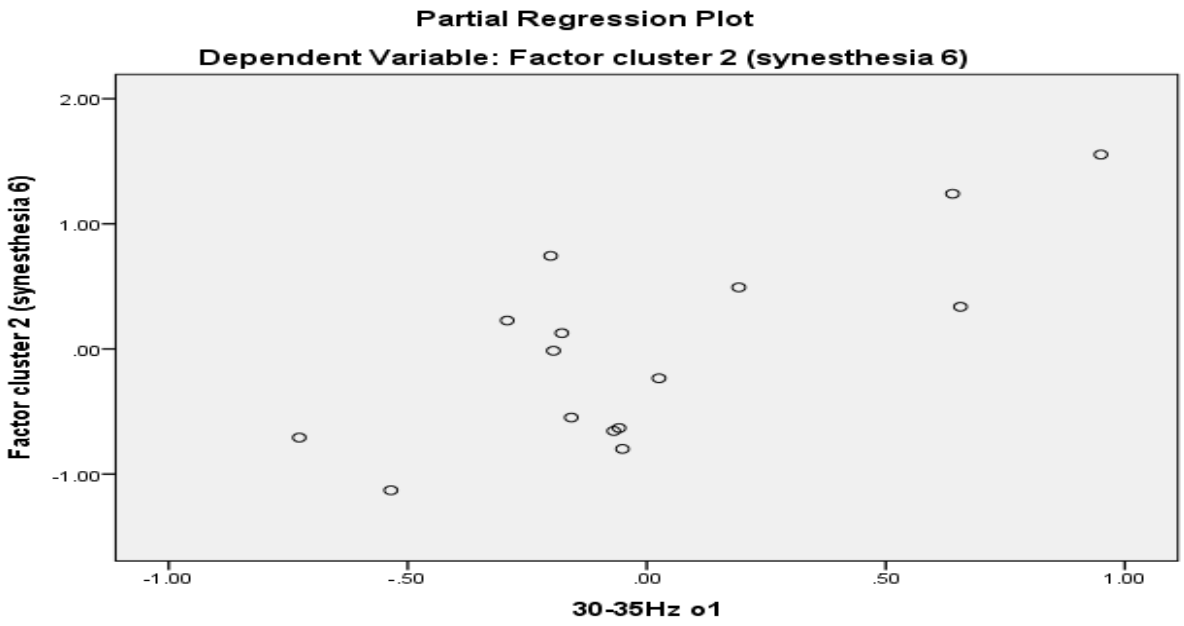

Figure 3.16 Synesthesia: 3rd Quantitative Electroencephalographic partial plot; Increase in 30-35Hz activity in the o1 sensor

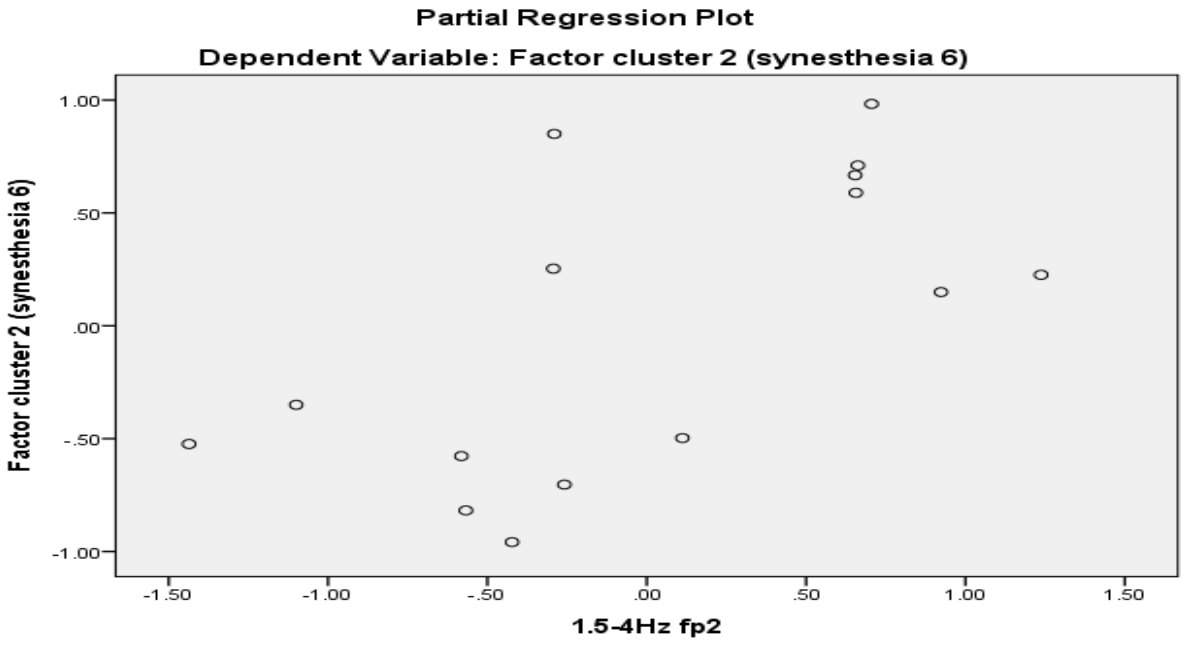

Figure 3.17 Synesthesia: 4th Quantitative Electroencephalographic partial plot; increase in 1.5-4Hz activity in the fp2 sensor

3.3.7 Factor 3: Enhanced Cognition Partial Plots

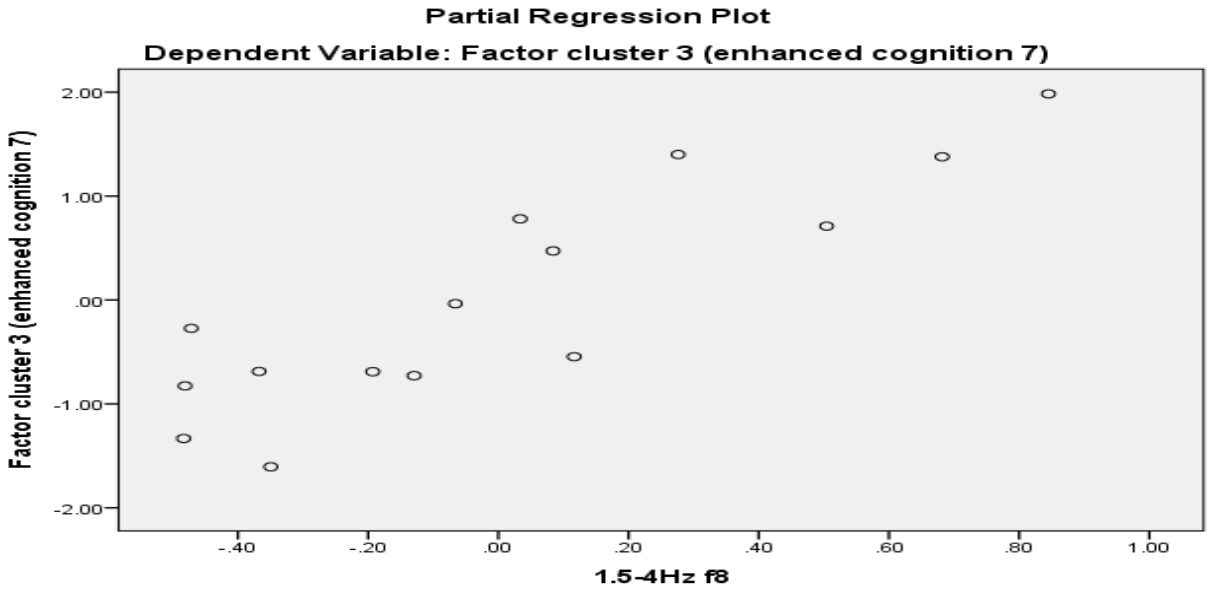

Figure 3.18 Enhanced Cognition: 1st Quantitative Electroencephalographic partial plot; increase in 1.5-4Hz activity in the f8 sensor

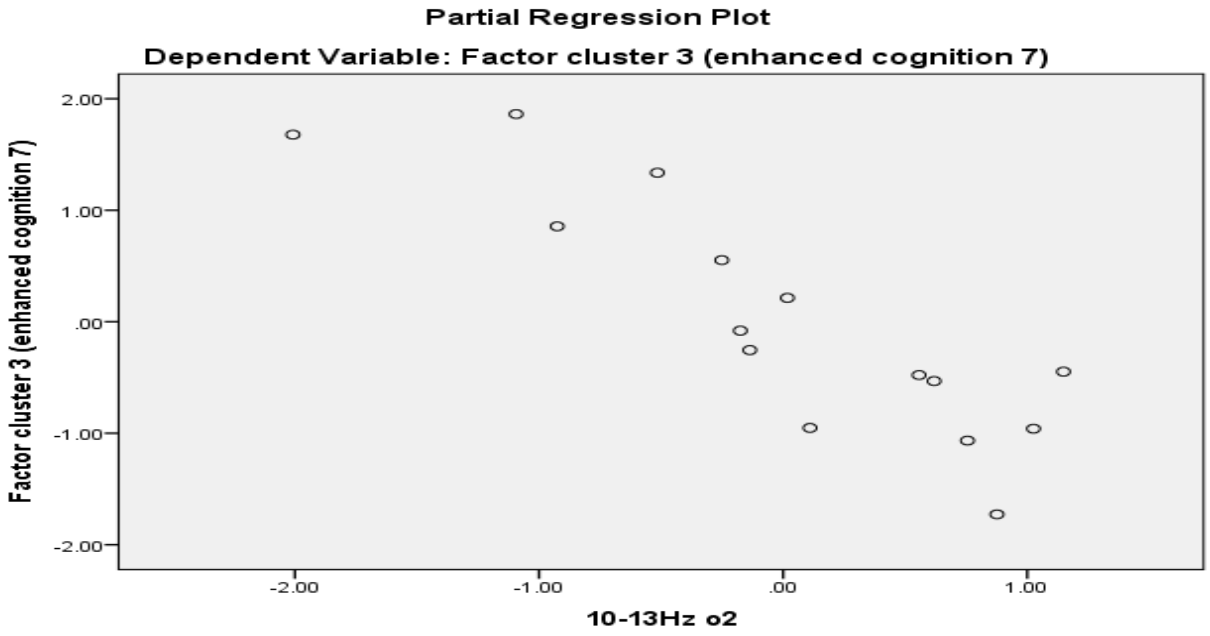

Figure 3.19 Enhanced Cognition: 2nd Quantitative Electroencephalographic partial plot; decrease in 10-13Hz activity in the o2 sensor

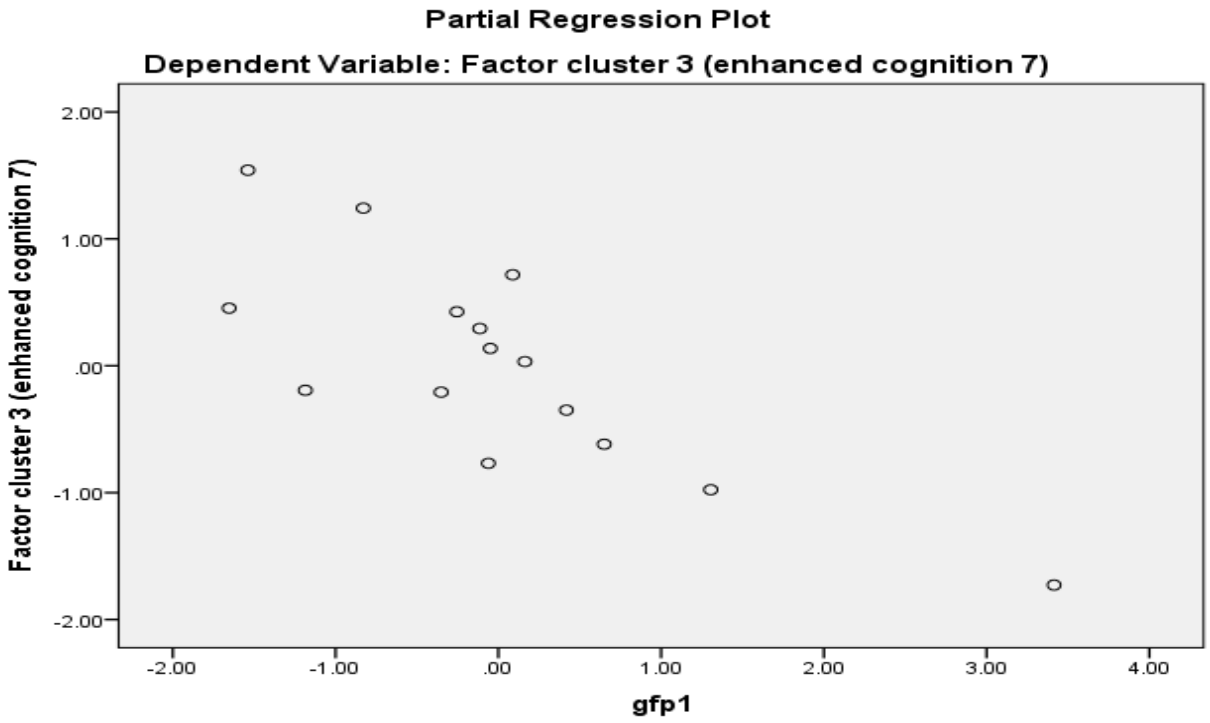

Figure 3.20 Enhanced Cognition: 3rd Quantitative Electroencephalographic partial plot; decrease in the number of global field potential peaks for microstate class A

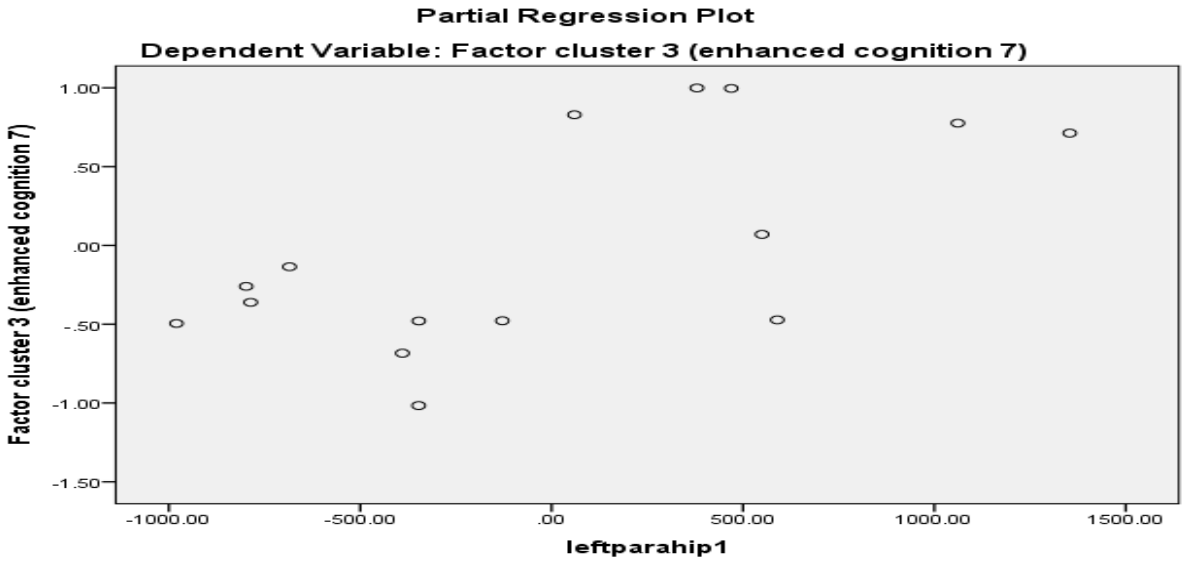

Figure 3.21 Enhanced Cognition: 4th Quantitative Electroencephalographic partial plot; increase in 1.5-4Hz activity within the left parahippocampus

3.3.8 Factor 5: Vivid Reminiscence Partial Plots

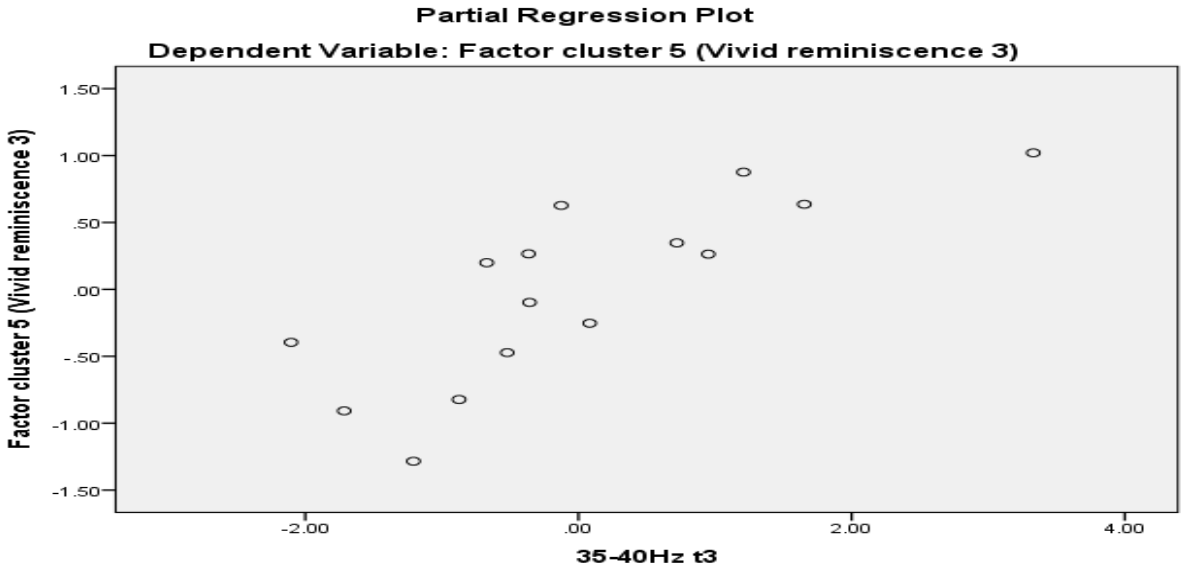

Figure 3.22 Vivid Reminiscence: 1st Quantitative Electroencephalographic partial plot; increase in 35-40Hz activity in the t3 sensor

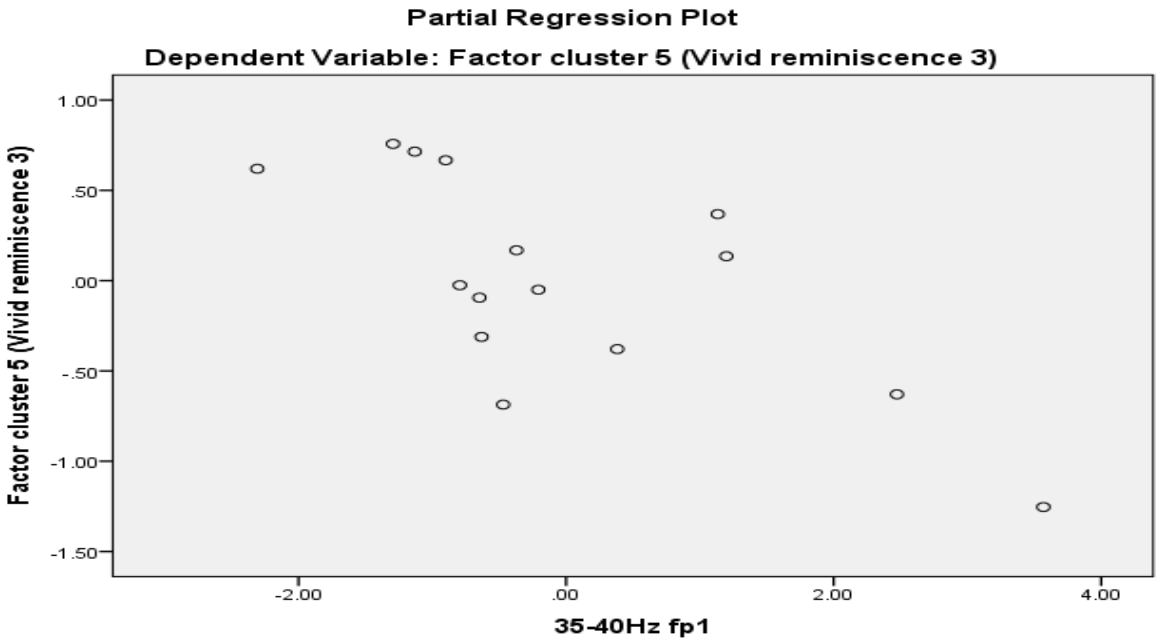

Figure 3.23 Vivid Reminiscence: 2nd Quantitative Electroencephalographic partial plot:; decrease in 35-40Hz activity in the fp1 sensor

3.3.9 Factor 6: Enhanced Awareness Partial Plots

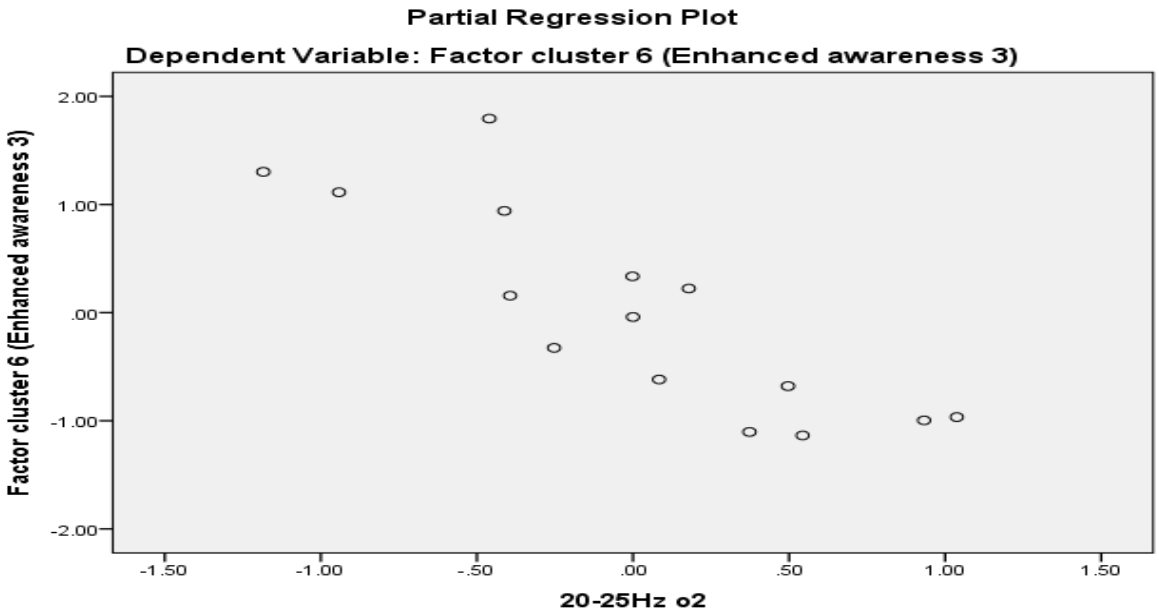

Figure 3.24 Enhanced Awareness: 1st Quantitative Electroencephalographic partial plot; decrease in 20-25Hz activity in the o2 sensor

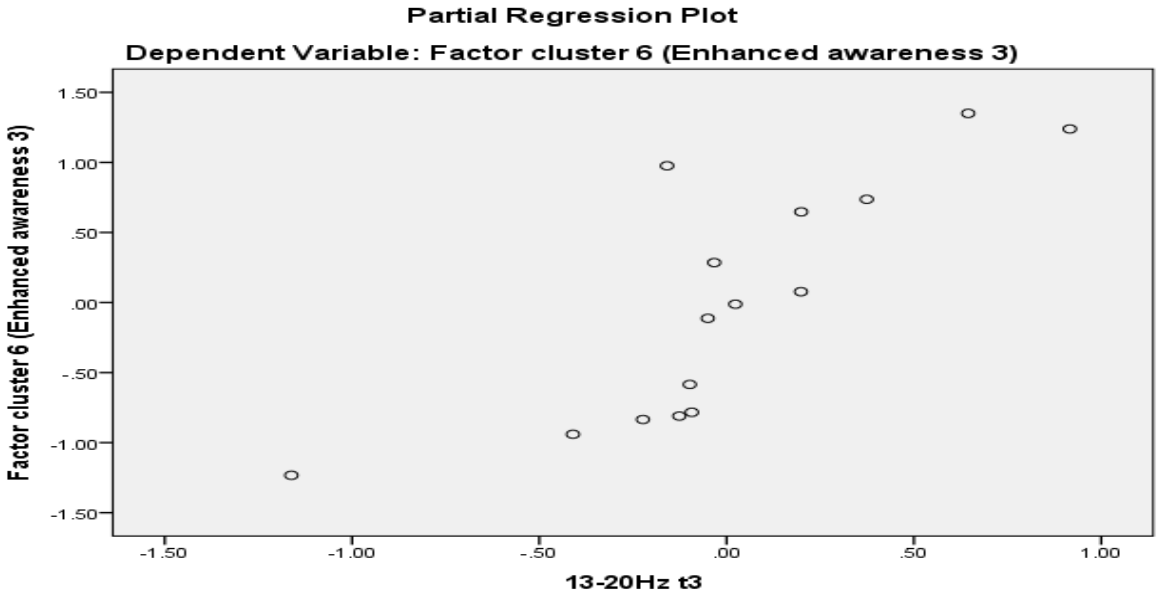

Figure 3.25 Enhanced Awareness: 2nd Quantitative Electroencephalographic partial plot; increase in 13-20Hz activity in the t3 sensor

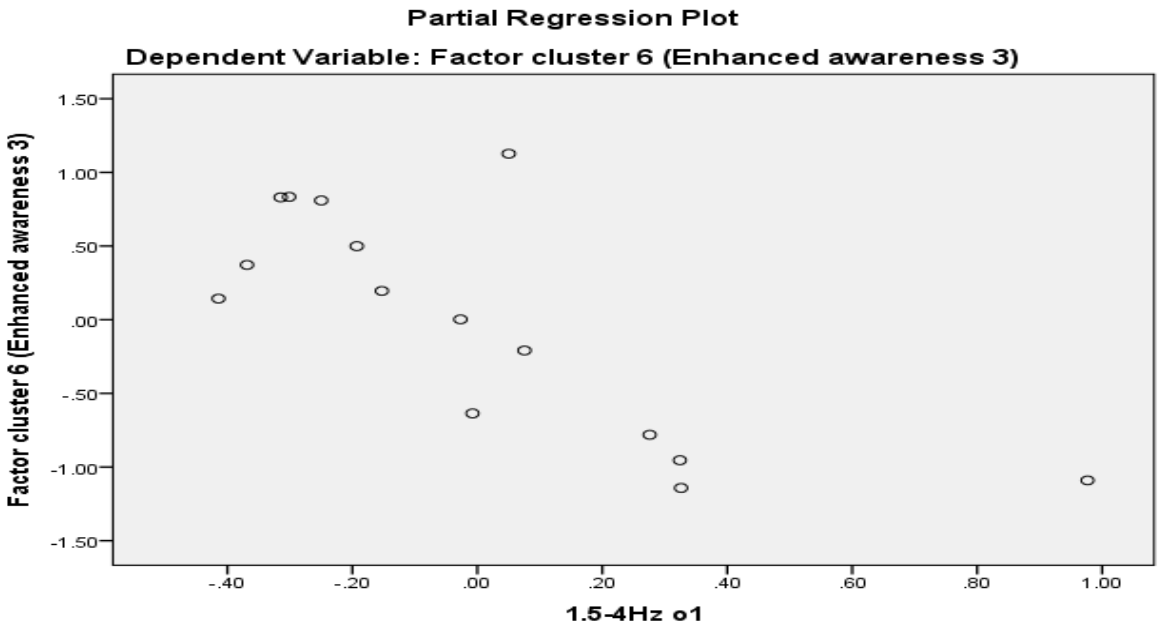

Figure 3.26 Enhanced Awareness: 3rd Quantitative Electroencephalographic partial plot; decrease in 1.5-4Hz activity in the o1 sensor

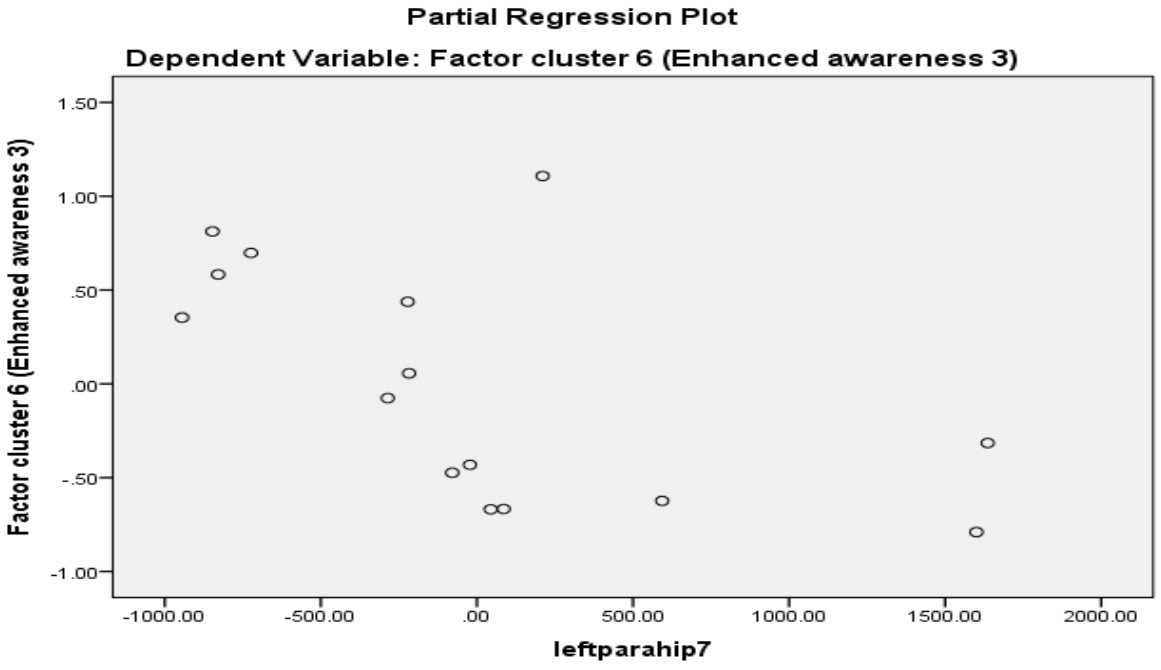

Figure 3.27 Enhanced Awareness: 4th Quantitative Electroencephalographic partial plot; decrease in 25-30Hz activity in the left parahippocampus

3.3.10 Content Cluster 2: Responsive to Inductive Stimuli Partial Plots

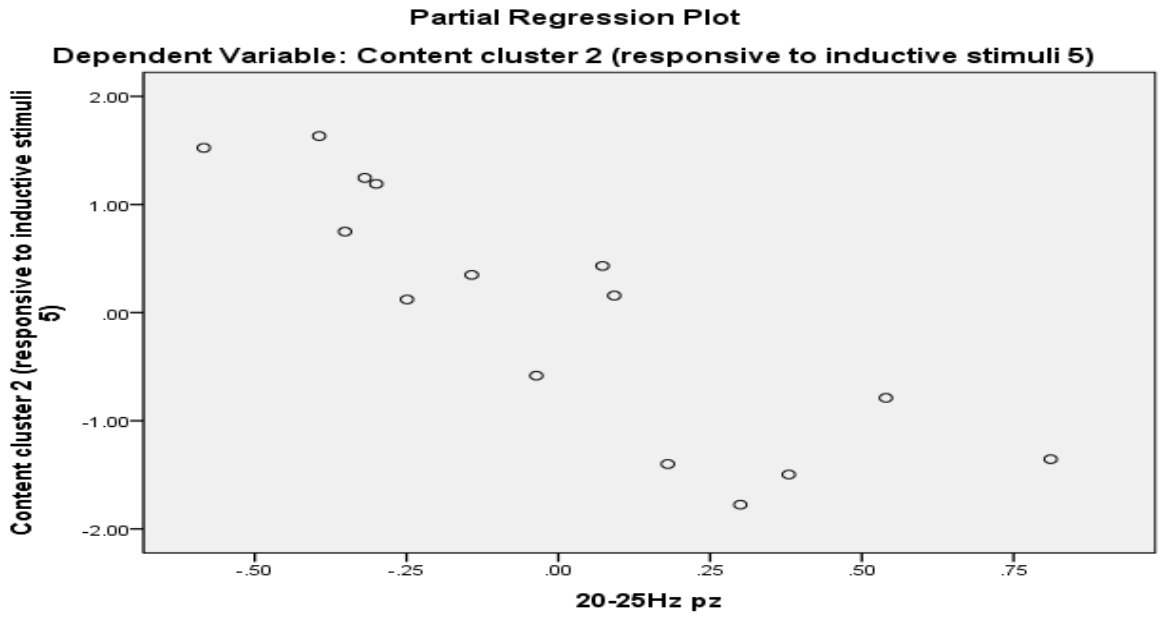

Figure 3.28 Responsive to Inductive Stimuli: 1st Quantitative Electroencephalographic partial plot; decrease in 20-25Hz activity in the pz sensor

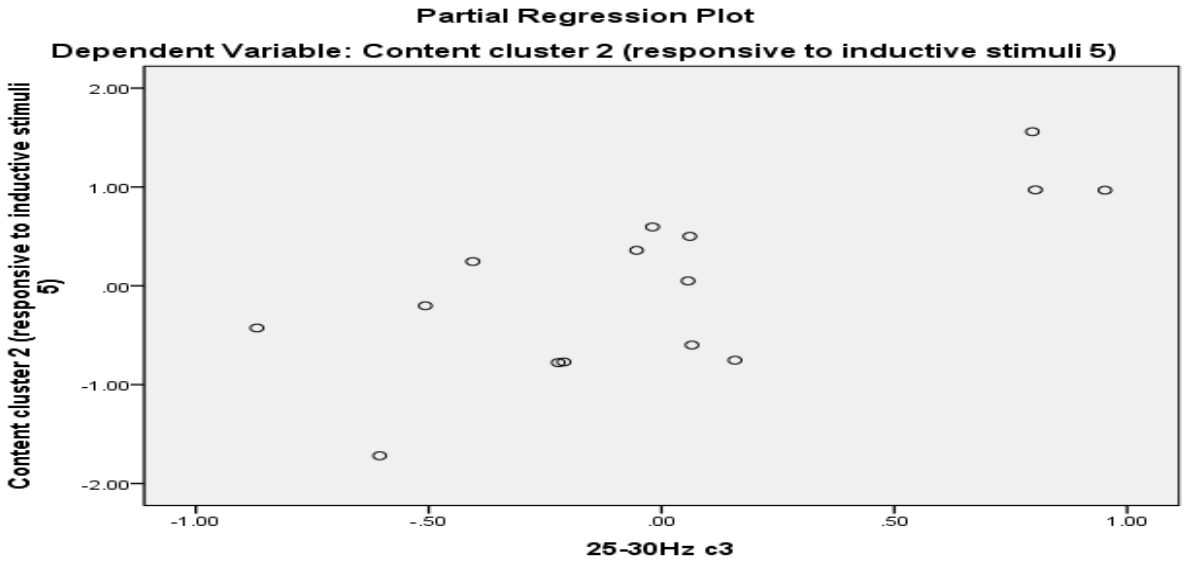

Figure 3.29 Responsive to Inductive Stimuli: 2nd Quantitative Electroencephalographic partial plot; increase in 25-30Hz activity in the c3 sensor

3.3.11 Content Cluster 3: Often Thinks In Images Partial Plots

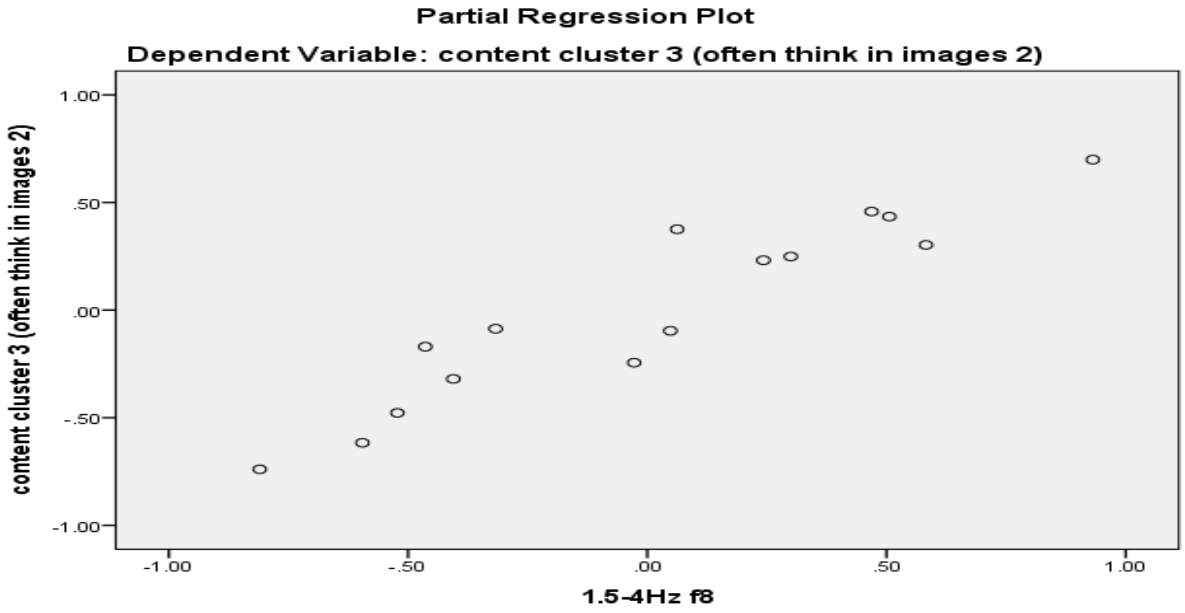

Figure 3.30 Often Thinks in Images: 1st Quantitative Electroencephalographic partial plot; increase in 1.5-4Hz activity in the f8 sensor

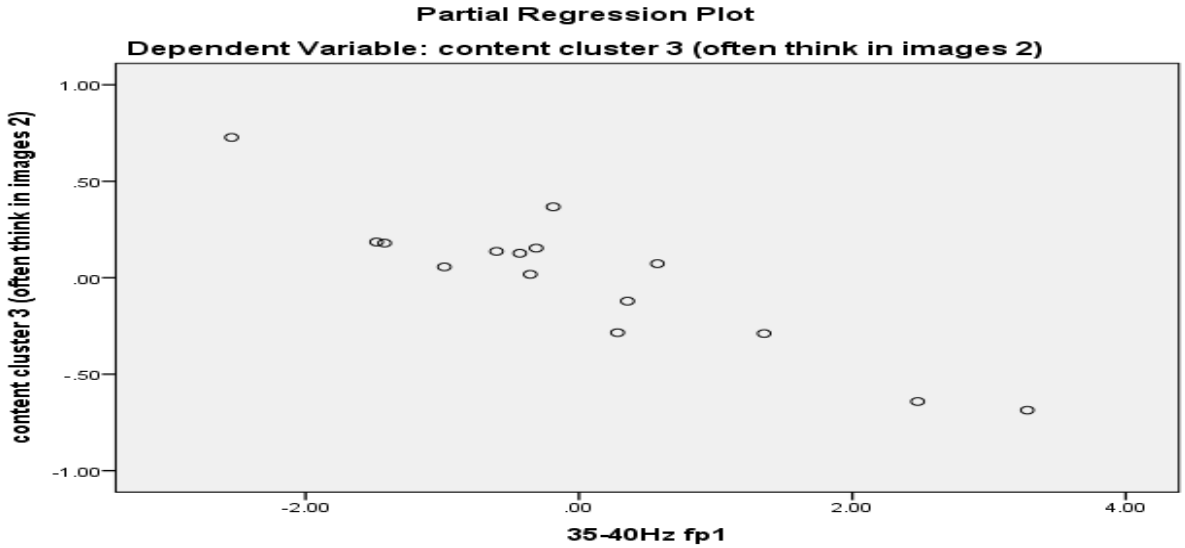

Figure 3.31 Often Thinks in Images: 2nd Quantitative Electroencephalographic partial plot; decrease in 35-40Hz activity in the fp1 sensor

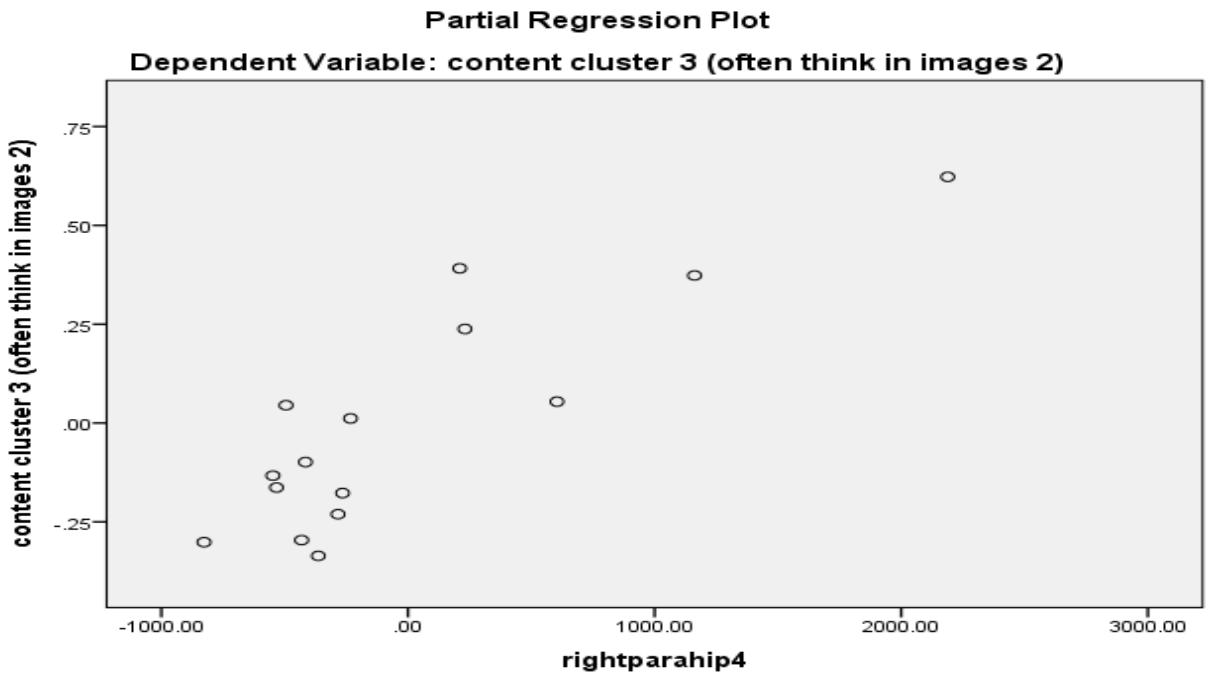

Figure 3.32 Often Thinks in Images: 3rd Quantitative Electroencephalographic partial plot; increase in 10-13Hz activity in the right parahippocampus

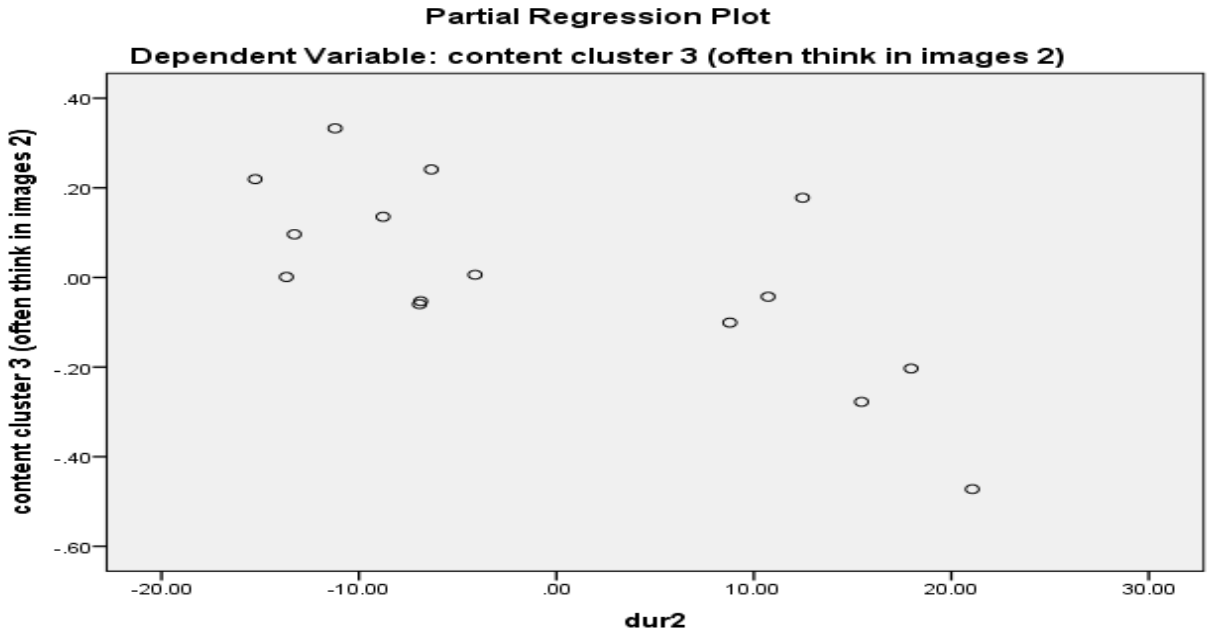

Figure 3.33 Often Thinks in Images: 4th Quantitative Electroencephalographic partial plot; decrease in the duration of microstate B

3.3.12 Content Cluster 5: Has "Crossmodal" Experiences Partial Plots

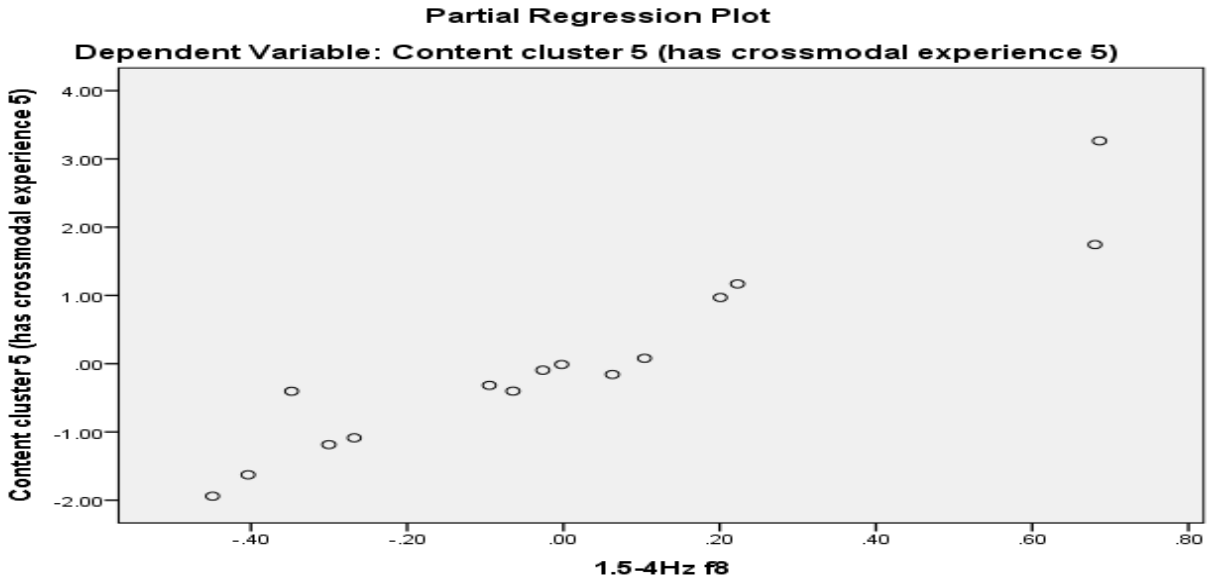

Figure 3.34 Has "Crossmodal" Experience: 1st Quantitative Electroencephalographic partial plot; increase in 1.5-4Hz activity in the f8 sensor

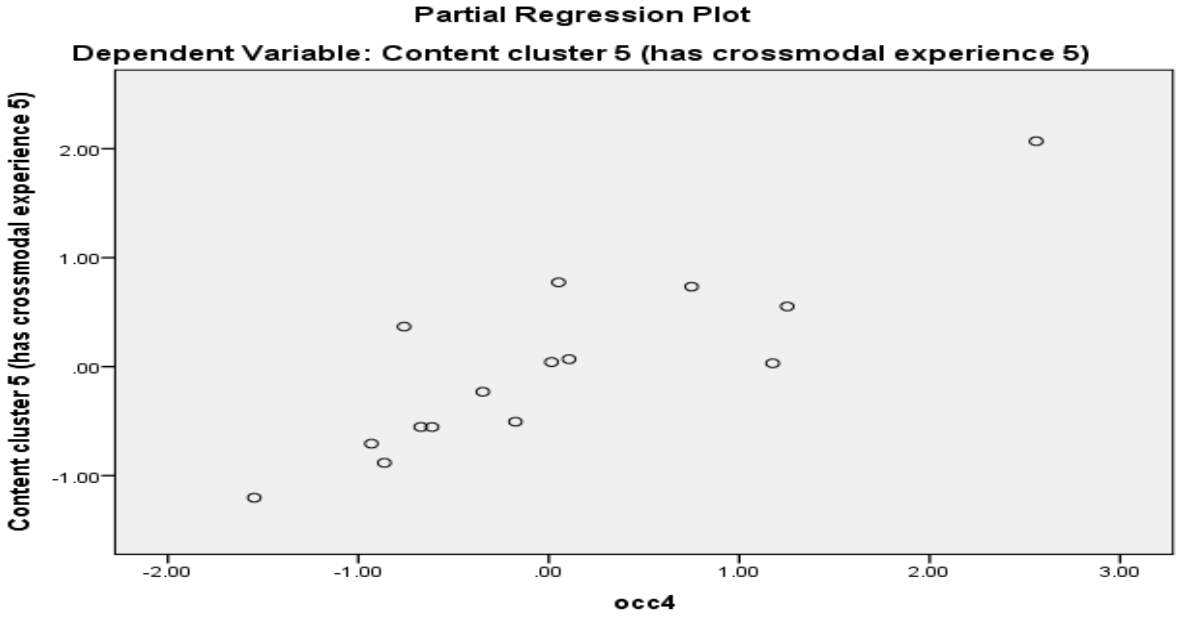

Figure 3.35 Has "Crossmodal" Experience: 2nd Quantitative Electroencephalographic partial plot; increase in the number of times that microstate D occurred

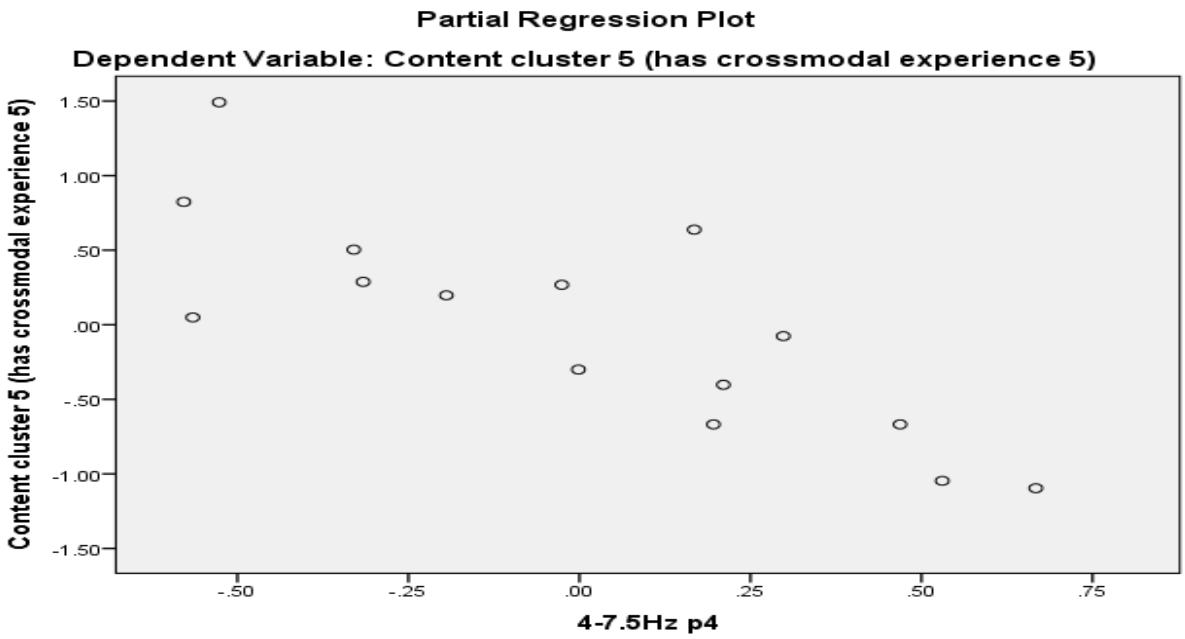

Figure 3.36 Has "Crossmodal" Experience: 3rd Quantitative Electroencephalographic partial plot; decrease in 4-7.5Hz activity in the p4 sensor

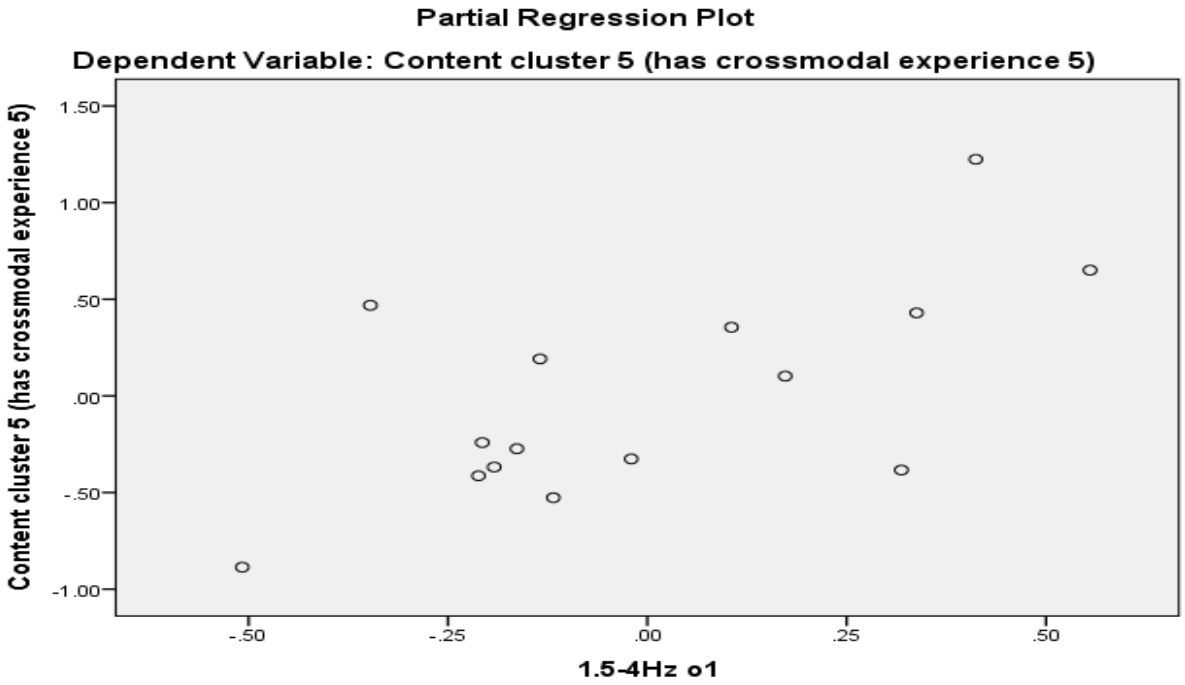

Figure 3.37 Has "Crossmodal" Experience: 4th Quantitative Electroencephalographic partial plot; increase in 1.5-4Hz activity in the o1 sensor

3.3.13 Content Cluster 6: Can Become Absorbed in Own Thoughts and Imaginings Partial Plots

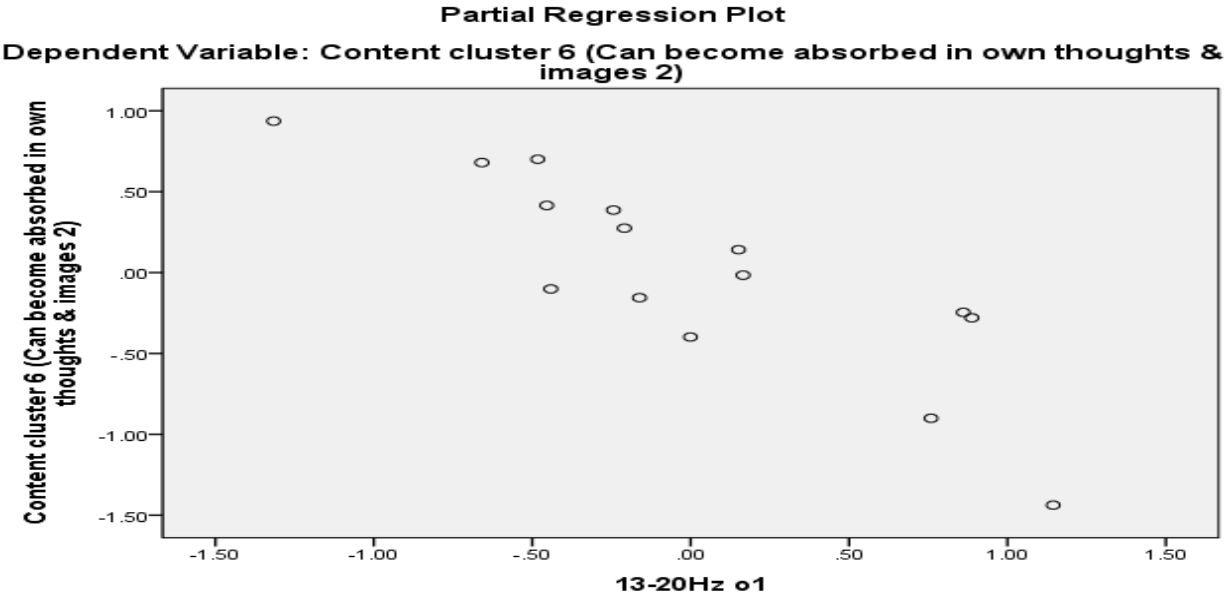

Figure 3.38 Can Become Absorbed in Own Thoughts and Imaginings: 1st Quantitative Electroencephalographic partial plot; decrease in 13-20Hz activity in the o1 sensor

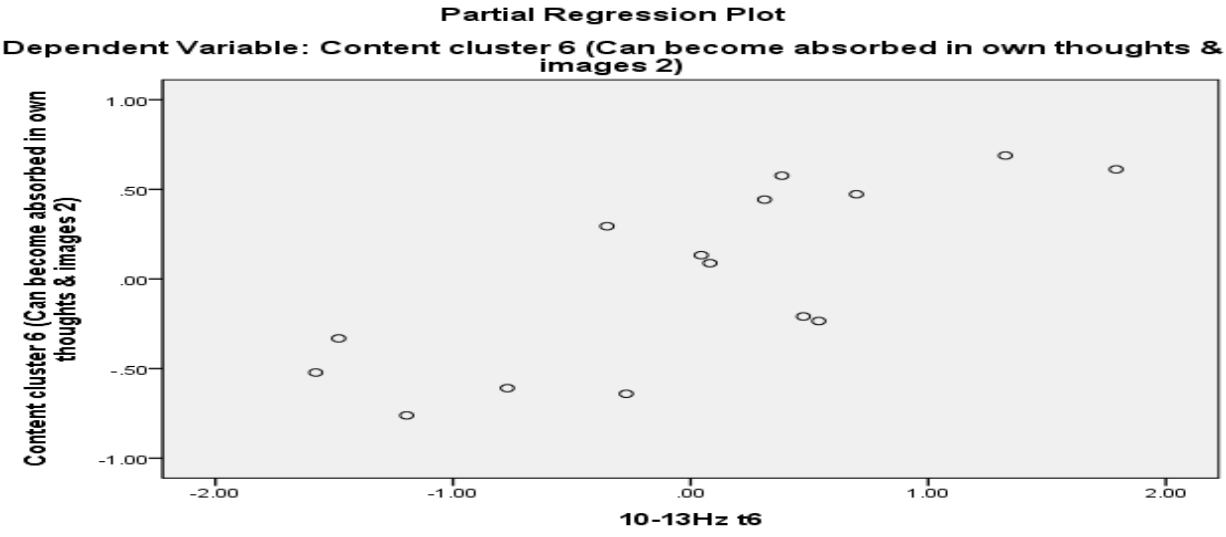

Figure 3.39 Can Become Absorbed in Own Thoughts and Imaginings: 2nd Quantitative Electroencephalographic partial plot; increase in 10-13Hz activity in the t6 sensor

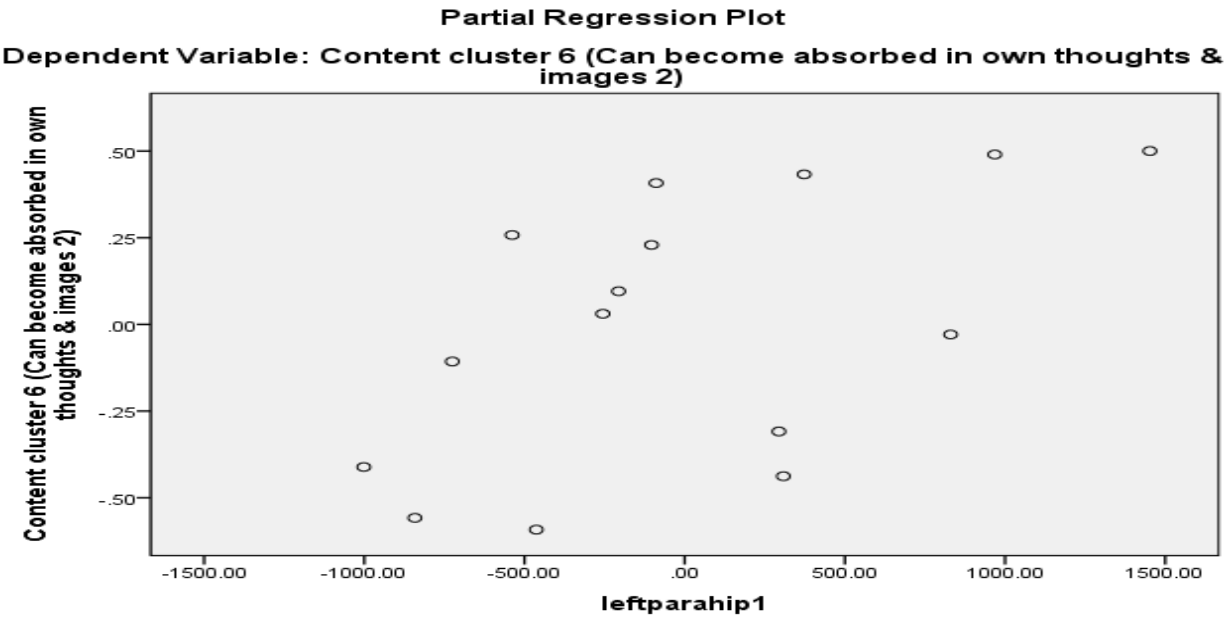

Figure 3.40 Can Become Absorbed in Own Thoughts and Imaginings: 3rd Quantitative Electroencephalographic partial plot; increase in 1.5-4Hz activity in the left parahippocampus

3.3.14 Content Cluster 7: Can Vividly Re-experience The Past Partial Plots

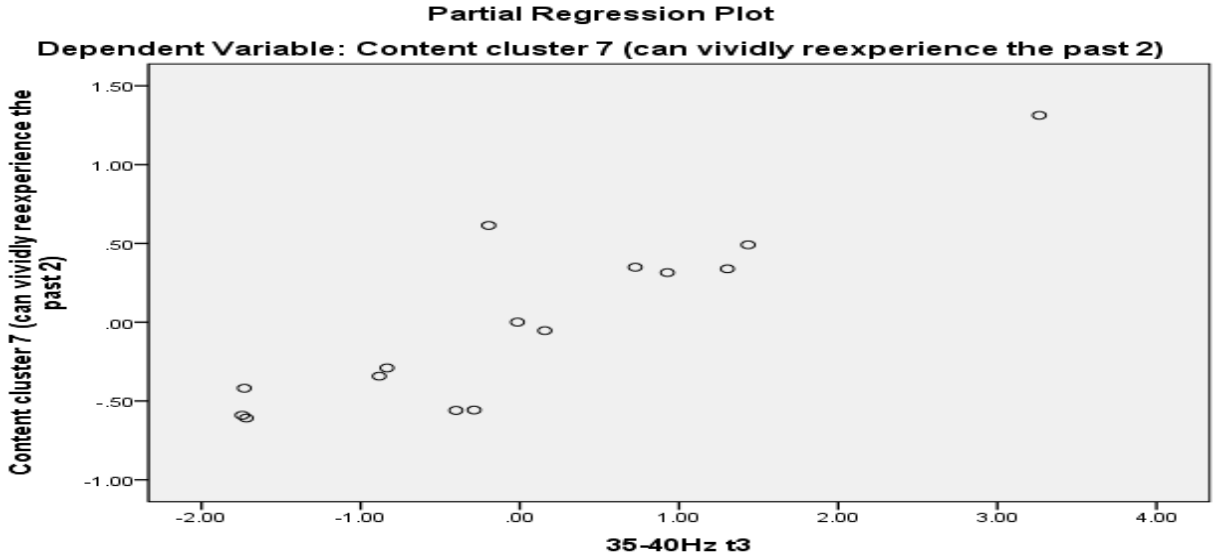

Figure 3.41 Can Vividly Re-experience The Past: 1st Quantitative Electroencephalographic partial plot; increase in 35-40Hz activity in the t3 sensor

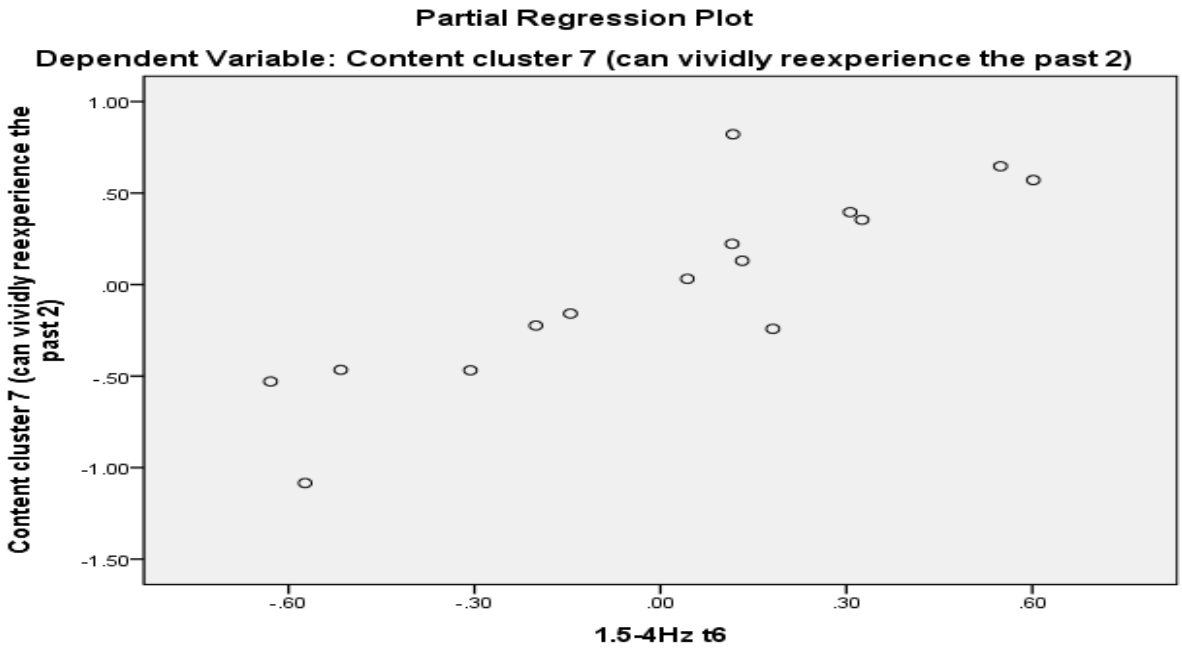

Figure 3.42 Can Vividly Re-experience The Past: 2nd Quantitative Electroencephalographic partial plot; increase in 1.5-4Hz activity in the t6 sensor

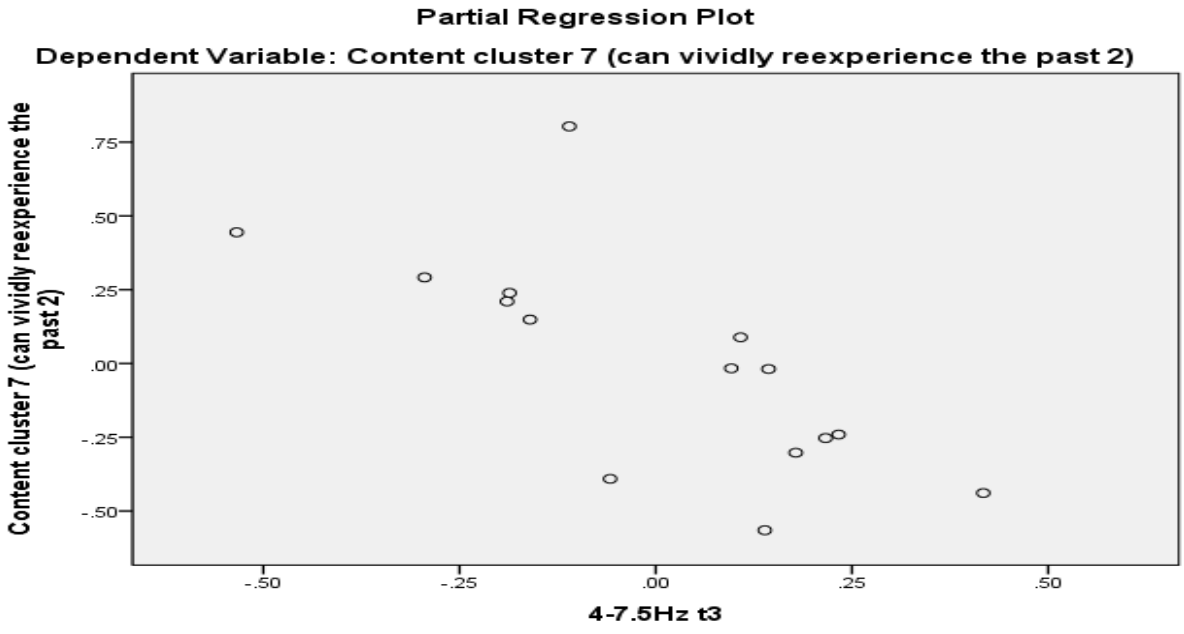

Figure 3.43 Can Vividly Re-experience The Past: 3rd Quantitative Electroencephalographic partial plot; decrease in 4-7.5Hz activity in the t3 sensor

3.3.15 Content Cluster 8: Has Episodes Of Expanded Awareness Partial Plots

Figure 3.44 Has Episodes of Expanded Awareness: 1st Quantitative Electroencephalographic partial plot; decrease in the number of Global Field Potential peaks for microstate A

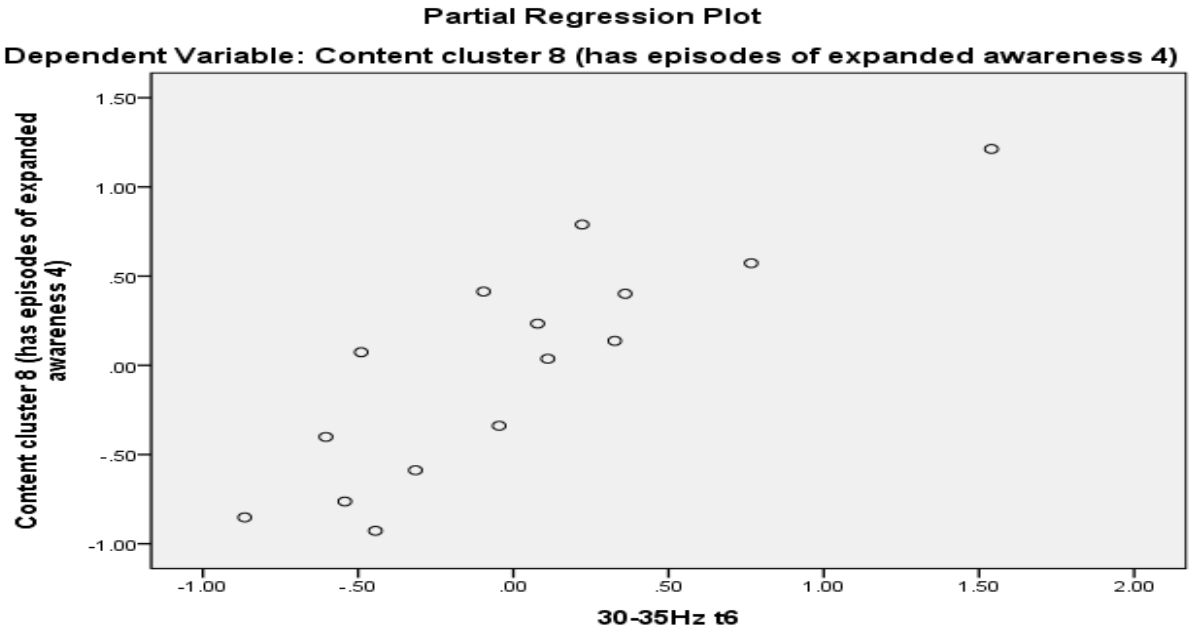

Figure 3.45 Has Episodes of Expanded Awareness: 2nd Quantitative Electroencephalographic partial plot; increase in 30-35Hz activity in the t6 sensor

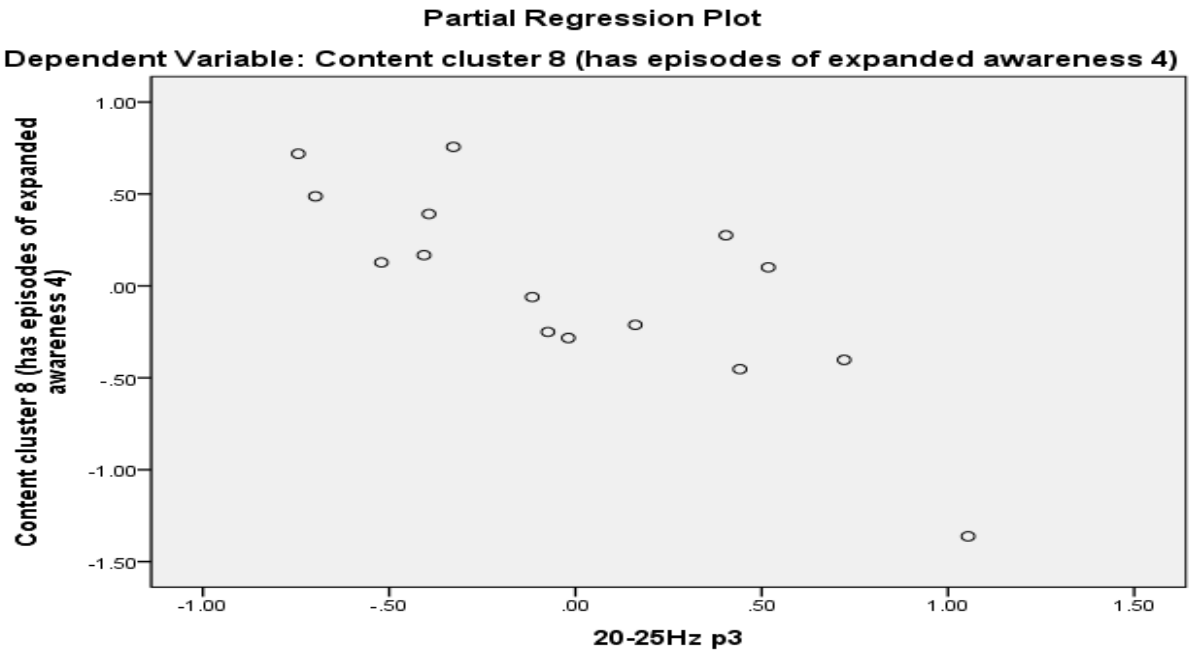

Figure 3.46 Has Episodes of Expanded Awareness: 3rd Quantitative Electroencephalographic partial plot; decrease in 20-25Hz activity in the p3 sensor

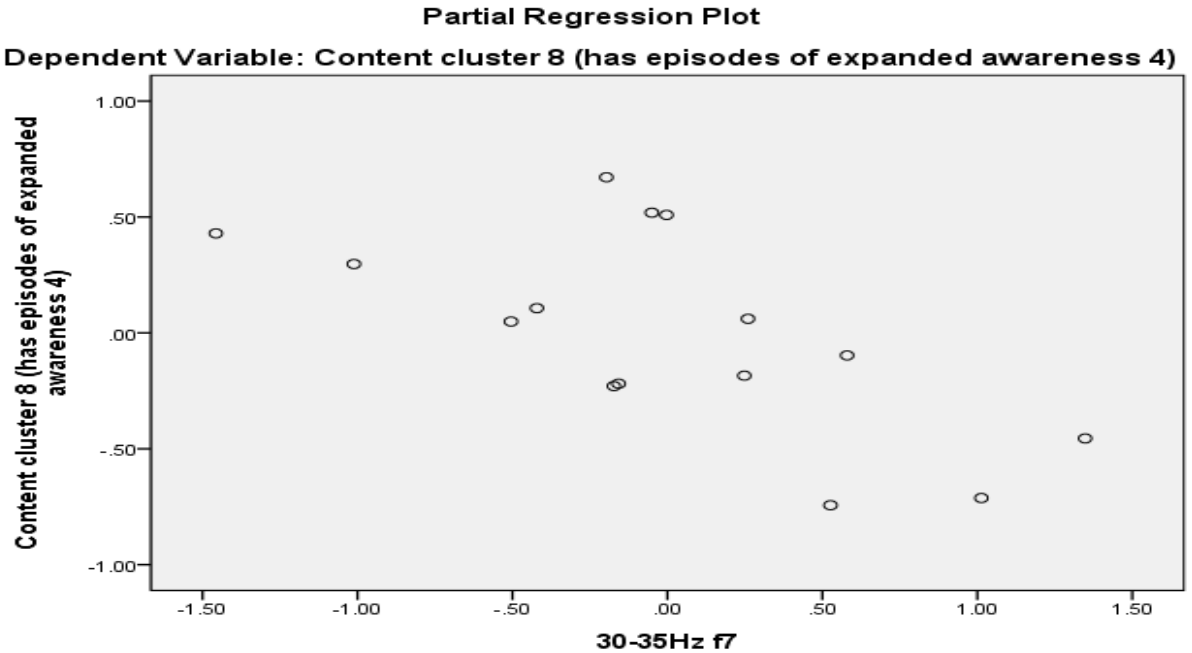

Figure 3.47 Has Episodes of Expanded Awareness: 4th Quantitative Electroencephalographic partial plot; decrease in 30-35Hz activity in the f7 sensor

3.3.16 Content Cluster 9: Experiences Altered States of Consciousness Partial Plots

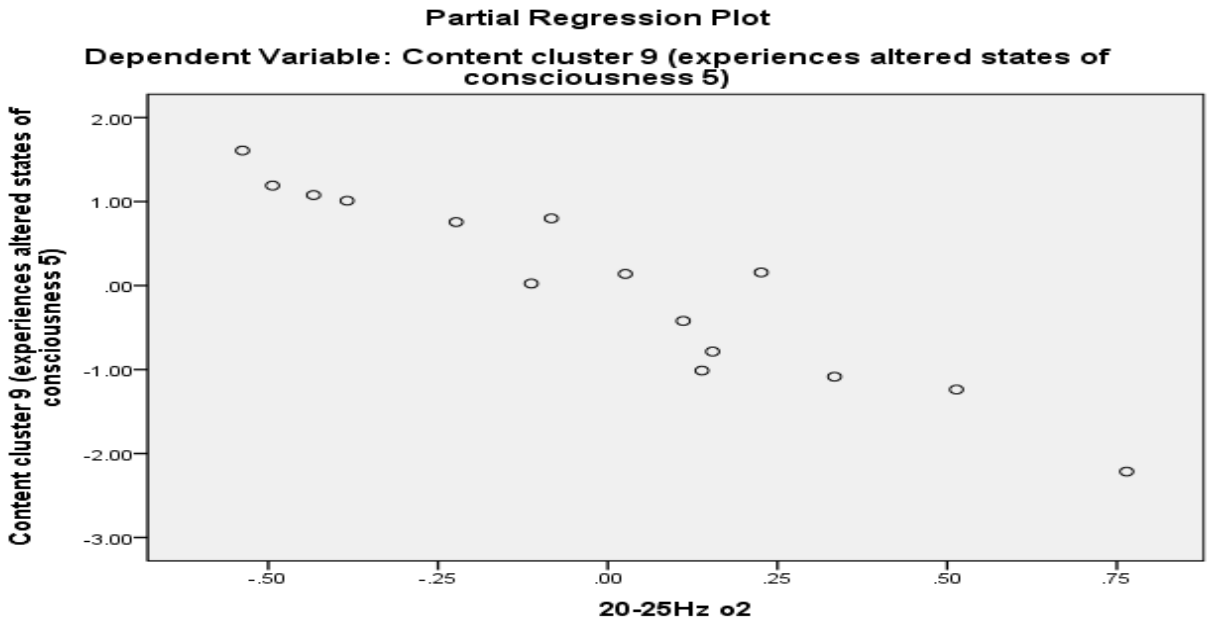

Figure 3.48 Experiences Altered States of Consciousness: 1st Quantitative Electroencephalographic partial plot; decrease in 20-25Hz activity in the o2 sensor

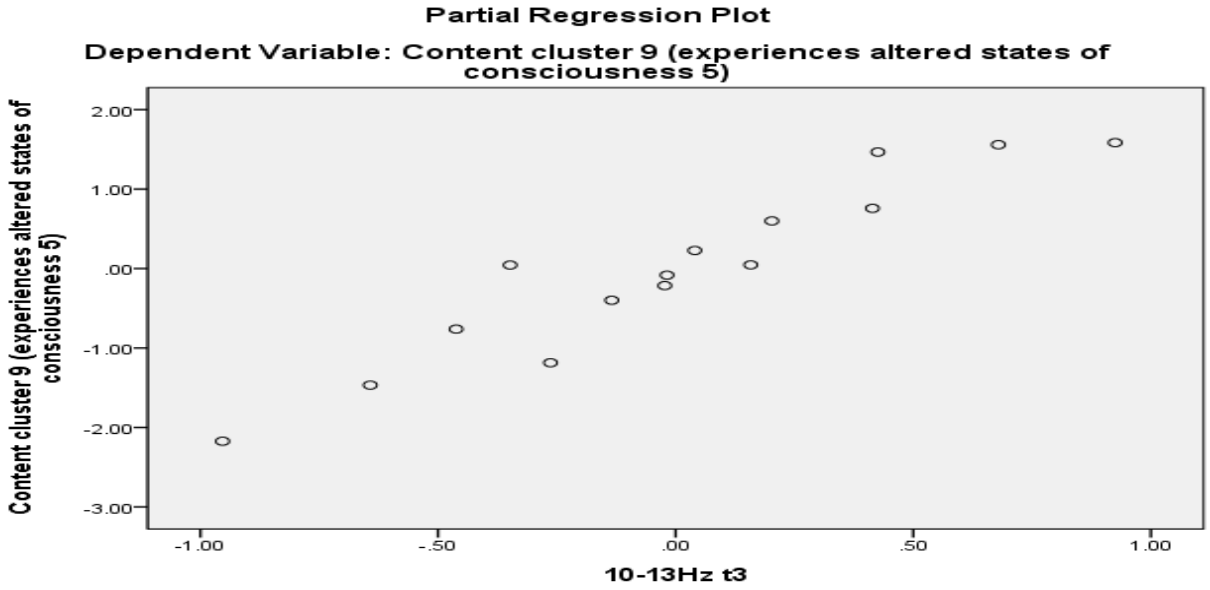

Figure 3.49 Experiences Altered States of Consciousness: 2nd Quantitative Electroencephalographic partial plot; increase in 10-13Hz activity in the t3 sensor

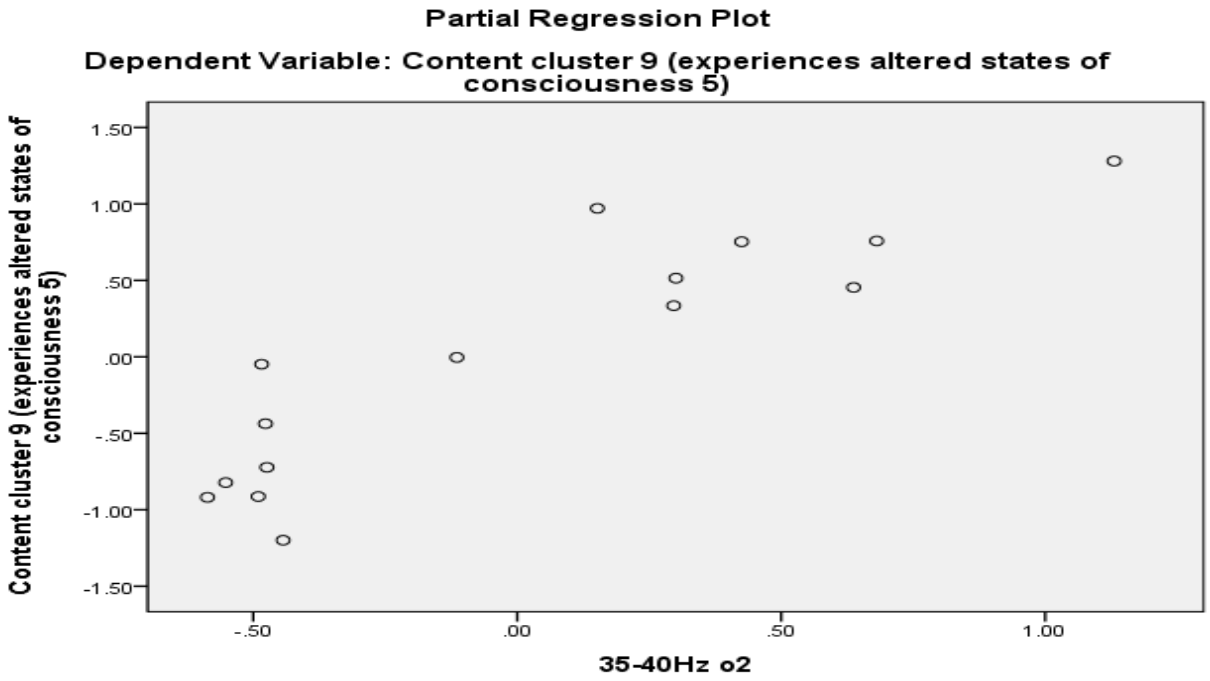

Figure 3.50 Experiences Altered Sates of Consciousness: 3rd Quantitative Electroencephalographic partial plot; increase in 35-40Hz activity in the o2 sensor

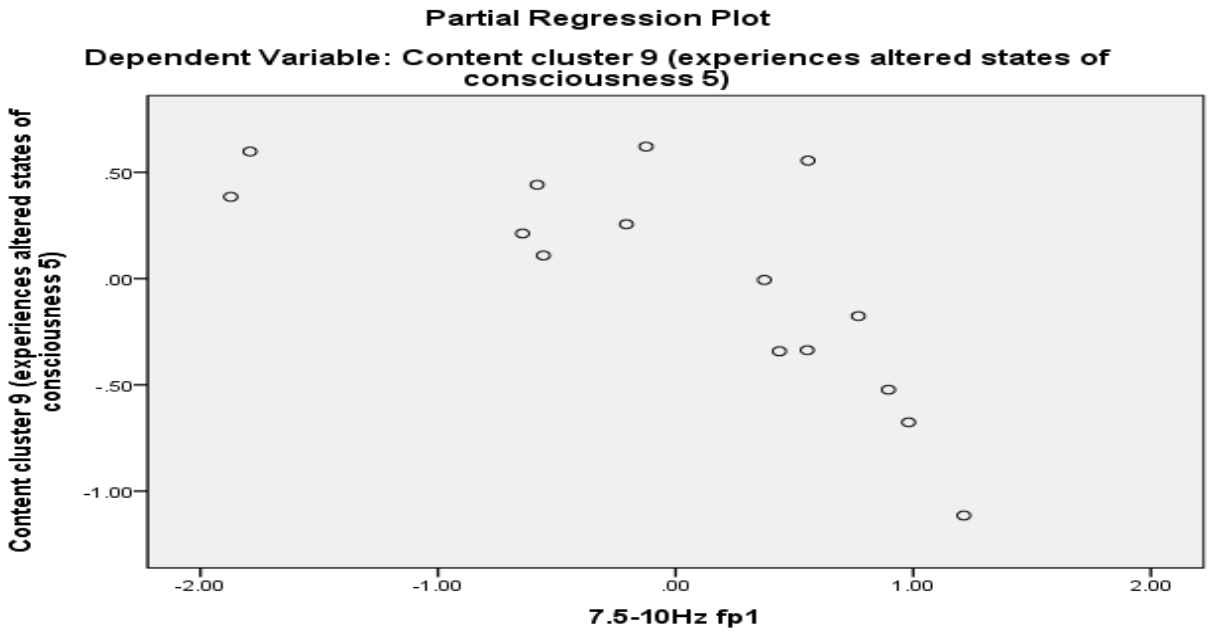

Figure 3.51 Experiences Altered Sates of Consciousness: 4th Quantitative Electroencephalographic partial plot; decrease in 7.5-10Hz activity in the fp1 sensor

These multiple regression results yielded a QEEG predictive equation for 17/18 of the TAS scales and subscales. The results can be observed in Table-3.17.

Table 3.17 Quantitative Electroencephalographic equation variables which predict Tellegen Absorption Scales and subscales

TAS Scale/subscale	QEEG Equation variable
Absorption ability Index	predAII=-15.26 (20-25Hz pz) + 9.29 (1.5-4Hz f8) + 9.98 (20-25Hz c3) -2.04 (7.5-10Hz f8)
Sentient	predsentience== -4.16 (20-25 Hz p3) +1.36 (10-13 Hz fp1) +7.29
Prone to altered and Imaginary States	predPTIS=-5.37 (20-25 Hz pz) + 3.60 (1.5-4 Hz f8) + 1.70 (35-40 Hz t3) + .10 (duration of microstate B) + 1.37
Responsive to Engaging Stimuli	predRTES=-3.15 (20-25Hz pz) + 1.20 (10-13Hz c3) + 3.29
Synesthesia	predS=-4.04 (4-7.5 Hz t3) + .01 (20-25 Hz right parahippocampus) + 1.3 (30-35 Hz o1) + .53 (1.5-4 Hz fp2).
Enhanced Cognition	predEC= +2.20 (1.5-4Hz f8) -1.06 (10-13Hz o2) -.54 (#GFP peaks for microstate A) + .00 (1.5-4Hz left parahippocampus)
Oblivious/Dissociative Involvement	predODI=-1.57 (20-25Hz pz sensor) + 3.91
Vivid Reminiscence	predVR= +.39 (35-40Hz t3) -.27 (35-40Hz fp1) + .002 (20-25Hz right parahippocampus) + 1.45
Enhanced Awareness	predEA= -1.28 (20-25Hz 02) + 1.45 (13-20Hz t3) -1.58 (1.5-4Hz 01) +.00 (25-30Hz left parahippocampus) + 5.15
Is Responsive To Engaging Stimuli	predIRTES= see predRTES
Is Responsive to Inductive stimuli	predIRTIS= - 2.56 (20-25Hz pz) + 1.18 (25-30Hz c3) + 3.53
Often Thinks in Images	predOTII= + .80 (1.5-4Hz f8) -.22 (35-40Hz fp1) + .00 (10-13Hz right parahippocampus) -.01(duration microstate B) -.02
Can summon vivid and suggestive images	predCSVSI=N/A
Has "crossmodal" experiences	predHCE= + 3.68 (1.5-4Hz f8) + .67 (# of times microstate D appeared) -1.43(4-7.5Hz p4) + 1.18 (1.5-4Hz p4) -10.20
Can Become Absorbed in own thoughts and images	predBAOTI= -.79 (13020Hz 01) + (10-13Hz t6) + .00 (1.5-4Hz left parahippocmapus) + 1.43
Can vividly Re-experience the past	predVRP= + .36 (35-40Hz t3) + 1.5-4Hz t6) – 1.08 (4-7.5Hz t3) -.01
Has Episodes of expanded awareness	predEEA= -.28 (#GFP peaks for microstate A) +.89 (30-35Hz t6) -.79 (20-25Hz p3) -.40 (30-35Hz f7) + 4.27
Experiences Altered States of Consciousness	predEASC= -2.75 (20-25Hz 02) + 2.10 (10-13Hz t3) + 1.28 (35-40Hz 02) -.40 (7.5-10Hz fp1) + 3.70

All questions which composed a scale or subscale were simultaneously entered into stepwise multiple-regression within SPSS in order to predict the relevant QEEG equation variable. The results are presented in Tables-3.18-3.32.

Table 3.18 Predicting the *predsentient* Quantitative Electroencephalographic equation variable with all Sentient (S) absorption related questions

Question	F-statement
Question 30	$F_{(1,13)}$=13.60, p<.01, η^2=.51, SEE=1.97
Question 33	$F_{(2,12)}$=14.29, p<.01, η^2=.70, SEE=1.59

Table 3.19 Predicting the predPTIS Quantitative Electroencephalographic equation variable with all Prone to Altered and imaginative State (PTIS) absorption related questions

Question	F-statement
Question 16	[$F_{(1,13)}$=9.98, p<.01, η^2=.43, SEE=2.75]
Question 13	[$F_{(2,12)}$=10.52, p<.01, η^2=.64, SEE=2.29]

Table 3.20 Predicting the *predRTES* Quantitative Electroencephalographic equation variable with all Responsive to Engaging Stimuli (IRTES/RTES) absorption related questions

Question	F-statement
Question 23	[$F_{(1,13)}$=17.25, p<.01, η^2=.57, SEE=1.03]

Table 3.21 Predicting the *predS* Quantitative Electroencephalographic equation variable with all Synesthesia (S) absorption related questions

Question	F-statement
Question 33	[$F_{(1,13)}$=14.62, p<.01, η^2=.53, SEE=1.20]
Question 27	[$F_{(2,12)}$=21.30, p<.01, η^2=.78, SEE=.85]
Question 30	[$F_{(3,11)}$=39.76, p<.01, η^2=.89, SEE=.55]

Table 3.22 Predicting the *predEC* Quantitative Electroencephalographic equation variable with all Enhanced Cognition (EC) absorption related questions

Question	F-statement
Question 31	[$F_{(1,13)}$=29.94, p<.01, η^2=.70, SEE=83]
Question 22	[$F_{(2,12)}$=62.52, p<.01, η^2=.91, SEE=.47]

Table 3.23 Predicting the *predVR* Quantitative Electroencephalographic equation variable with all Vivid Reminiscence (VR) absorption related questions

Question	F-statement
Question 19	[$F_{(1,13)}$=.49, p<.01, η^2=.49, SEE=.54]

Table 3.24 Predicting the predEA Quantitative Electroencephalographic equation variable with all Enhanced Awareness (EA) absorption related questions

Question	F-statement
Question 5	[$F_{(1,13)}$=12.94, p<.01, η^2=.50, SEE=.74]
Question 9	[$F_{(2,12)}$=14.75, p<.01, η^2=.71, SEE=.58]
Question 11	[$F_{(3,11)}$=15.26, p<.01, η^2=.81, SEE=.50]

Table 3.25 Predicting the *predIRTIS* Quantitative Electroencephalographic equation variable with all Is Responsive to Inductive Stimuli (IRTIS) absorption related questions

Question	F-statement
Question 30	[$F_{(1,13)}$=30.85, p<.01, η^2=.70, SEE=.58]
Question 21	[$F_{(2,12)}$=30.91, p<.01, η^2=.84, SEE=.44]

Table 3.26 Predicting the *predOTII* Quantitative Electroencephalographic equation variable with all Often Thinks In Images (OTII) absorption related questions

Figure-42.	
Question	F-statement
Question 22	[$F_{(1,13)}$=18.28, p<.01, η^2=.58, SEE=.42]
Question 32	[$F_{(2,12)}$=125.96, p<.01, η^2=.96, SEE=.14]

Table 3.27 Predicting the predCSVSI Quantitative Electroencephalographic equation variable with all Can Summon Vivid and Suggestive Images (CSVSI) absorption related questions

Question	F-statement
N/A	N/A

Table 3.28 Predicting the *predHCE* Quantitative Electroencephalographic equation variable with all Has "Crossmodal" Experiences (HCE) absorption related questions

Question	F-statement
Question 33	$F_{(1,13)}$=26.77, p<.01, η^2=.67, SEE=.83
Question 27	$F_{(2,12)}$=38.39, p<.01, η^2=.87, SEE=.56
Question 26	$F_{(3,11)}$=36.39, p<.01, η^2=.91, SEE=.48
Question 17	$F_{(4,10)}$=67.30, p<.01, η^2=.96, SEE=.31

Table 3.29 Predicting the *predBOATI* Quantitative Electroencephalographic equation variable with all Can Become Absorbed in Own Thoughts and Imaginings (BOATI) absorption related questions

Question	F-statement
Question 18	[$F_{(1,13)}$=12.98, p<.01, η^2=.50, SEE=.44]
Question 7	[$F_{(2,12)}$=22.62, p<.01, η^2=.79, SEE=.29]

Table 3.30 Predicting the *predVRP* Quantitative Electroencephalographic equation variable with all Can Vividly Re-experience the Past (VRP) absorption related questions

Question	F-statement
Question 19	[$F_{(1,13)}$=18.58, p<.01, η^2=.59, SEE=.45]
Question 1	[$F_{(2,12)}$=18.97, p<.01, η^2=.76, SEE=.36]

Table 3.31 Predicting the *predEEA* Quantitative Electroencephalographic equation variable with all Has Episodes of Expanded Awareness (EEA) absorption related questions

Question	F-statement
Question 31	[$F_{(1,13)}$=19.52, p<.01, η^2=.60, SEE=.54]

Table 3.32 Predicting the *predASC* Quantitative Electroencephalographic equation variable with all Experiences Altered States of Consciousness (ASC) absorption related questions

Question	F-statement
Question 9	[$F_{(1,13)}$=30.67, p<.01, η^2=.70, SEE=.80]
Question 5	[$F_{(2,12)}$=56.55, p<.01, η^2=.90, SEE=.47]

When each question which makes up a scale or subscale is individually entered into regression analysis in order to predict the relevant QEEG equation variable, the results can be observed in Tables- 3.33-3.48.

Table 3.33 Predicting the predAAI Quantitative Electroencephalographic equation variable with each relevant individual AAI Tellegen Absorption scale question

Question	F-statement	Question	F-statement
Question 2	$F_{(1,13)}$=5.01, p<.05, η^2=.28, SEE=5.34	Question 21	$F_{(1,13)}$=12.73, p<.01, η^2=.50, SEE=4.47
Question 7	$F_{(1,13)}$=9.32, p<.01, η^2=.42, SEE=4.80	Question 23	$F_{(1,13)}$=15.09, p<.01, η^2=.54, SEE=4.27
Question 13	$F_{(1,13)}$=13.65, p<.01, η^2=.51, SEE=4.39	Question 27	$F_{(1,13)}$=4.75, p<.05, η^2=.27, SEE=5.38
Question 15	$F_{(1,13)}$=6.58, p<.03, η^2=.34, SEE=5.12	Question 30	$F_{(1,13)}$=7.11, p<.02, η^2=.35, SEE=5.05
Question 16	$F_{(1,13)}$=10.01, p<.01, η^2=.44, SEE=4.72	Question 31	$F_{(1,13)}$=5.96, p<.03, η^2=.31, SEE=5.20
Question 17	$F_{(1,13)}$=4.90, p<.05, η^2=.27, SEE=5.36	Question 33	$F_{(1,13)}$=4.82, p<.05, η^2=.27, SSE=5.37

Table 3.34 Predicting the *predptis* Quantitative Electroencephalographic equation variable with each relevant individual PTIS Tellegen Absorption Scale question

Question	F-statement
Question 5	$F_{(1,13)}$=8.56, p<.02, η^2=.40, SEE=2.84
Question 7	$F_{(1,13)}$=7.42, p<.02, η^2=.36, SEE=2.92
Question 9	$F_{(1,13)}$=6.55, p<.03, η^2=.34, SEE=2.98
Question 13	$F_{(1,13)}$=8.16, p<.02, η^2=.39, SEE=2.87
Question 16	$F_{(1,13)}$=9.98, p<.01, η^2=.43, SEE=2.75
Question 19	$F_{(1,13)}$=4.93, p<.05, η^2=.28, SEE=3.11
Question 21	$F_{(1,13)}$=9.50, p<.01, η^2=.42, SEE=2.78
Question 31	$F_{(1,13)}$=5.75, p<.04, η^2=.31, SEE=3.05

Table 3.35 Predicting the *predRTIS* Quantitative Electroencephalographic equation variable with each relevant individual RTES and IRTES Tellegen Absorption Scale question

Question	F-Statement
Question 2	N/A
Question 6	$F_{(1,13)}$=6.67, p<.03, η^2=.34, SEE=1.28
Question 15	$F_{(1,13)}$=11.70, p<.01, η^2=.47, SEE=1.14
Question 23	$F_{(1,13)}$=17.25, p<.01, η^2=.57, SEE=1.03
Question 34	$F_{(1,13)}$=10.07, p<.01, η^2=.44, SEE=1.18

Table 3.36 Predicting the *predsynesthesia* Quantitative Electroencephalographic equation variable with each relevant individual S Tellegen Absorption scale question

Question	F-statement
Question 10	N/A
Question 17	$F_{(1,13)}$=13.71, p<.01, η^2=.51, SEE=1.22
Question 26	N/A
Question 27	$F_{(1,13)}$=14.47, p<.01, η^2=.53, SEE=1.20
Question 30	$F_{(1,13)}$=12.87, p<.01, η^2=.50, SEE=1.24
Question 33	$F_{(1,13)}$=14.62, p<.01, η^2=.53, SEE=1.20

Table 3.37 Predicting the *predEC* Quantitative Electroencephalographic equation variable with each relevant individual EC Tellegen Absorption Scale question

Questions	F-statements
Question 13	$F_{(1,13)}$=11.68, p<.01, η^2=.47, SEE=1.10
Question 31	$F_{(1,13)}$=29.93, p<.01, η^2=.70, SEE=.83

Table 3.38 Predicting the *predODI* Quantitative Electroencephalographic equation variable with each relevant individual ODI Tellegen Absorption Scale question

Questions	F-statement
Question 3	N/A
Question 7	$F_{(1,13)}$=19.46, p<.01, η^2=.60, SEE=.61
Question 16	$F_{(1,13)}$=5.75, p<.04, η^2=.31, SEE=.80
Question 18	N/A
Question 21	$F_{(1,13)}$=5.78, p<.01, η^2=.31, SEE=.80

Table 3.39 Predicting the *predVR* Quantitative Electroencephalographic equation variable with each relevant individual VR Tellegen Absorption Scale question

Question	F-statement
Question 19	[$F_{(1,13)}$=.49, p<.01, η^2=.49, SEE=.54]

Table 3.40 Predicting the *predEA* Quantitative Electroencephalographic equation variable with each relevant individual EA Tellegen Absorption Scale question

Question	F-statement
Question 5	$F_{(1,13)}$=12.94, p<.01, η^2=.50, SEE=.74
Question 9	$F_{(1,13)}$=12.02, p<.01, η^2=.48, SEE=.75
Question 11	$F_{(1,13)}$=7.28, p<.02, η^2=.36, SEE=.84

Table 3.41 Predicting the *predIRTIS* Quantitative Electroencephalographic equation variable with each relevant individual IRTIS Tellegen Absorption Scale question

Question	F-statement
Question 3	N/A
Question 21	[$F_{(1,13)}$=10.21, p<.01, η^2=.44, SEE=.79]
Question 30	[$F_{(1,13)}$=30.85, p<.01, η^2=.70, SEE=.58]

Table 3.42 Predicting the *predOTII* Quantitative Electroencephalographic equation variable with each relevant individual OTII Tellegen Absorption Scale question

Question	F-statement
Question 22	$F_{(1,13)}$=18.28, p<.01, η^2=.58, SEE=.42
Question 32	$F_{(1,13)}$=13.11, p<.01, η^2=.50, SEE=.46

Table 3.43 Predicting the *predCSVSI* Quantitative Electroencephalographic equation variable with each relevant individual CSVSI Tellegen Absorption Scale question

Question	F-statement
N/A	N/A

Table 3.44 Predicting the *predHCE* Quantitative Electroencephalographic equation variable with each relevant individual HCE Tellegen Absorption Scale question

Question	F-statement
Question 17	[$F_{(1,13)}$=7.98, p<.02, η^2=.38, SEE=1.15]
Question 26	[$F_{(1,13)}$=6.57, p<.03, η^2=.34, SEE=1.19]
Question 27	[$F_{(1,13)}$=12.47, p<.01, η^2=.49, SEE=1.04]
Question 33	[$F_{(1,13)}$=26.77, p<.01, η^2=.67, SEE=.83]

Table 3.45 Predicting the *predBOATI* Quantitative Electroencephalographic equation variable with each relevant individual BOATI Tellegen Absorption Scale question

Question	F-statement
Question 18	[$F_{(1,13)}$=12.98, p<.01, η^2=.50, SEE=.44]

Table 3.46 Predicting the *predVRP* Quantitative Electroencephalographic equation variable with each relevant individual VRP Tellegen Absorption Scale questions

Question	F-statement
Question 19	[$F_{(1,13)}$=18.58, p<.01, η^2=.59, SEE=.45]

Table 3.47 Predicting the *predEEA* Quantitative Electroencephalographic equation variable with each relevant individual EEA Tellegen Absorption Scale question

Question	F-statement
Question 28	[$F_{(1,13)}$=6.51, p<.03, η^2=.33, SEE=.69]
Question 31	[$F_{(1,13)}$=19.52, p<.01, η^2=.60, SEE=.54]

Table 3.48 Predicting the *predASC* Quantitative Electroencephalographic equation variable with each relevant individual ASC Tellegen Absorption Scale question

Question	F-statement
Question 5	[$F_{(1,13)}$=15.06, p<.01, η^2=.54, SEE=1.00]
Question 9	[$F_{(1,13)}$=30.67, p<.01, η^2=.70, SEE=.80]
Question 16	[$F_{(1,13)}$=8.78, p<.02, η^2=.40, SEE=1.13]

When multiple regression analysis was conducted for each *individual* frequency and sensor as predictors of each TAS scale and sub-scale, the results can be observed in Table-3.49.

Table 3.49 Tellegen Absorption Scales and subscales predicted by individual Quantitative Electroencephalographic frequency and sensors

Predicting Absorption ability index by frequency	**F-statement**
Delta	
Increase in delta within f8 sensor	$F_{(1,13)}$=5.88, p<.04, η^2=.31, SEE=.5.44
Beta2	
Decrease in beta2 within pz sensor	$F_{(1,13)}$=10.10, p<.01, η^2=.44, SEE=.4.92
Increase in beta2 within fz sensor	$F_{(2,12)}$=9.21, p<.01, η^2=.61, SEE=.4.29
Beta3	
Decrease in beta3 within pz sensor	$F_{(1,13)}$=5.64, p<.04, η^2=.30, SEE=5.48
Increase in beta3 within t6 sensor	$F_{(2,12)}$=6.17, p<.02, η^2=.51, SEE=4.80
Predicting absorption ability index by sensor	
Increase in delta within f8 sensor	$F_{(1,13)}$=5.88, p<.04, η^2=.31, SEE=5.44
Decrease in delta within c3 sensor	$F_{(1,13)}$=5.52, p<.04, η^2=.30, SEE=5.50
Decrease in beta2 within cz sensor	$F_{(1,13)}$=4.91, p<.05, η^2=.27, SEE=5.59
Decrease in delta within c4 sensor	$F_{(1,13)}$=4.77, p<.05, η^2=.27, SEE=5.61
Decrease in beta2 within p3 sensor	$F_{(1,13)}$=6.78, p<.03, η^2=.34, SEE=5.32
Increase in alpha2 within p3 sensor	$F_{(2,12)}$=7.39, p<.01, η^2=.55, SEE=4.57
Decrease in beta2 within pz sensor	$F_{(1,13)}$=10.10, p<.01, η^2=.44, SEE=4.92
Decrease in beta2 within p4 sensor	$F_{(1,13)}$=5.49, p<.04, η^2=.30, SEE=5.50
Predicting Sentience by frequency	
Delta	
Decrease in delta within t3 sensor	$F_{(1,13)}$=5.48, p<.04, η^2=.30, SEE=2.81
Theta	
Decrease in theta within t3 sensor	$F_{(1,13)}$=5.81, p<.04, η^2=.31, SEE=2.78
Beta2	
Decrease in beta2 within p3 sensor	$F_{(1,13)}$=8.22, p<.02, η^2=.39, SEE=2.62
Increase in beta2 within f4 sensor	$F_{(2,12)}$=9.78, p<.01, η^2=.62, SEE=2.15
Predicting sentience by sensor	
Decrease in theta within t3 sensor	$F_{(1,13)}$=5.81, p<.04, η^2=.31, SEE=2.78
Decrease in beta2 within p3 sensor	$F_{(1,13)}$=8.22, p<.02, η^2=.39, SEE=2.62
Increase in alpha2 within p3 sensor	$F_{(2,12)}$=10.65, p<.01, η^2=.64, SEE=2.09
Increase in beta3 within p3 sensor	$F_{(3,11)}$=11.04, p<.01, η^2=.75, SEE=1.82
Decrease in beta2 within pz sensor	$F_{(1,13)}$=8.07, p<.02, η^2=.38, SEE=2.63
Predicting prone to imaginary and altered states by frequency	
Beta2	

Decrease in beta2 within pz sensor	$F_{(1,13)}$=6.50, p<.03, η^2=.33, SEE=3.21
Predicting prone to imaginary and altered states by sensor	
Decrease in beta2 within pz sensor	$F_{(1,13)}$=6.50, p<.03, η^2=.33, SEE=3.21
Predicting responsive to engaging stimuli by frequency	
Delta	
Decrease in delta within c3 sensor	$F_{(1,13)}$=6.30, p<.03, η^2=.33, SEE=1.58
Beta2	
Decrease in beta2 within pz sensor	$F_{(1,13)}$=9.37, p<.01, η^2=.42, SEE=1.46
Beta3	
Decrease in beta3 within f8 sensor	$F_{(1,13)}$=7.29, p<.02, η^2=.36, SEE=1.54
Predicting responsive to engaging stimuli by sensor	
Decrease in beta3 within f8 sensor	$F_{(1,13)}$=7.29, p<.02, η^2=.36, SEE=1.54
Decrease in delta within c3 sensor	$F_{(1,13)}$=6.30, p<.03, η^2=.33, SEE=1.58
Decrease in beta3 within cz sensor	$F_{(1,13)}$=5.17, p<.05, η^2=.29, SEE=1.63
Decrease in delta within c4 sensor	$F_{(1,13)}$=6.09, p<.03, η^2=.32, SEE=1.59
Decrease in delta within t4 sensor	$F_{(1,13)}$=4.78, p<.05, η^2=.27, SEE=1.64
Decrease in beta2 within p3 sensor	$F_{(1,13)}$=7.55, p<.02, η^2=.37, SEE=1.53
Increase in alpha2 within p3 sensor	$F_{(2,12)}$=10.50, p<.01, η^2=.64, SEE=1.21
Decrease in beta2 within pz sensor	$F_{(1,13)}$=9.37, p<.01, η^2=.42, SEE=1.46
Increase in alpha2 within pz sensor	$F_{(2,12)}$=10.28, p<.01, η^2=.63, SEE=1.21
Decrease in beta2 within p4 sensor	$F_{(1,13)}$=7.28, p<.02, η^2=.36, SEE=1.54
Increase in alpha2 within p4 sensor	$F_{(2,12)}$=8.12, p<.01, η^2=.58, SEE=1.30
Predicting Synesthesia by frequency	
Delta	
Increase in delta within f8 sensor	$F_{(1,13)}$=6.40, p<.03, η^2=.33, SEE=1.50
Alpha2	
Increase in alpha2 within fp1 sensor	$F_{(1,13)}$=6.32, p<.03, η^2=.33, SEE=1.50
Decrease in alpha2 within c3 sensor	$F_{(2,12)}$=9.69, p<.01, η^2=.62, SEE=1.18
Gamma1	
Increase in gamma1 within f4 sensor	$F_{(1,13)}$=5.94, p=.03, η^2=.31, SEE=1.52
Decrease in gamma1 within c4 sensor	$F_{(2,12)}$=6.35, p<.02, η^2=.51, SEE=1.33
Increase in gamma1 within t6 sensor	$F_{(3,11)}$=10.93, p<.01, η^2=.75, SEE=1.00
Gamma2	
Increase in gamma2 within f4 sensor	$F_{(1,13)}$=5.86, p<.04, η^2=.31, SEE=1.52
Decrease in gamma2 within c4 sensor	$F_{(2,12)}$=6.96, p=.01, η^2=.54, SEE=1.30
Increase in gamma2 within t6 sensor	$F_{(3,11)}$=8.94, p<.01, η^2=.71, SEE=1.07
Predicting Synesthesia by sensor	
Increase in alpha2 within fp1 sensor	$F_{(1,13)}$=6.32, p<.03, η^2=.33, SEE=1.50
Decrease in theta within fp1 sensor	$F_{(2,12)}$=7.94, p<.01, η^2=.57, SEE=1.25
Increase in alpha2 within fp2 sensor	$F_{(1,13)}$=6.29, p<.03, η^2=.33, SEE=1.50
Increase in alpha2 within f7 sensor	$F_{(1,13)}$=5.37, p<.04, η^2=.29, SEE=1.54
Increase in gmma1 within f4 sensor	$F_{(1,13)}$=5.94, p=.03, η^2=.31, SEE=1.52

Increase in delta within f8 sensor	$F_{(1,13)}$=6.40, p<.03, η^2=.33, SEE=1.50
Decrease in theta within t3 sensor	$F_{(1,13)}$=8.07, p<.02, η^2=.38, SEE=1.44
Predicting enhanced cognition by frequency	
Delta	
Increase in delta within f8 sensor	$F_{(1,13)}$=11.73, p<.01, η^2=.47, SEE=1.17
Predicting enhanced cognition by sensor	
Increase in delta within f8 sensor	$F_{(1,13)}$=11.73, p<.01, η^2=.47, SEE=1.17
Predicting oblivious/dissociative involvement by frequency	
Beta1	
Decrease in beta1 within c3 sensor	$F_{(1,13)}$=9.20, p=.01, η^2=.41, SEE=1.10
Beta2	
Decrease in beta2 within pz sensor	$F_{(1,13)}$=10.51, p<.01, η^2=.45, SEE=1.07
Beta3	
Decrease in beta3 within pz sensor	$F_{(1,13)}$=5.74, p<.04, η^2=.31, SEE=1.20
Increase in beta3 within p3 sensor	$F_{(2,12)}$=8.77, p<.01, η^2=.59, SEE=.95
Predicting oblivious/dissociative involvement by sensor	
Decrease in beta1 within c3 sensor	$F_{(1,13)}$=9.19, p=.01, η^2=.41, SEE=1.10
Decrease in beta2 within cz sensor	$F_{(1,13)}$=7.86, p<.02, η^2=.38, SEE=1.14
Decrease in beta1 within c4 sensor	$F_{(1,13)}$=7.96, p<.02, η^2=.38, SEE=1.13
Decrease in beta1 within p3 sensor	$F_{(1,13)}$=6.04, p<.03, η^2=.32, SEE=1.19
Decrease in beta2 within pz sensor	$F_{(1,13)}$=10.51, p<.01, η^2=.45, SEE=1.07
Decrease in beta2 within p4 sensor	$F_{(1,13)}$=7.41, p<.02, η^2=.36, SEE=1.15
Decrease in beta2 within o1 sensor	$F_{(1,13)}$=7.77, p<.02, η^2=.37, SEE=1.14
Decrease in beta1 within o2 sensor	$F_{(1,13)}$=5.04, p<.05, η^2=.28, SEE=1.22
Decrease in beta2 within pz sensor	$F_{(1,13)}$=10.51, p<.01, η^2=.45, SEE=1.07
Predicting vivid reminiscence by frequency	
Beta1	
Increase in beta1 within t3 sensor	$F_{(1,13)}$=7.88, p<.02, η^2=.38, SEE=.69
Beta2	
Increase in beta2 within t3 sensor	$F_{(1,13)}$=8.78, p<.02, η^2=.40, SEE=.68
Decrease in beta2 within fp1 sensor	$F_{(2,12)}$=8.22, p<.01, η^2=.58, SEE=.59
Beta3	
Increase in beta3 within t3 sensor	$F_{(1,13)}$=9.65, p<.01, η^2=.43, SEE=.66
Decrease in beta3 within fp1 sensor	$F_{(2,12)}$=9.81, p<.01, η^2=.62, SEE=.56
Gamma1	
Increase in gamma1 within t3 sensor	$F_{(1,13)}$=8.87, p<.02, η^2=.41, SEE=.68
Decrease in gamma1 within fp1 sensor	$F_{(2,12)}$=9.63, p<.01, η^2=.62, SEE=.57
Gamma2	
Increase in gamma2 within t3 sensor	$F_{(1,13)}$=11.02, p<.01, η^2=.46, SEE=.65
Decrease in gamma2 within fp1 sensor	$F_{(2,12)}$=11.06, p<.01, η^2=.65, SEE=.54
Predicting vivid reminiscence by sensor	
Increase in gamma2 within t3 sensor	$F_{(1,13)}$=11.02, p<.01, η^2=.46, SEE=.65
Increase in beta2 within t4 sensor	$F_{(1,13)}$=5.35, p<.04, η^2=.29, SEE=.74

Predicting enhanced awareness by frequency	
Decrease in beta2 within o2 sensor	$F_{(1,13)}$=5.54, p<.04, η^2=.30, SEE=.98
Predicting enhanced awareness by sensor	
Decrease in beta2 within o2 sensor	$F_{(1,13)}$=5.54, p<.04, η^2=.30, SEE=.98
Predicting responsive to engaging stimuli by frequency	
Delta	
Decrease in delta within c3 sensor	$F_{(1,13)}$=6.30, p<.03, η^2=.33, SEE=1.58
Beta2	
Decrease in beta2 within pz sensor	$F_{(1,13)}$=9.37, p<.01, η^2=.42, SEE=1.46
Beta3	
Decrease in beta3 within f8 sensor	$F_{(1,13)}$=7.29, p<.02, η^2=.36, SEE=1.54
Predicting responsive to engaging stimuli by sensor	
Decrease in beta3 within f8 sensor	$F_{(1,13)}$=7.29, p<.02, η^2=.36, SEE=1.54
Decrease in delta within c3 sensor	$F_{(1,13)}$=6.30, p<.03, η^2=.33, SEE=1.58
Decrease in beta3 within cz sensor	$F_{(1,13)}$=5.17, p<.05, η^2=.29, SEE=1.63
Decrease in delta within c4 sensor	$F_{(1,13)}$=6.09, p<.03, η^2=.32, SEE=1.59
Decrease in delta within t4 sensor	$F_{(1,13)}$=4.78, p<.05, η^2=.27, SEE=1.64
Decrease in beta2 within p3 sensor	$F_{(1,13)}$=7.55, p<.02, η^2=.37, SEE=1.53
Increase in alpha2 within p3 sensor	$F_{(2,12)}$=10.50, p<.01, η^2=.64, SEE=1.21
Decrease in beta2 within pz sensor	$F_{(1,13)}$=9.37, p<.01, η^2=.42, SEE=1.46
Increase in alpha2 within pz sensor	$F_{(2,12)}$=10.28, p<.01, η^2=.63, SEE=1.21
Decrease in beta2 within p4 sensor	$F_{(1,13)}$=7.28, p<.02, η^2=.36, SEE=1.54
Increase in alpha2 within p4 sensor	$F_{(2,12)}$=8.12, p<.01, η^2=.58, SEE=1.30
Predicting is responsive to inductive stimuli by frequency	
Delta	
Decrease in delta within o2 sensor	$F_{(1,13)}$=7.90, p<.02, η^2=.38, SEE=.97
Theta	
Decrease in theta within t3 sensor	$F_{(1,13)}$=9.75, p<.01, η^2=.43, SEE=.93
Alpha1	
Decrease in alpha1 within c3 sensor	$F_{(1,13)}$=5.30, p<.04, η^2=.29, SEE=1.04
Increase in alpha1 within o1 sensor	$F_{(2,12)}$=6.40, p<.02, η^2=.52, SEE=.89
Decrease in alpha1 within t3 sensor	$F_{(1,13)}$=, p<.01, η^2=.42, SEE=1.46
Alpha2	
Decrease in alpha2 within pz sensor	$F_{(1,13)}$=9.16, p=.01, η^2=.37, SEE=.94
Increase in alpha2 within fp2 sensor	$F_{(2,12)}$=11.95, p<.01, η^2=.61, SEE=.74
Increase in alpha2 within t6 sensor	$F_{(3,10)}$=12.24, p<.01, η^2=.71, SEE=.64
Beta1	
Decrease in beta1 within p3 sensor	$F_{(1,13)}$=11.17, p<.01, η^2=.46, SEE=.90
Increase in beta1 within t5 sensor	$F_{(2,12)}$=35.15, p<.01, η^2=.85, SEE=.49
Beta2	
Decrease in beta2 within pz sensor	$F_{(1,13)}$=11.48, p<.01, η^2=.47, SEE=.89
Predicting is responsive to inductive stimuli	

by sensor	
Decrease in theta within f7 sensor	$F_{(1,13)}$=4.79, p<.05, η^2=.27, SEE=1.05
Decrease in theta within t3 sensor	$F_{(1,13)}$=9.75, p<.01, η^2=.43, SEE=.93
Decrease in beta1 within c3 sensor	$F_{(1,13)}$=7.50, p<.02, η^2=.37, SEE=.98
Decrease in beta1 within cz sensor	$F_{(1,13)}$=7.45, p<.02, η^2=.36, SEE=.98
Decrease in beta1 within c4 sensor	$F_{(1,13)}$=10.85, p<.01, η^2=.46, SEE=.91
Decrease in beta1 within p3 sensor	$F_{(1,13)}$=11.17, p<.01, η^2=.46, SEE=.90
Decrease in beta2 within pz sensor	$F_{(1,13)}$=11.48, p<.01, η^2=.47, SEE=.89
Decrease in beta1 within p4 sensor	$F_{(1,13)}$=9.38, p<.01, η^2=.42, SEE=.94
Decrease in delta within o2 sensor	$F_{(1,13)}$=7.90, p<.02, η^2=.38, SEE=.97
Decrease in beta1 within left parahippocampal	$F_{(1,13)}$=8.08, p<.02, η^2=.38, SEE=.96
Predicting often thinks in images by frequency	
Delta	
Increase in delta within f8 sensor	$F_{(1,13)}$=16.35, p<.01, η^2=.56, SEE=.44
Alpha2	
Increase in alpha2 within t6 sensor	$F_{(1,13)}$=12.73, p<.01, η^2=.50, SEE=.47
Decrease in alpha2 within c3 sensor	$F_{(2,12)}$=11.77, p<.01, η^2=.66, SEE=.40
Beta3	
Decrease in beta3 within p4 sensor	$F_{(1,13)}$=4.85, p<.05, η^2=.27, SEE=.57
Increase in beta3 within fz sensor	$F_{(1,13)}$=5.89, p<.02, η^2=.50, SEE=.49
Predicting often thinks in images by sensor	
Increase in delta within f7 sensor	$F_{(1,13)}$=10.72, p<.01, η^2=.45, SEE=.49
Increase in delta within f8 sensor	$F_{(1,13)}$=16.35, p<.01, η^2=.56, SEE=.44
Increase in alpha2 within t3 sensor	$F_{(1,13)}$=8.84, p<.02, η^2=.41, SEE=.51
Increase in alpha2 within t4 sensor	$F_{(1,13)}$=8.46, p<.02, η^2=.39, SEE=.52
Increase in alpha2 within t5 sensor	$F_{(1,13)}$=6.35, p<.03, η^2=.33, SEE=.54
Increase in alpha2 within p4 sensor	$F_{(1,13)}$=6.49, p<.03, η^2=.33, SEE=.54
Decrease in beta3 within p4 sensor	$F_{(2,12)}$=10.36, p<.01, η^2=.63, SEE=.42
Increase in alpha2 within t6 sensor	$F_{(1,13)}$=12.73, p<.01, η^2=.50, SEE=.47
Increase in alpha2 within o1 sensor	$F_{(1,13)}$=5.02, p<.05, η^2=.28, SEE=.56
Increase in "best of fitness" (Koenig and Lehmann)	$F_{(1,13)}$=7.66, p<.02, η^2=.37, SEE=.53
Decrease in the # of times microstate D appeared	$F_{(1,13)}$=6.44, p<.03, η^2=.33, SEE=.54
Predicting can summon vivid and suggestive images	(No variables loaded)
Predicting has crossmodal experiences by frequency	
Delta	
Increase in delta within f8 sensor	$F_{(1,13)}$=10.65, p<.01, η^2=.45, SEE=1.13
Alpha2	
Increase in alpha2 within fp1 sensor	$F_{(1,13)}$=9.34, p<.01, η^2=.42, SEE=1.16
Decrease in alpha2 within o2 sensor	$F_{(2,12)}$=9.43, p<.01, η^2=.61, SEE=.99
Gamma1	
Increase in gamma1 within f4 sensor	$F_{(1,13)}$=7.21, p<.02, η^2=.36, SEE=1.22

Decrease in gamma1 within c4 sensor	$F_{(2,12)}$=7.53, p<.01, η^2=.56, SEE=1.05
Increase in gamma1 within t6 sensor	$F_{(3,11)}$=15.27, p<.01, η^2=.81, SEE=.73
Gamma2	
Increase in gamma2 within f4 sensor	$F_{(1,13)}$=6.30, p<.03, η^2=.33, SEE=1.25
Decrease in gamma2 within c4 sensor	$F_{(2,12)}$=7.61, p<.01, η^2=.56, SEE=1.05
Increase in gamma2 within t6 sensor	$F_{(3,11)}$=13.03, p<.01, η^2=.78, SEE=.77
Predicting has crossmodal experiences by frequency	
Increase in alpha2 within fp1 sensor	$F_{(1,13)}$=8.75, p<.02, η^2=.40, SEE=1.17
Decrease in theta within fp1 sensor	$F_{(2,12)}$=10.21, p<.01, η^2=.63, SEE=.96
Increase in alpha2 within fp2 sensor	$F_{(1,13)}$=9.34, p<.01, η^2=.42, SEE=1.16
Increase in alpha2 within f7 sensor	$F_{(1,13)}$=8.24, p<.02, η^2=.39, SEE=1.19
Increase in gamma1 within f4 sensor	$F_{(1,13)}$=7.21, p<.02, η^2=.36, SEE=1.22
Increase in delta within f8 sensor	$F_{(1,13)}$=10.65, p<.01, η^2=.45, SEE=1.13
Increase in beta3 within right parahippocampus	$F_{(1,13)}$=5.21, p=.04, η^2=.29, SEE=1.28
Predicting can become absorbed in own thoughts and images by frequency	
Delta	
Increase in delta within f7 sensor	$F_{(1,13)}$=4.87, p<.05, η^2=.27, SEE=.60
Beta1	
Decrease in beta1 within o1 sensor	$F_{(1,13)}$=5.11, p<.05, η^2=28., SEE=.60
Beta3	
Decrease in beta3 within o2 sensor	$F_{(1,13)}$=4.80, p<.05, η^2=.27, SEE=.60
Predicting can become absorbed in own thoughts and images by sensor	
Increase in delta within f7 sensor	$F_{(1,13)}$=4.87, p<.05, η^2=.27, SEE=60
Decrease in theta within f7 sensor	$F_{(2,12)}$=8.73, p<.01, η^2=.59, SEE=.47
Decrease in beta1 within o1 sensor	$F_{(1,13)}$=5.11, p<.05, η^2=.28, SEE=.59
Increase in alpha1 within o1 sensor	$F_{(2,12)}$=7.04, p=.01, η^2=.54, SEE=.50
Decrease in beta3 within o2 sensor	$F_{(1,13)}$=4.80, p<.05, η^2=.27, SEE=.60
Predicting can vividly re-experience the past by frequency	
Delta	
Increase in delta within t6 sensor	$F_{(1,13)}$=6.93, p<.03, η^2=.35, SEE=.61
Beta2	
Increase in beta2 within t3 sensor	$F_{(1,13)}$=5.82, p<.04, η^2=.31, SEE=.62
Beta3	
Increase in beta3 within t3 sensor	$F_{(1,13)}$=6.33, p<.03, η^2=.33, SEE=.62
Gamma1	
Increase in gamma within t3 sensor	$F_{(1,13)}$=8.86, p<.02, η^2=.41, SEE=.58
Gamma2	
Increase in gamma2 within t3 sensor	$F_{(1,13)}$=11.22, p<.01, η^2=.46, SEE=.55
Predicting can vividly re-experience the past by sensor	
Increase in gamma2 within t3 sensor	$F_{(1,13)}$=11.22, p<.01, η^2=.46, SEE=.55

Increase in delta within t5 sensor	$F_{(1,13)}$=5.63, p<.04, η^2=.30, SEE=.63
Increase in delta within t6 sensor	$F_{(1,13)}$=6.93, p<.03, η^2=.35, SEE=.61
Predicting has episodes of expanded awareness by frequency	
Decrease in # of gfp peaks for class A	$F_{(1,13)}$=4.78, p<.05, η^2=.27, SEE=.78
Predicting experiences altered states of consciousness by frequency	
Beta2	
Decrease in beta2 within o2 sensor	$F_{(1,13)}$=7.59, p<.02, η^2=.37, SEE=1.20
Increase in beta2 within t3 sensor	$F_{(2,12)}$=8.47, p<.01, η^2=.59, SEE=1.01
Predicting experiences altered states of consciousness by sensor	
Decrease in beta2 within p4 sensor	$F_{(1,13)}$=6.25, p<.03, η^2=.33, SEE=1.24
Decrease in beta2 within o1 sensor	$F_{(1,13)}$=6.23, p<.03, η^2=.33, SEE=1.24
Decrease in beta2 within o2 sensor	$F_{(1,13)}$=7.59, p<.02, η^2=.37, SEE=1.20

3.3.17 TAS Results from study 2

Tellegen Absorption Scale (TAS) scores from the participants included in this study were entered into multiple regression analysis in order to predict Remote Behavioural Guessing (RBG) accuracy during the pre-treatment condition. The results are shown in Table-3.50.

Table 3.50 Multiple Regression results; predicting Remote Behavioural Guessing accuracy with Tellegen Absorption Scale scores

Predictor	**F-statement**
Content cluster 4 (Can summon vivid and suggestive images)	[η^2=.49, $F_{(1,15)}$=14.29, p=.002, SEE=.29]
Content Cluster 6 (Can become absorbed in own thought and imaginings)	[η^2=.66, $F_{(2,14)}$=13.47, p=.001, SEE=.24]
Content Cluster 2 (Responsive to inductive stimuli)	[η^2=.75, $F_{(3,13)}$=13.04, p=.002, SEE=.29]

One-way analysis of variance revealed the relevant TAS*RBG accuracy relationship. This is shown in Figures- 3.52-3.53.

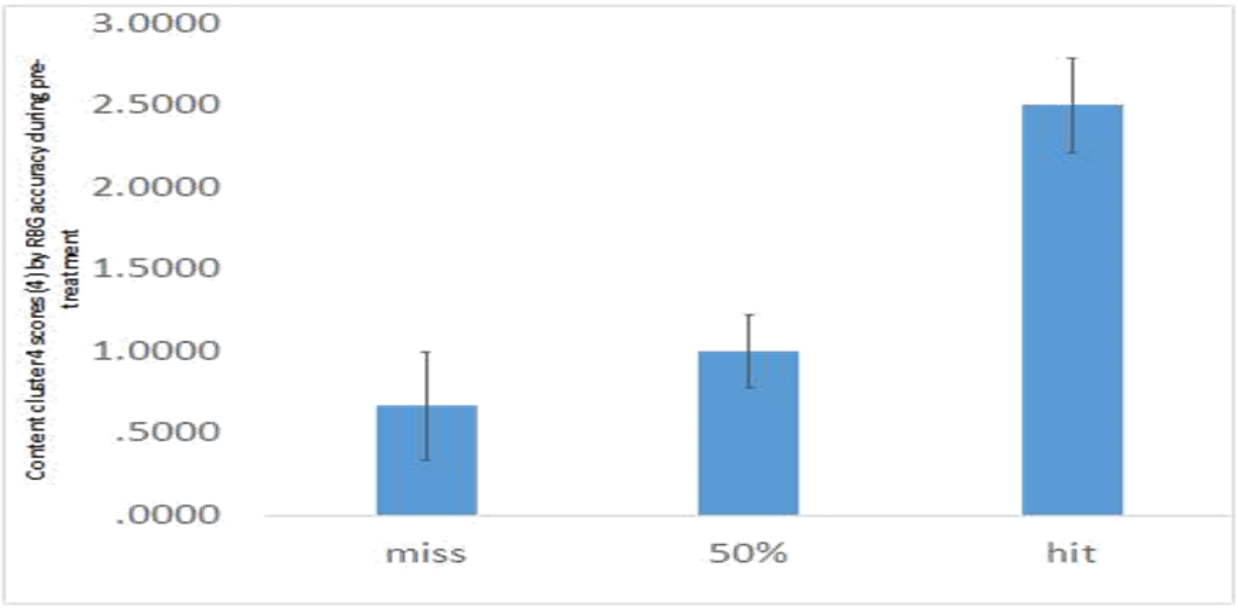

Figure 3.52 Tellegen Absorption Scale content cluster 4 (Can Summon Vivid and Suggestive Images) scores (/4) by Remote Behavioural accuracy during pre-treatment within human testing conditions

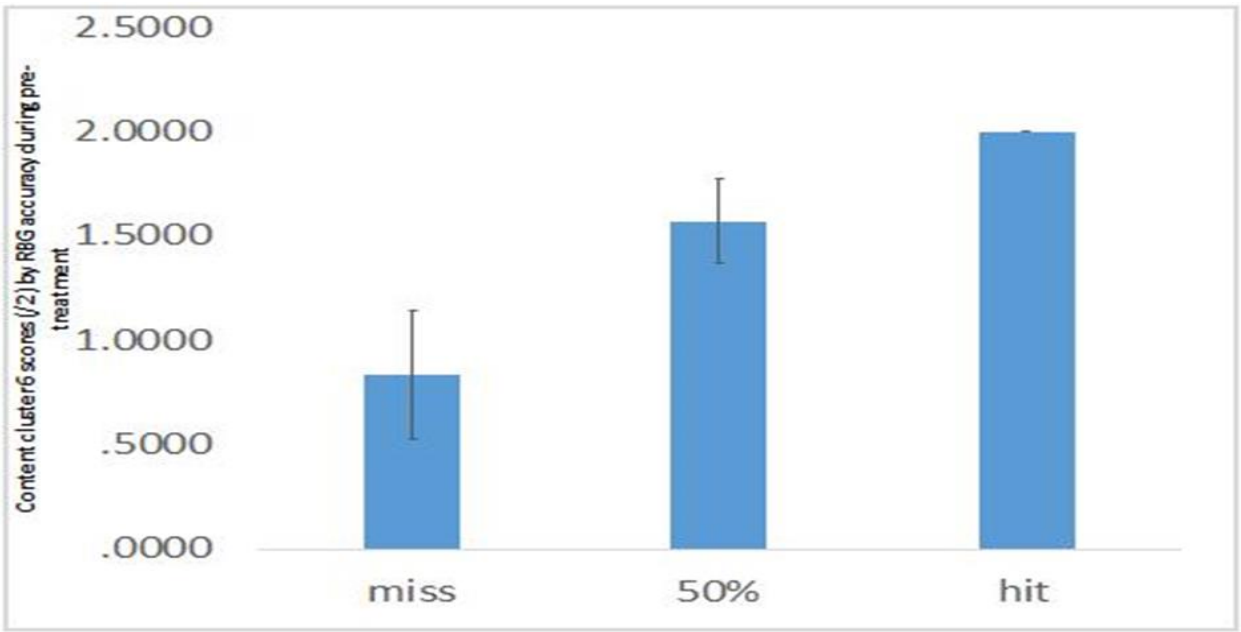

Figure 3.53 Tellegen Absorption Scale content cluster 6 (Can Become Absorbed in own Thought and imaginings) scores (/2) by Remote Behavioural Guessing accuracy during pre-treatment within human testing conditions

Analyses also indicated that factor cluster 5 (Vivid reminiscence) [η^2=.39,F(1,13)=8.24, p<.02, SEE=.30] and content cluster 5 (Has "crossmodal" experience) [η^2=.70, F(2,12)=14.27, p=.001, SEE=.22] entered the model to predict post-treatment RBG accuracy. *Post hoc* analysis indicated that participants who had a 'miss' scored significantly higher on factor 5 then participants who had a 'hit' in RBG accuracy during the post-treatment condition.

The Δ no-field RBG accuracy was computed (post-treatment RBG accuracy – pre-treatment RBG accuracy), and then entered into multiple regression analysis as the dependent variable along with TAS scores and field condition RBG scores as the prediction variables. The results can be observed in Table-3.51.

Table 3.51 Multiple regression results; predicting Δ no-field RBG accuracy with Tellegen Absorption Scale (TAS) scores and field condition Remote Behavioural Guessing accuracy

Model	Predictor of Δ no-field RBG accuracy	F-statement
1	TAS Factor 5 (Vivid Reminiscence)	[η^2=.72, $F_{(1,12)}$=30.77, p<.001, SEE=.33]
2	TAS Content cluster 7 (Can vividly re-experience the past)	[η^2=.83, $F_{(2,11)}$=25.93, p<.001, SEE=.27]
3	RBG scores during 1st Burst-X treatment	[η^2=.89, $F_{(3,10)}$=27.02, p<.001, SEE=.22]
4	RBG scores during 1st Thomas Pulse treatment	[η^2=.93, $F_{(4,9)}$=30.64, p<.001, SEE=.19]

One-way analysis of variance revealed the relationship between the TAS Factor 5 and content cluster 7 scores and Δ no-field RBG accuracy which can be observed in Figures 3.54-3.55.

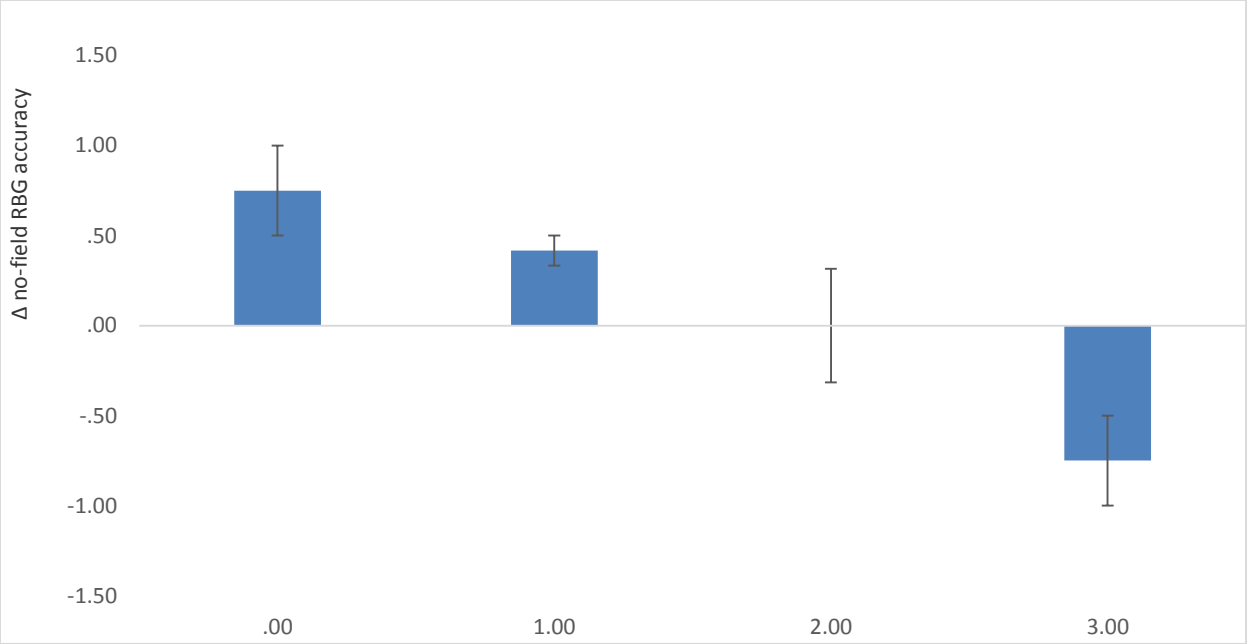

Figure 3.54 Δ No-field Remote Behavioural Guessing accuracy by Tellegen Absorption Scale factor 5 (Vivid reminiscence) scores (/3)

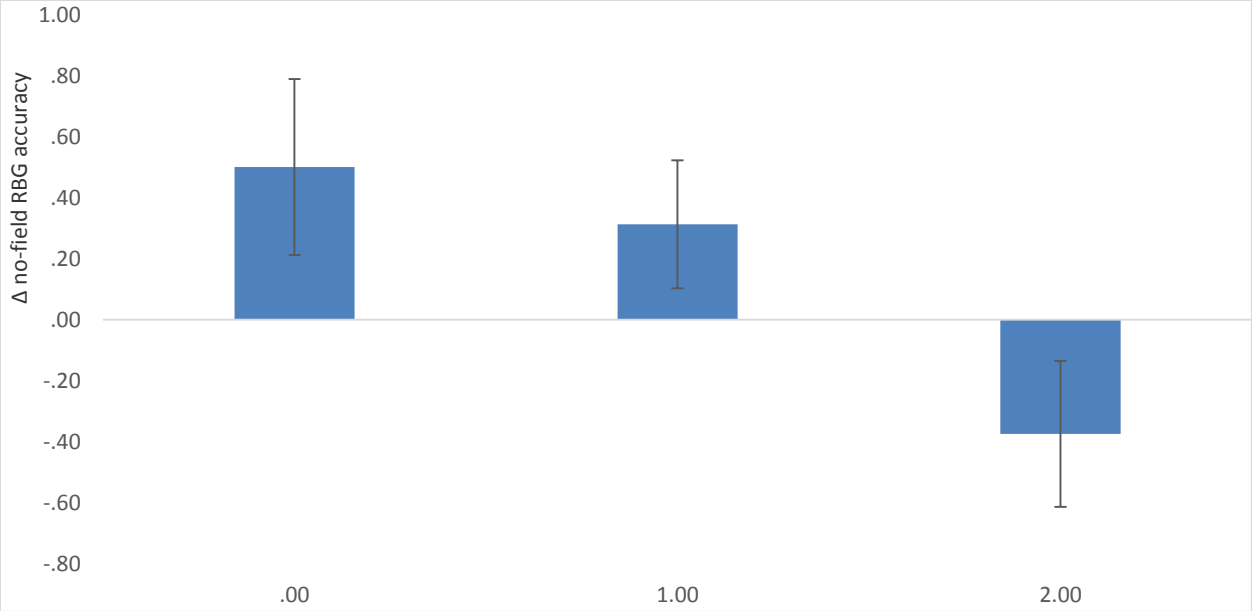

Figure 3.55 Δ No-field Remote Behavioural Guessing accuracy by Tellegen Absorption Scale content cluster 7 (Can vividly re-experience the past) scores (/2)

3.3.18 TAS Results from Study 3

When the participants within study 3 were divided into halves (N 1 half=30; N 2nd half=31) within the dataset for purposes of multiple regression analysis with TAS scores acting as predictors of POMS profiles during the pre-treatment condition within the study, the results indicate that the TAS absorption ability index (determined by the number of "true" responses to absorption related questions (scored out of 29) was able to accommodate pre-treatment vigor-activity POMS component scores [η^2=.25, F(1,28)=9.17, p<.01, SEE=3.85]. The resulting equation was:

predpreV=(.312*TASindex) + 3.571

When this equation was used to create a new variable (predpreV), correlational analysis performed on the 1st half of the database indicated that it was positively correlated with the unstandardized predicted value derived from the multiple regression analysis [Pearson r(30)=1.00, rho(30)=1.00, p<.001] suggesting that it was calculated correctly. Furthermore predpreV is also correlated with the baseline vigor-activity component scores (PreV) within the 1st half of the database with a Pearson r value equal to that obtained from the multiple regression analysis [Pearson r(30)=.497, rho(30)=.423, p<.01] (Figure-3.56).

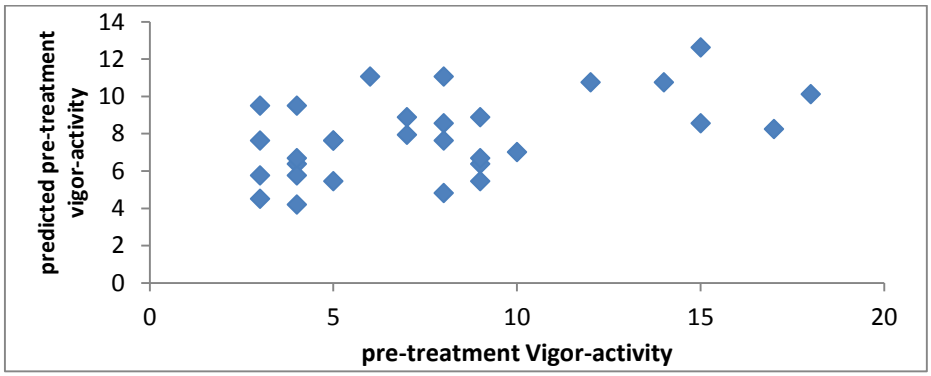

Figure 3.56 Significant correlation: predicted baseline Profile of Mood States vigor-activity score regression variable and observed baseline vigor-activity scores in the 1st half of the dataset

Correlational analyses performed on the 2nd half of the database indicated that predpreV was positively correlated with the baseline vigor-activity component scores [Pearson $r_{(31)}$=.393, rho=.474, p<.01] (Figure-3.57) as well as with the TAS absorption ability index variable [Pearson $r_{(31)}$=1.00, $rho_{(31)}$=1.00, p<.01].

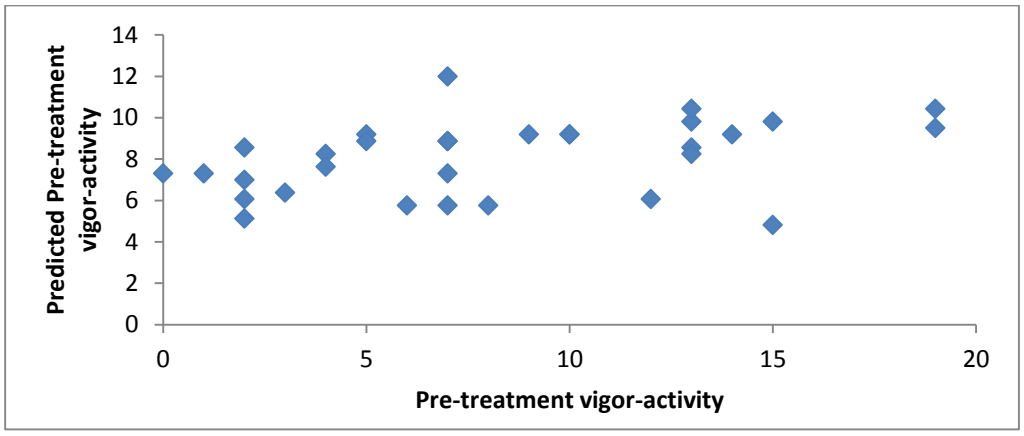

Figure 3.57 Significant correlation: predicted baseline Profile of Mood States vigor-activity score regression variable and observed baseline vigor-activity scores in the 2nd half of the dataset

The application of the treatment (Burst-X EM fields) within this study appeared to have an effect on the relationship between the vigor-activity POMS subscale and the TAS AAI. Multiple regression analysis was performed on the 1st half of a database containing 61 participants (N=30, N=31). "Prediction" of *post*-treatment vigor-activity with TAS scales and subscales significance was found [$F_{(1,28)}$=11.47, p=.002, η^2=.29].The results indicate that the TAS AAI significantly accommodated post-treatment vigor-activity yielding the following equation:

predpostv=.389*(tasindex) + .650.

Correlational analysis performed on the 1st half of the dataset indicated the variable "predpostv" was significantly correlated with post-treatment Vigor-activity (postV) yielding a Pearson r value equal to the R value obtained from the regression analysis [Pearson $R_{(30)}$=.54, rho=.53, p<.002] (figure-3.58).

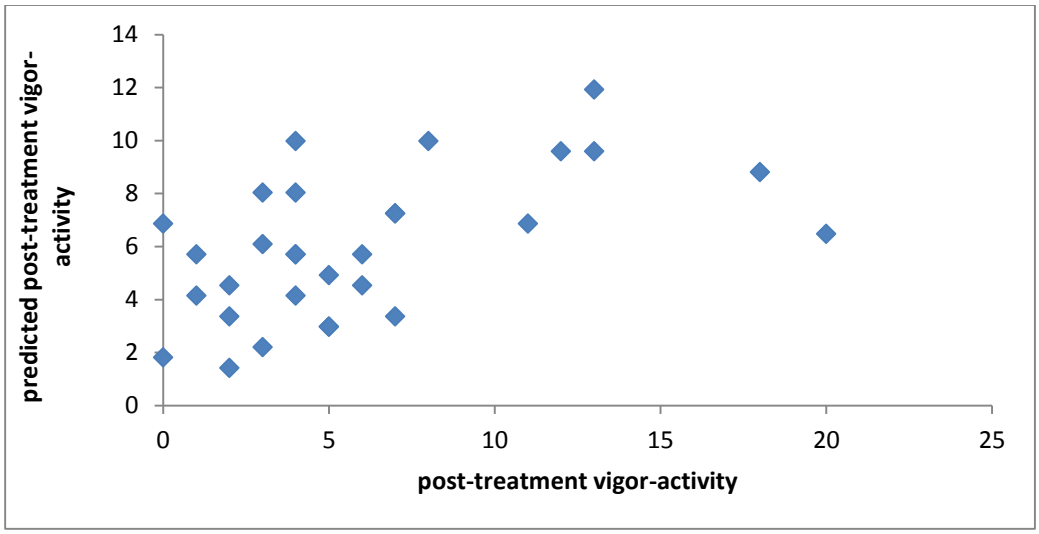

Figure 3.58 Significant correlation: predicted post-treatment Profile of Mood States vigor-activity score regression variable and observed post-treatment Vigor-activity scores in the 1st half of the dataset

Correlational analysis performed on the 2nd half of the dataset indicates that predpostv was significantly correlated with post-treatment Vigor-activity [Pearson $r_{(31)}$=.49, rho=.53, p=.002] (figure-3.59).

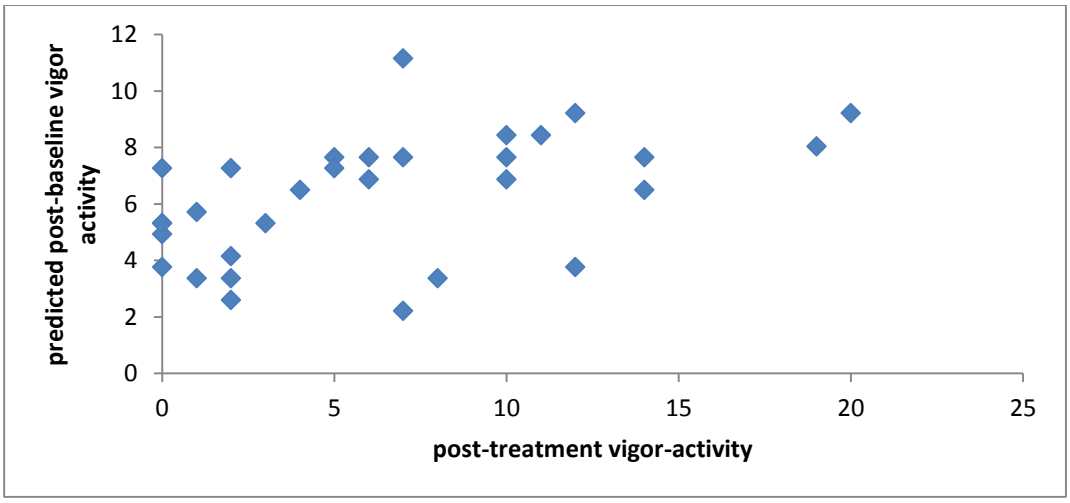

Figure 3.59 Significant correlation: Predicted post-treatment Profile of Mood States vigor-activity score regression variable and observed post-treatment vigor-activity scores within the 2nd half of the dataset

The correlation between predicted vigor-activity (computed from TAS absorption ability index) and observed vigor-activity within the 2nd half of the dataset was greater in post-treatment (see above) then it is in baseline conditions [Pearson $r_{(31)}$=.39, rho=.47, p<.01] even though there was an evident decrease in vigor-activity throughout the duration of the experiment (figure-3.60.). However this difference in magnitude of coefficients was not significant when assessed by transformed r values (z <1.96).Figure-3.60 displays an evident decrease in vigor-activity across the majority of experimental conditions. Figure-3.61 displays baseline, post-treatment, and change in vigor-activity for all participants. Finally Figure-3.62 displays vigor-activity for both females and males.

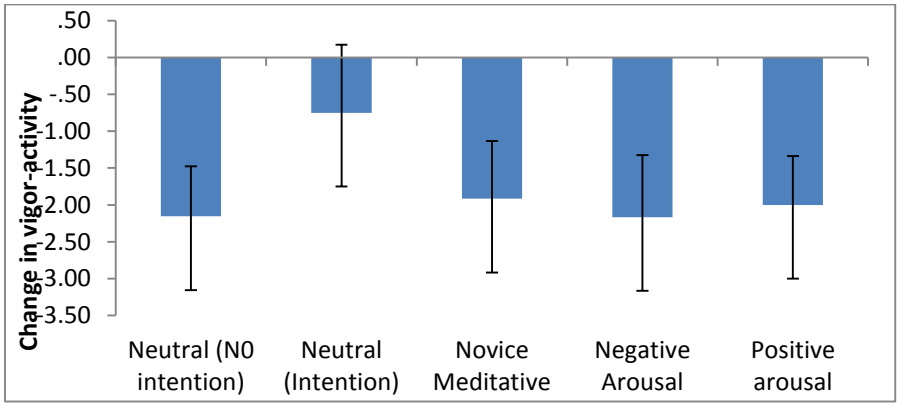

Figure 3.60 Delta vigor-activty POMS subscale after post-treatment across experimental conditions

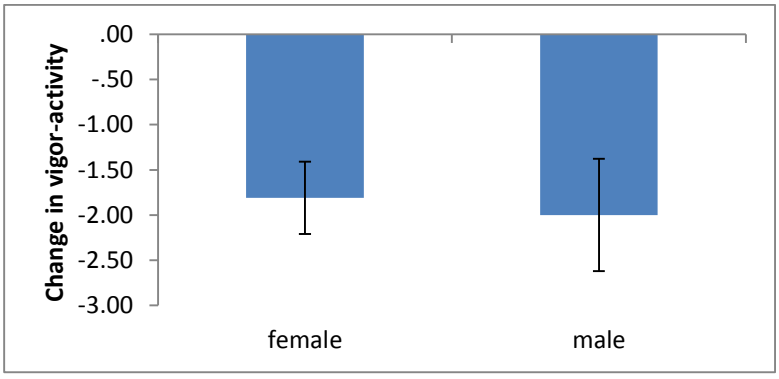

Figure 3.61 Delta vigor-activity POMS subscale after post-treatment by gender

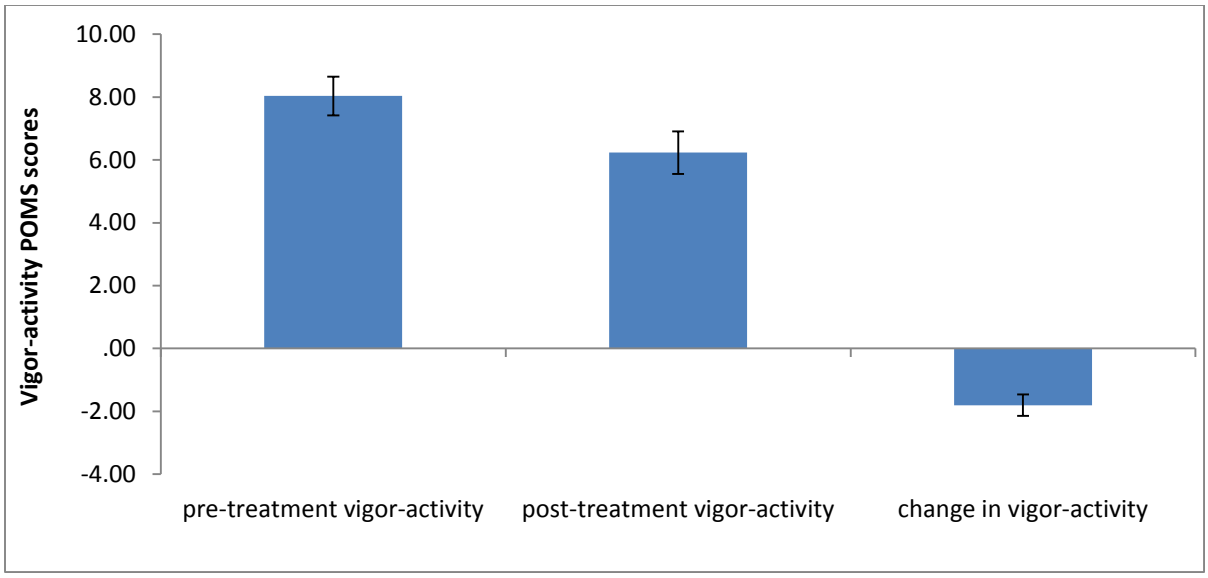

Figure 3.62 Pre-treatment, post-treatment and change in vigor-activity scores over the course of the experiment

When TAS Sentient scores and RNG z-scores pre-treatment were split into high and low scores and assessed by chi-squared analyses significant dis-concordance was observed [$X^2_{(1,61)}$=7.22, p<.01]. The results indicated that those individuals who scored low on the sentient subscale also scored low on the RNG pre-treatment z-score as displayed in Table-3.52.

Table 3.52 Sentient scores split data by Random Number Generator z-scores split data during pre-treatment

	Sentient		**Total**
Z-score pre-treatment	**Low**	**Hi**	
Miss	21	10	31
Hit	10	20	30
Total	31	30	61

With regard to intention on the RNG pre-treatment, multiple regression analysis indicated that IRTES [$F_{(1,59)}$=10.95, η^2=.16, p<.01, SEE=.92], OTII [$F_{(2,58)}$=9.33, η^2=.24, p<.01, SEE=.88], and IRTIS [$F_{(3,57)}$=9.33, η^2=.30, p<.01, SEE=.86] explained 30% of the variance in pre-treatment RNG z-scores. When these z-score values for the RNG during intention post-treatment along with TAS factor 3 EC were split into hi and low values and analyzed by chi-squared significant dis-concordance was observed [$X^2_{(1,61)}$=3.70, p<.05]. The results indicated that those individuals who scored highly on the EC TAS factor had a lower hit rate with regard to RNG intention during field exposure then individuals who scored lower on EC (Table-3.53).

Table 3.53 Enhanced Cognition scores split data by Random Number Generator z-scores split data during post-treatment

	Enhanced Cognition		**Total**
Z-score post-treatment	**Low**	**Hi**	
Miss	12	19	31
Hit	19	11	30
Total	31	30	61

3.3.19 TAS Results from Studies 2 & 3

To adequately test the construct validity of the TAS and the hypothesis that it measures the individual's expression of the trait of absorption and not some other confounding variables, daily geophysical variables were considered. They included: Geomagnetic AA Index (nT), Sunspot Number (SIDC), Penticton Canada Average Solar Flux Unit (W/m^2 Hz), Penticton Canada Average Solar Flux Unit (W/m^2 Hz) (corrected for variations in the Earth-Sun distance), NOAA Penticton Solar Flux Unit (W/m2 Hz) (measure @ 2000UT), Average Seismic Energy (J); total, .01-1M, 1.01-2M, 2.01-3M, 3.01-4M, 4.01-5M, 5.01-6M, >6M, Sum Total Seismic Energy (J); total, .01-1M, 1.01-2M, 2.01-3M, 3.01-4M, 4.01-5M, 5.01-6M, >6M, Average Distance of Total

Earthquakes from Laurentian (km); total, .01-1M, 1.01-2M, 2.01-3M, 3.01-4M, 4.01-5M, 5.01-6M,>6M,Total number of earthquakes registered; >.01M, .01-1M, 1.01-2M, 2.01-3M, 3.01-4M, 4.01-5M, 5.01-6M, >6M]. These values were obtained for the days of, before and after the test was completed by the subject. They were added to the database to see if these variables had a relationship with TAS scoring. Figure-3.61 displays the mean number of significant correlations between these geophysical variables and TAS scores from two studies of interest (study 1- N=61, study 2- N=17; Total=78). Figure-3.63 displays the average strength of these correlations from each study by each TAS scale and subscale.

Table 3.54 Tellegen Absorption Scale variables and visual Representation

Variable	**Representation**	**Variable**	**Representation**
Tasindex	Absorption index	Con1	Responsive to engaging stimuli
Sent	Sentience	Con2	responsive to inductive stimuli
PTIS	Proneness to imaginative and altered states	Con3	often think in images
Fac1	Responsive to engaging stimuli	Con4	can summon vivid and suggestive images
Fac2	synesthesia	Con5	has “crossmodal” experience
Fac3	enhanced cognition	Con6	Can become absorbed in own thoughts& images
Fac4	Oblivious/Dissociative Involvement	Con7	can vividly re-experience the past
Fac5	Vivid reminiscence	Con8	has episodes of expanded awareness
Fac6	Enhanced awareness	Con9	experiences altered states Of consciousness

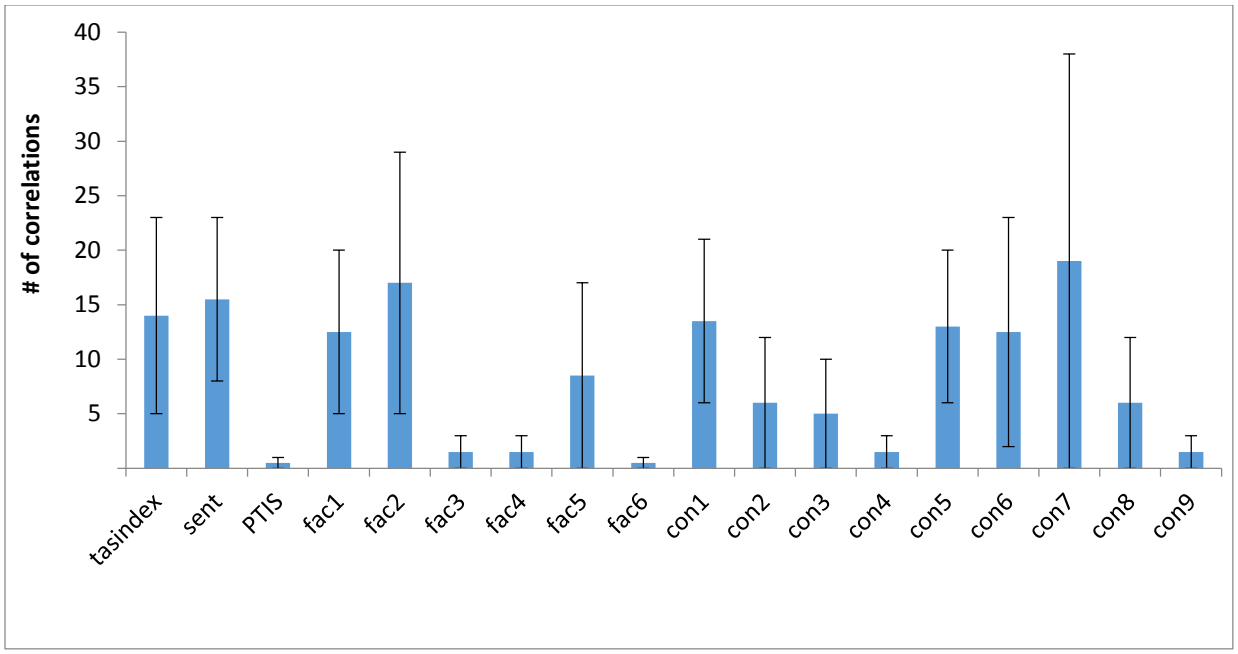

Figure 3.63 Number of significant correlations between Tellegen Absorption Scales and subscales and select space weather variables

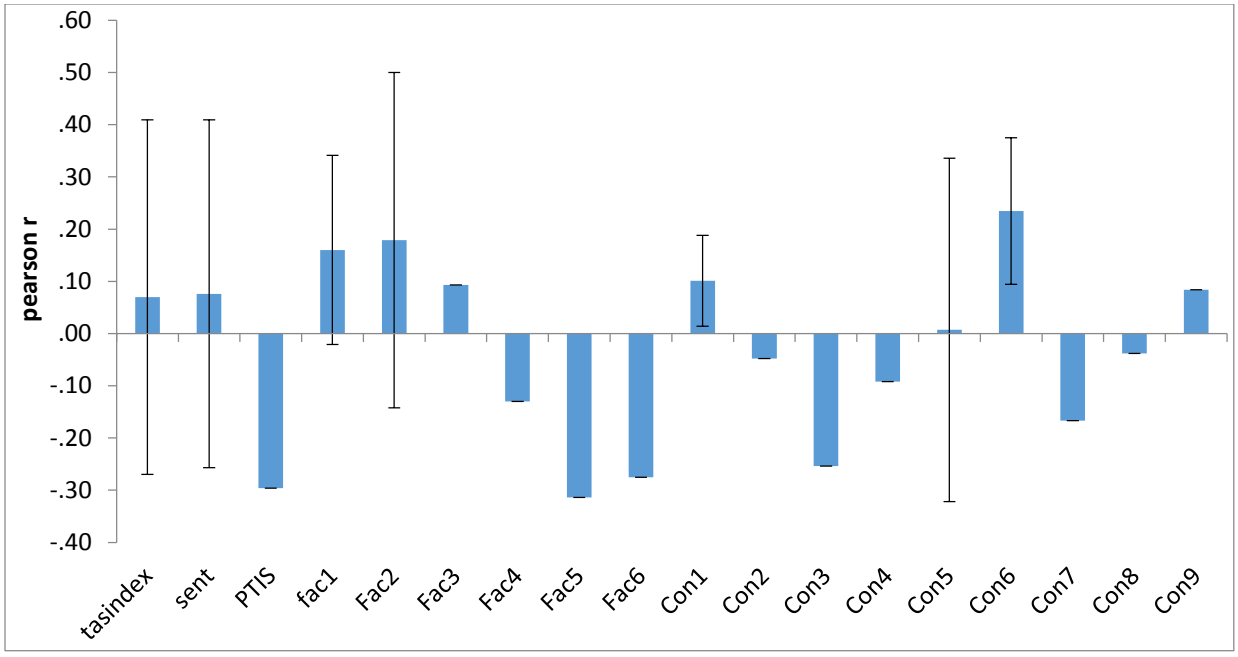

Figure 3.64 Average strength of correlation between Tellegen Absorption Scales and subscales and select space weather variables

3.4 Discussion:

The quantitative approach in this experiment facilitated an understanding by which subjective experience could contribute to successful/unsuccessful "PK ability" as inferred by the magnitude and direction of deviation from random variations of the RNG. The process of identifying the absorption related traits measured by the Tellegen Absorption Scale (TAS) allowed for correct classification of individuals who subsequently exhibited significant differences in several PK tasks including influencing on a REG and correct identifications in Remote Behavioral Guessing (RBG) tasks.

The construct validity of the TAS appears to be verified through QEEG analysis. Baseline measures recorded prior to the completion of the questionnaire were significantly associated with the scores on 17/18 measures on the subjective experience questionnaire. Localized fluctuations of power within brain activity loaded as TAS predictors and were intuitively congruent with what might be expected from Absorption related traits.

Predictors for several absorption related traits displayed the same QEEG activations as psychic "superstar" and sensitive Sean Harribance during an 'intuitive state' condition (Persinger & Saroka, 2012). Elevated scores for Synesthesia, Vivid reminiscence, and "Often thinks in images" was associated with increased activity in the right parahippocampus. This was observed for Mr. Harribance. It has been suggested that the right parahippocampal structure might be involved with the extraction of information from the environment through non-classical senses or pathways (Venkatasubramanian et al., 2008). This parahippocampal region is also considered the gatekeepers of the hippocampal formation (hippocampus and dentate gyrus). The

parahippocampal area because mediates all information from diverse areas of the cerebral cortices to the hippocampal formation through the operation of the fusiform (occipitotemporal) gyrus, and the collateral sulcus within the space between the posterior portion of the parahippocampal gyrus which is caudal to the posterior border of the entorhinal cortices (Gloor, 1997).

QEEG predictors of absorption related traits also appeared to mimic the psi-coupled brain activity of Ingo Swann who demonstrated proportions of unusual 7-Hz and slow wave activity over the right temporal-occipital lobes which was found to be moderately correlated (rho=.50) with accuracy regarding distal hidden stimuli (Persinger et al., 2002). The absorption related traits which were predicted by slower wave (theta range) fluctuations over the occipital lobes included: Enhanced Awareness and "crossmodal" experience. In the case of Enhanced awareness- decreased delta activity loaded as the 3rd frequency to predict the factor along with (1) decreased beta2 activity in the right occipital lobe, (2) increased beta1 within the rostral lateral portion of the left temporal lobe (t3 sensor) sensor and (4) decreased beta3 activity within the left parahippocampus. The cluster "has "crossmodal" experiences: was predicted by an increase in delta within the left occipital lobe (o1 sensor) after variance explained from (1) increased delta within the caudal lateral region of the right frontal lobe (f8 sensor), (2) an increase in the number of times that microstate D appeared, and (3) a decrease in theta within the rostral medial region of the right parietal lobe (p4 sensor) have been accommodated. These results suggest that Mr. Swann may have relied upon variations in Enhanced Awareness and experiencing "crossmodal" experience during his remote viewing procedure.

The fact that the QEEG profiles were collected prior to the TAS questionnaire was completed is of interest and should not be overlooked as *states* and other individual measures available to discern individual differences may not be as consistent over time as absorption traits appear to be. Even IQ may not be static from birth to death. There may be changes that occur during learning (Haan, 1963), or growth (Ment et al., 2003) or after Traumatic Brain Injury (TBI) acquisition (Parker & Rosenblum, 1996).

The experimenter effect (Kennedy & Taddonio, 1976), or experimenter expectation also was reduced insofar as the baseline QEEG measures used within the study were collected from the NED (Neuroscience Electroencephalographic Database) and were not collected by the researcher analyzing the data. The fact that the factor Enhanced cognition was significantly higher in the NRG database is noteworthy insofar as scores from several members within this group were also a part of the 2013 Neuropsychology student and 2011 Laurentian University Community. These results suggest that this trait was developed within or selected for the Neuroscience Research Group.

The finding that baseline vigor scores could predict the numbers of true responses on the Absorption ability index is a novel characteristic of absorption. The fact that the relationship between vigor and the AAI index became stronger after EM field stimulation suggests that the applied field (Burst-X) which has been found to reduce depression and pain and to stimulate opiate like conditions for clinical populations (Baker-Price & Persinger, 1996) strengthened the neurophysiological pathways of the vigorous expression of the trait of absorption.

The weak to moderate correlations between space-weather collected on the day of, before and after the TAS was completed were not unexpected. Such "subtle" energies have been found to interfere with electronics, human health and animal behavior. These correlations were much weaker than those found between pen and paper TAS results and QEEG measures collected well in advance with r^2 values ranging from .44~.94. However given the transience and "weak" effect size of "intention" related phenomena one would expect relatively low strength correlations between these geophysical variables and behavior. One reason might be that the combining of the many variables that cause these phenomena is so infrequent that the coherence with solar geophysical variables is obscured within the dominant average.

In summary, it appears as if the TAS measures have strong construct validity with regard to what it is actually supposed to measure, that is to say that the cerebral activity that enter as Independent variables as predictors of the dependent variable TAS measures were that which is to be expected. The fact that scores on individual questions within the TAS component in question were able to predict the QEEG equation variable for that absorption related trait in 17/18 cases suggests a potentially functional relationship between self-identified absorption levels and baseline QEEG measures. The only TAS subscale which was not predicted by QEEG profiles was 'Can summon vivid and suggestive images'.

There were very large numbers of variables involves with these analyses and despite the sample of about 80 subjects the intrinsic limitation of these procedures is appreciated. However care was taken to ensure minimum artifacts and distorting influences from outliers as can be discerned by inspecting the scatter within the figures. One would expect multiple intercorrelations between

QEEG and TAS variables because both are strongly internally coherent because of the nature of the processes which would be consistent with the concept of a "field" of QEEG patterns and a "field" of cognition. What is relatively clear is that QEEG measures of brain activity and reports of subjective experiences are consistently correlated in the population. These same classes of variables are associated with the deviation of "random" numbers and changes in electron conduction across random number devices. This could be considered the first empirical step to relating the quantification of brain activity and psychometric representations of the classic "mind" experiences to the types of subtle physical mechanisms at the quantum level that might explain "intention" effect specifically and "psychokinesis" in general.

4 Chapter 4: Excess Correlation Between Two Non-Local Random Event Generators By Electromagnetic Field Applications

4.1 Introduction

Entanglement which has been widely studied since the term was first introduced by Erwin Schrodinger remains an ambiguous and multifaceted phenomenon. This assumes of course there is only one source or form of entanglement that may or may not be correct. A more preferred label is excess correlation between reactions in two spaces that are not juxtaposed but behave as if there has been a transposition of axis. The occurrence of this "spooky action at a distance", to reiterate a description attributed to Albert Einstein, has been found to occur at the macro-level between several physical chemical reactions separated by significant distances.

In a series of 24 experiments; inverse shifts in pH were noted in two quantities of spring water separated by 10 meters that shared rotating magnetic fields with changing angular velocities when one solution was injected with proton donors (weak acetic acid). It was also found that the associated fixed amount of energy of 10^{-21}J per molecule from the coordinated fields in the two loci was related to the change in numbers of H^+ within these volumes and predicted the time required to produce the maximum shift in pH (Dotta et al., 2013).

Excess correlation is not exclusive to pH shifts in water but also applies to electron spins and gases (Ahn et al., 2000; Fickler et al., 2012; Hoffman et al., 2012; Julsaarg et al., 2001) as well in non-local human interaction. Excess correlation has been found up to 300 km. Discrete changes in power within the cerebral space of the non-local subject was experimentally demonstrated when the pair were exposed to specific configurations of circular magnetic fields with changing

angular velocities that dissociated the phase and group components. These non-local discrete changes in power occurred when the local participant was exposed to sound pulses but not light flash frequencies (Burke et al., 2013). The signal to noise ratio within excess correlation with regard to human cerebrums seems to be heightened when the pairs of individuals have had proximal space-time relations from previous relations. When 'pairs' were separated by 75 m, ~50% of the variance of the "simultaneous" electroencephalographic power was shared between the pairs of brains. Positive correlations were found within the alpha and gamma bands within the temporal and frontal lobes. However the mutual power within the alpha and theta bands were found to be negatively correlated for pairs of people who had a protracted history of interaction (Dotta et al., 2009).

All human brains on planet earth are immersed within the same medium, the earth's naturally occurring electromagnetic field. Quantitative solutions have indicated that the intensities from the 'transcerebral' fields are in the same order of magnitude as the values associated with cognitive processes and altered expressions of proteins within the human brain (Persinger, 2013). The facilitation of these events should fall under the domain of random events which have been demonstrated to be significantly altered from chance expectations under the influence of active human participation (Caswell et al., 2013). The presence of excess correlation between electronic, or inorganic, systems whose structure share similarities to the functional and fundamental structure of the brain within which consciousness has been assume to emerge or to be correlated could help separate the confusion between the type of matter that composes consciousness and it excess correlation and the structure of these relationships independent of the constituents. The RNG micro-circuits involve PN junctions whose interface is very similar to

that of the synapse of the human brain. The widths of the functional zones are about 1 micrometer. The separation is within the range of visible wavelengths. The present experiment was designed to discern if excess correlation could occur between two random number generators. If excess correlation emerged from the property of random fluctuations and whatever process that drives it, then the quintessential property of entangled systems should emerge. Here the property would be, if the two systems were entangled, a deviation from change in one direction within one locus at the same time there was a deviation in the other direction at the non-local area. In the present experiment this "entanglement" was accomplished by the same dual-coupled circular magnetic field array with rotating magnetic fields display changing angular velocities as was required for the display of excess correlation in the photon emissions and water pH shifts.

4.2 Methods

An experimental procedure was conducted over 25 days of testing with two Random Event Generators (REG's) and two "Octopus devices" in two remote locations within the consciousness lab at Laurentian University (Figure-4.1).

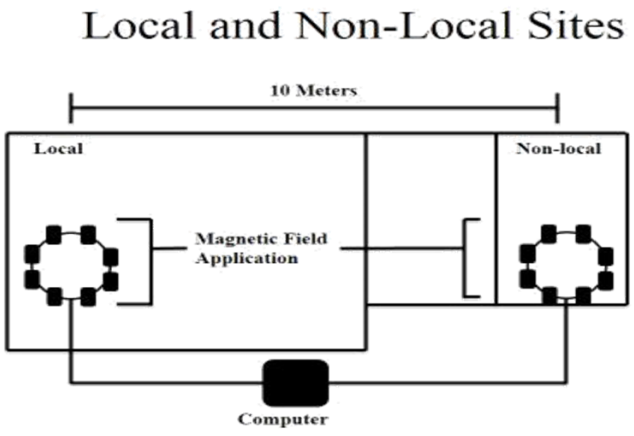

Figure 4.1 Visual representation of local and non-local sites in the Random Event Generator excess correlation paradigm

The two octopus devices produced weak fields that were about 1 microTesla within the center within which the RNGs were placed. The strength is equivalent to 1,000 nT which approaches the intensities that occur over large areas during some geomagnetic storms. The devices produced the fields through eight small solenoids placed around REG's. The REG's manufactured by Psyleron. They generate random 1's and 0's by utilizing the quantum wave-functions of electrons when using two streams of random generation from two transistor chips which undergo Boolean Exclusive-OR logic gate operation procedures.

The experimental REG 'entanglement' procedure included nine 2 minute conditions spaced by 1 minute intervals which commenced in the following order: baseline 1 (BL1), baseline 2 (BL2), Thomas 1 (T1), Thomas 2 (T2), Burst-X 1 (B1), Burst-X 2 (B2), Burst-X 3 (B3), baseline 3 (BL3), baseline 4 (BL4). The REG's were synchronized through stop watches which ran continuously throughout the experiment. All field conditions involved 1,1 ms delay between points and point duration presentations. Several variables were collected from each REG in each condition including: overall z-score, mean, standard deviation, max/min z-score value and min/max z-score location within output.

4.3 Results

When min z-scores were entered into one-way analysis by REG location (Local/non-local) during the 2nd Thomas condition and 1st Burst-X condition, a significant shift in the displacement or random variation was observed (Table-4.1).

Table 4.1 Significant differences in REG values during field conditions prior to the 2nd Burst-X exposure condition

Significant Condition & Variable By REG	F-Statement
Thomas 2 Min Z-score	[$F_{(1,47)}$=7.40, p<.01, η^2=.14]
Burst-X 1 Min Z-score	[$F_{(1,47)}$=6.63, p=.01, η^2=.12]

Post-hoc analysis indicated that the non-local REG deviated significantly further from chance expectation in the 0 direction in comparison to the local REG during the 2nd Thomas condition [$F_{(1,47)=}$7.40, p=<.01, η^2=.14] (figure-4.2)

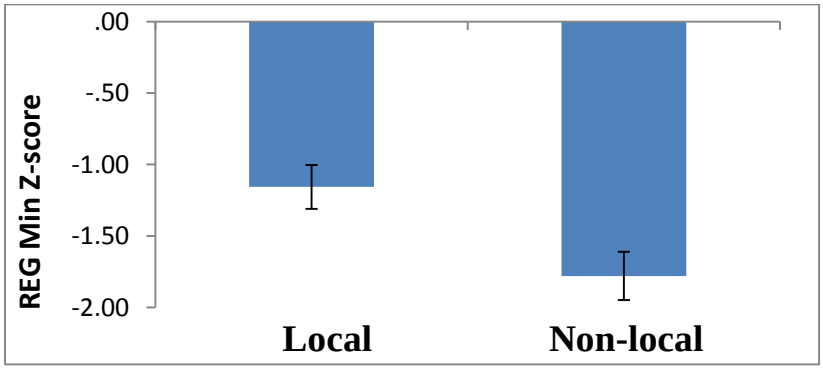

Figure 4.2 REG Min Z-score values during the 2nd Thomas Pulse exposure by location

It was also determined through *post-hoc* analysis that the local REG deviated further from chance expectations in the 0 direction in comparison to the non-local REG during the 1st Burst-X condition [$F_{(1,47)}$=6.63, p=.01, η^2=.12] (Figure4.3).

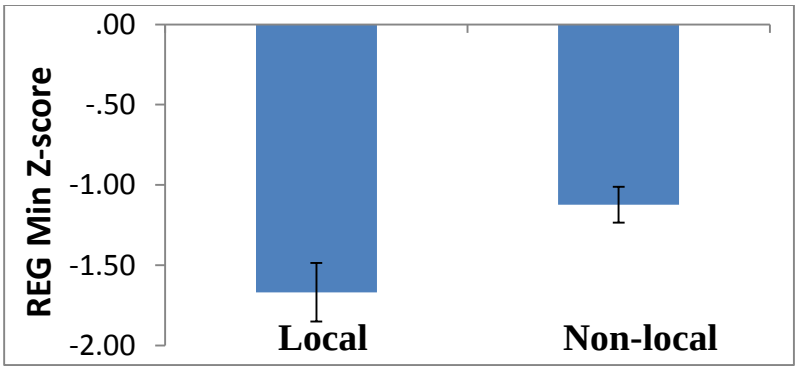

Figure 4.3 REG Min z-score values during the 1st Burst-X exposure by location

When mean scores, max z-scores, min z-scores, and overall z-scores were entered into one-way analysis as a function of REG location (local vs nonlocal) during the 2nd Burst-X condition, significant effects were observed (Table-4.2).

Table 4.2 Significant variable by Random Event Generator location results during 2nd Burst-X exposure

Variable	F-statement by REG location
Mean during Burst-X 2	[$F_{(1,47)}$=10.16, p<.01, η^2=.18]
Max Z-score during Burst-X 2	[$F_{(1,47)}$=7.14, p=.01, η^2=.13]
Min Z-score during Burst-X 2	[$F_{(1,47)}$=13.97, p=.001, η^2=.23]
Overall Z-score during Burst-X 2	[$F_{(1,47)}$=10.2, p<.01, η^2=.18]

The results indicated that the local REG deviated significantly away from chance expectations in the 1 direction and the non-local REG deviated significantly away from chance expectations specifically in the 0 direction when observing mean scores by REG during the 2nd Burst-X condition [$F_{(1,47)}$=10.16, p=<.01, η^2=.18] (Figure-4.4).

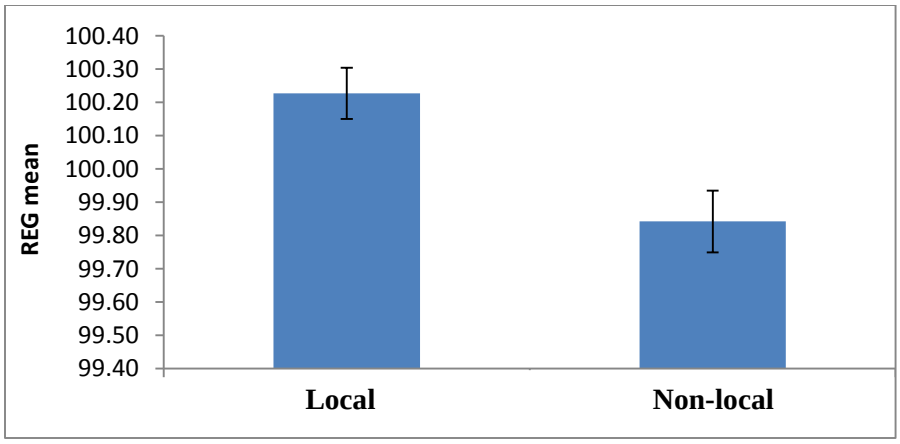

Figure 4.4 Significant differences in Random Event Generator means (# of 1's/200) by location (local/non-local) during the 2nd Burst-X exposure

One-way analysis of variance conducted on max z-scores by location indicated that the local REG significantly deviated further in the 1 direction in relation to the non-local REG during the 2nd Burst-X condition [$F_{(1,47)}$=7.14, p=.01, η^2=.13] (Figure-4.5).

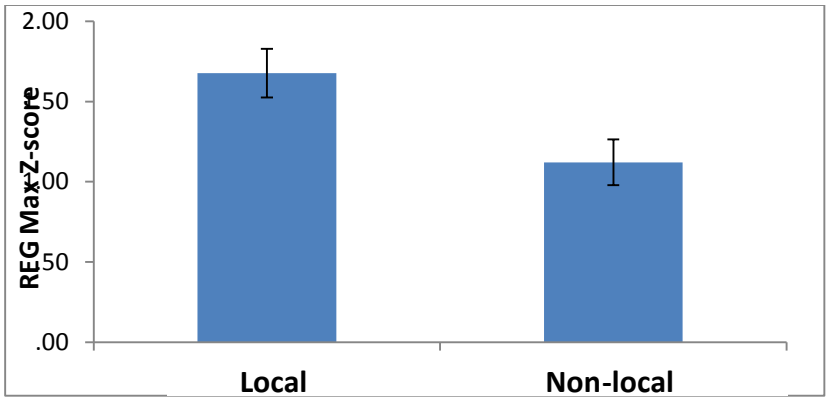

Figure 4.5 Significant differences in Max z-score means by Random Event Generator location (local/non-local) during the 2nd Burst-X exposure

Min z-scores displayed significant mean differences by REG location during the 2nd Burst-X condition. The non-local REG significantly deviated further in the 0 direction in relation to the local REG [$F_{(1,47)}$=13.97, p=.001, η^2=.23] (Figure-4.6).

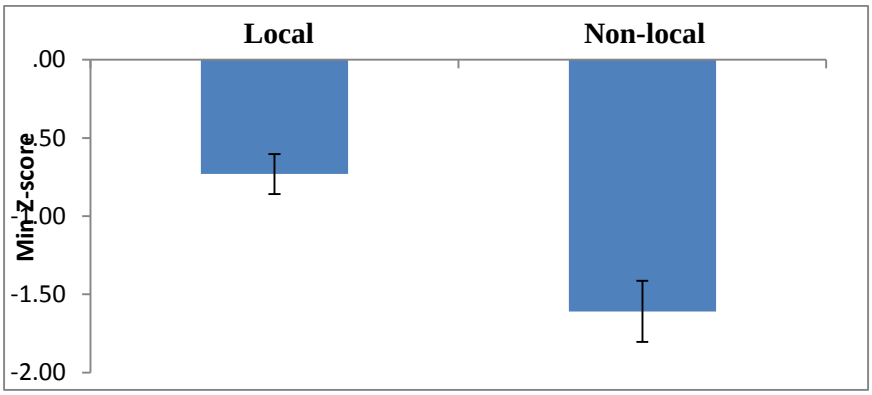

Figure 4.6 Significant differences in min z-score means by Random Event Generator location (local/non-local) during the 2nd Burst-X exposure

Overall z-scores by REG during the 2nd Burst-X condition resembled mean scores by REG during this condition insofar as the Local REG deviated significantly away from chance expectations specifically in the 1 direction. The non-local REG deviated significantly away from chance expectations in the 0 direction [$F_{(1,47)}$=10.20, p=<.01, η^2=.18] (Figure-4.7).

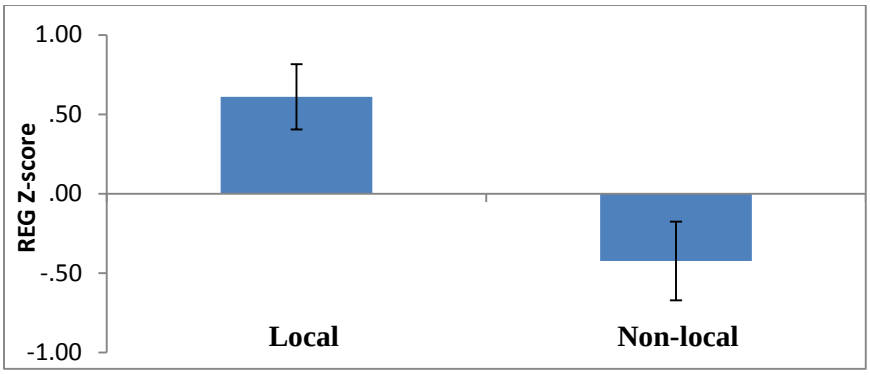

Figure 4.7 Significant differences in Overall z-score means by Random Event Generator location (local/non-local) during the 2nd Burst-X exposure

When mean scores, standard deviation scores, max z-scores, min z-scores, and overall z-scores were entered into a discriminant analysis within SPSS in order to predict membership to REG location (Local/non-local), a marked differentiation occurred [$\chi_{(3)}$=22.20, p=<.001, =.57]. As shown in Tables 4.3-4.4 the function was based on min z-scores during the 1st Burst-X condition [Δ(1-)=.17], min z-scores during the 2nd Burst-X condition [Δ(1-)=.21], and overall z-scores during baseline 4 [Δ(1-)=.06]. This function correctly identified 75% of cases in a cross-validation analysis.

Table 4.3 REG Means and Standard Deviations between location (local/non-local) for select Random Event Generator variables which were significantly different between non-local locations

Variable	REG location	Mean	SD
Min Z-scores during B1*	Local	-1.67	.89
	Non-local	-1.12	.56
Min Z-scores during B2**	Local	-.73	.63
	Non-local	-1.61	.97
Overall Z-scores during Bl4	Local	.05	.89
	Non-local	-.27	1.12

***p<.05, **p=.001**

Table 4.4 Canonical discriminant function coefficients; accommodating location with select Random Event Generator variables

				Canonical function coefficients	
	Δ(1-)[a]	**Rao's V**	**V Change**	**Unstandardized**	**Standardized**
Min Z-scores during B1	.17	8.26**	8.26**	-1.28	-.96
Min Z-scores during B2	.21	24.43***	16.17***	1.04	.87
Overall Z-scores during Bl4	.06	30.93***	6.50*	.49	.49
(Constant)				-.48	

***p<.05,**p<.01, ***p<.001**

When average values were calculated for REG variables (Overall z-scores, mean, max z-scores, min z-scores, and standard deviation scores) at 2-4 minutes of field exposure during Thomas and Burst-X conditions and then entered into one-way analysis by REG location (Local/non-local) differences were statistically significant (Table-4.4.).

Table 4.5 Average REG values for select variables (overall z-score, mean, max z-score, min z-score, and Standard Deviation) after 4 minutes of field exposure from Thomas Pulse and Burst-X by REG location

Variable	**F-statement by REG**
Overall Z-score average	[$F_{(1,48)}$=10.06, p=<.01, η^2=.17]
Mean average	[$F_{(1,48)}$=10.01, p=<.01, η^2=.17]
Max Z-score average	[$F_{(1,48)}$=15.66, p=<.001, η^2=.25]
Min Z-score average	[$F_{(1,48)}$=22.50, p=<.001, η^2=.32]
SD average	[$F_{(1,48)}$=0, p=.99, η^2=.00]

With regard to average values at 2-4 minutes of field exposure during Thomas and Burst-X conditions for overall z-scores, the local REG deviated significantly away from chance expectations specifically in the up (1) direction. On the other hand the non-local REG deviated significantly away from chance expectations in the 0 direction [$F_{(1,48)}$=10.06, p=<.01, η^2=.17] (Figure-4.8).

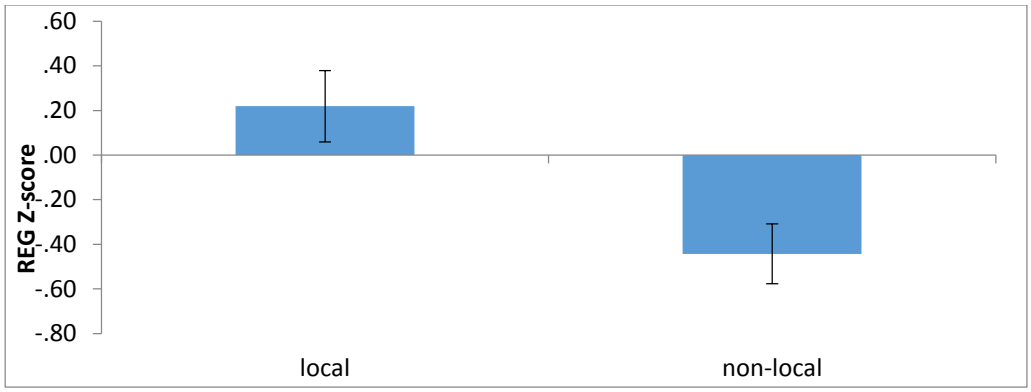

Figure 4.8 REG Z-score values by location (local/non-local) at 4 minutes of field exposure (Thomas Pulse and Burst-X)

With regard to average values at 2-4 minutes of field exposure from Thomas and Burst-X conditions for mean values by REG, the local REG deviated significantly away from chance expectations in the 1 direction. The non-local REG deviated significantly away from chance expectations in the 0 direction [$F_{(1,48)}$=10.01, p=<.01, η^2=.17.] (Figure-4.9).

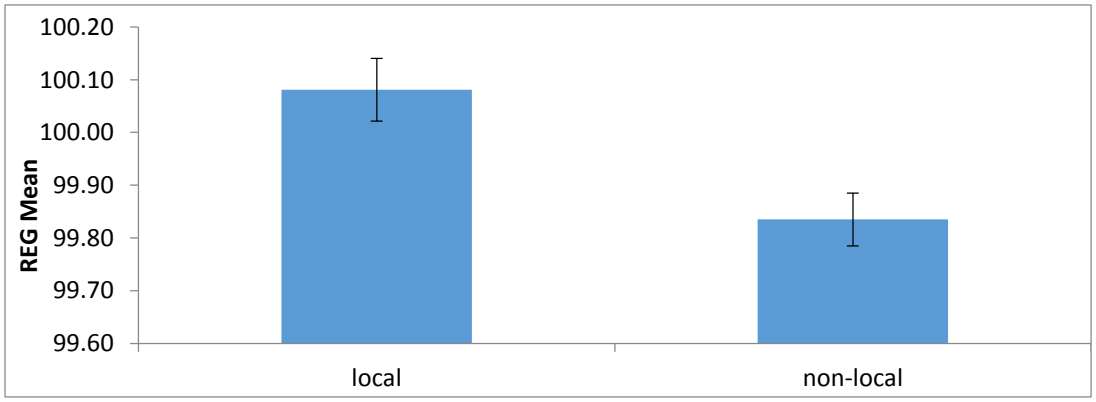

Figure 4.9 REG Mean values by location (non-local/local) at 4 minutes of field exposure (Thomas Pulse & Burst-X)

Average values for max z-scores by REG during 2-4 minutes of field exposure from Thomas and Burst-X condition revealed the local REG deviated significantly further from chance expectations in the 1 direction in relation to the non-local REG [$F_{(1,48)}$=15.66, p=<.001, η^2=.25] (Figure-4.10).

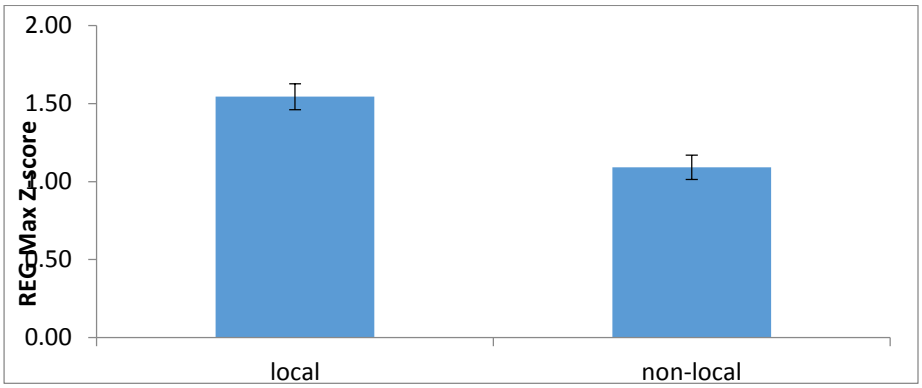

Figure 4.10 REG Max z-score values by location (local/non-local) at 4 minutes of field exposure (Thomas Pulse & Burst-X)

Average values for min z-scores by REG during 2-4 minutes of field exposure from Thomas and Burst-X conditions demonstrated that the non-local REG deviated further from chance expectations in the 0 direction in relation to the local REG [$F_{(1,48)}$=22.50, p=<.001, η^2=.32] (Figure-4.11).

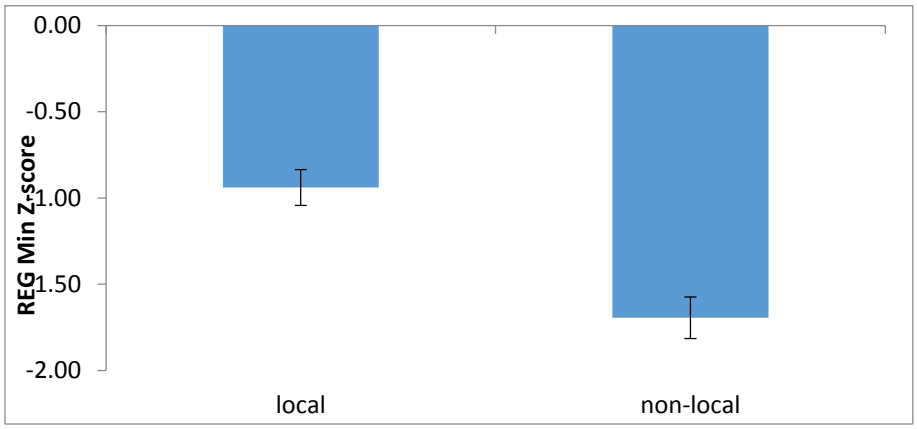

Figure 4.11 REG Min z-scores values by location (local/non-local) at 4 minutes of field exposure (Thomas Pulse & Burst-X)

Interestingly, average values for standard deviation scores of REG scores during minutes 2-4 of field exposure from Thomas and Burst-X conditions was not found to be significant [$F_{(1,48)}$=0, p=.99, η^2=.0] (Figure-4.12).

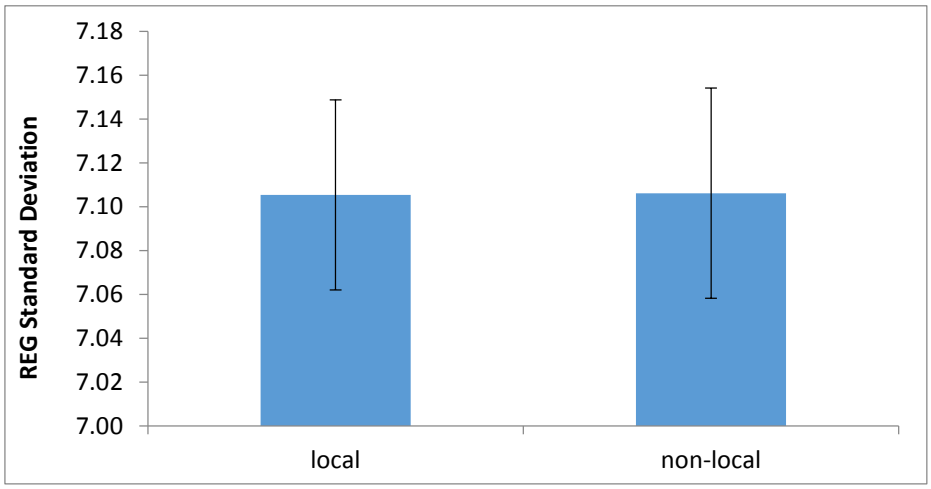

Figure 4.12 REG Standard Deviation values by location (local/non-local) at 4 minutes field exposure (Thomas Pulse and Burst-X)

When these average values at 2-4 minutes of field exposure during Thomas and Burst-X exposure were entered into a discriminant analysis in order to predict membership of REG location a significant function emerged [$\chi_{(3)}$=18.26, p=<.001, =.68]. It was based on average min z-scores at 2-4 minutes of field exposure during Thomas and Burst-X conditions [Δ(1-)=.32] (Tables 4.6-4.7).

Table 4.6 Means and standard deviations for REG Min z-score values by location (local/non-local) at 2-4 minutes of field exposure (Thomas Pulse and Burst-X)

Variable	REG location	Mean	SD
Average Min Z-scores during 2-4 minutes of EM-field exposure	Local	-.94	.52
from Thomas & Burst-X*	Non-local	-1.69	.60

***p<.001**

Table 4.7 Canonical discriminant function coefficients (2): accommodating Random Event Generator location (local/non- local) by average Min z-score values at 2-4 minutes of field exposure (Thomas Pulse and Burst-X)

				Canonical function coefficients	
	Δ(1-)[a]	Rao's V	V Change	Unstandardized	Standardized
Average Min Z-scores during 2-4 minutes of EM-field exposure from Thomas & Burst-X					
(Constant)	.32	22.50*	22.50*	1.78	1.00
				2.34	

Overall field condition scores (Thomas pulse =p1, p2; Burst-X= e1,e2) for REG mean, standard deviation, max z-score, and min z-score can be observed in Figures 4.13-4.16.

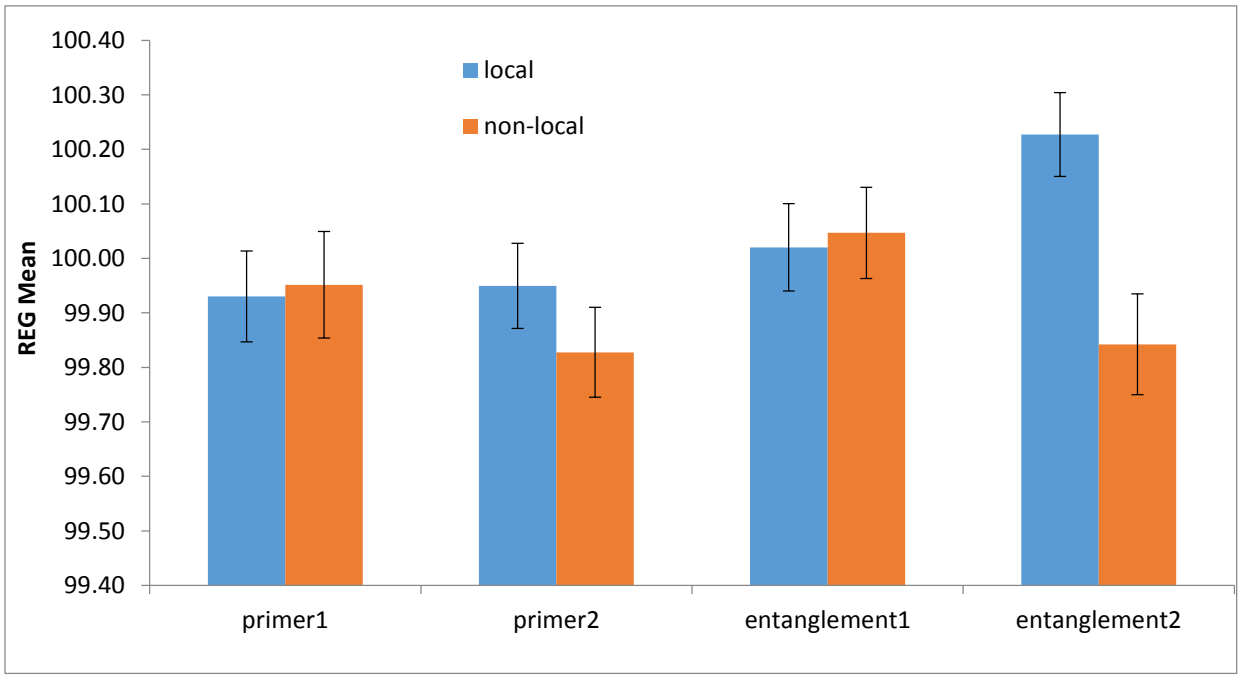

Figure 4.13 REG mean values by location (local/non-local) during primer and entanglement conditions

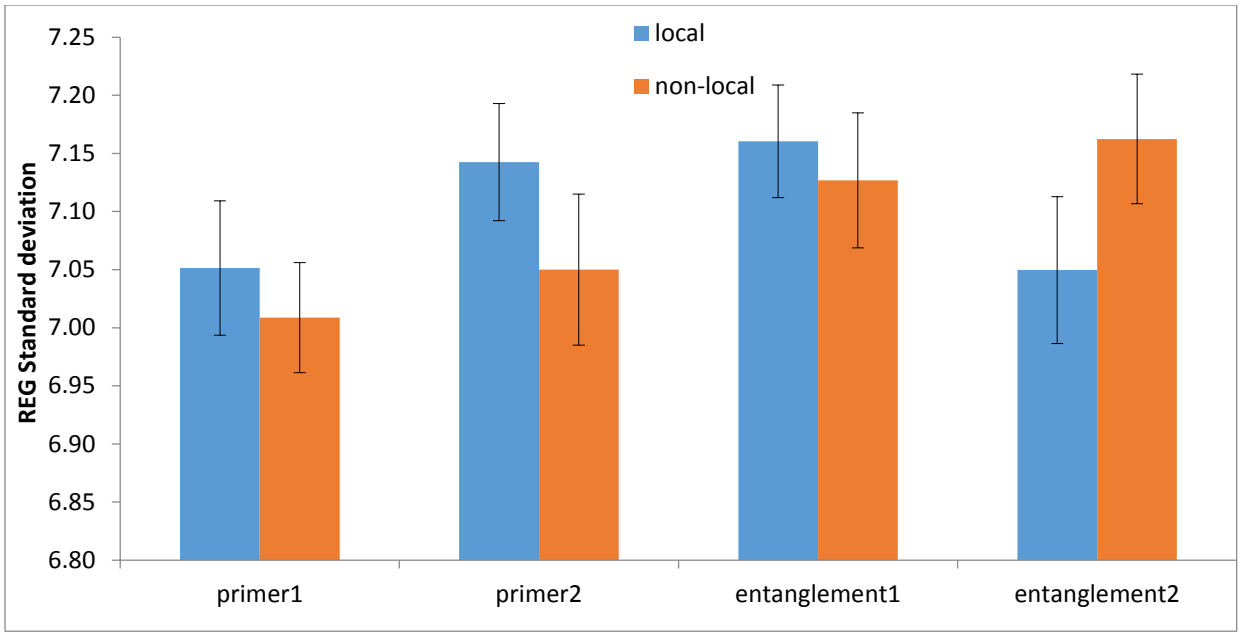

Figure 4.14 REG Standard Deviation values by location (local/non-local) during primer and entanglement conditions

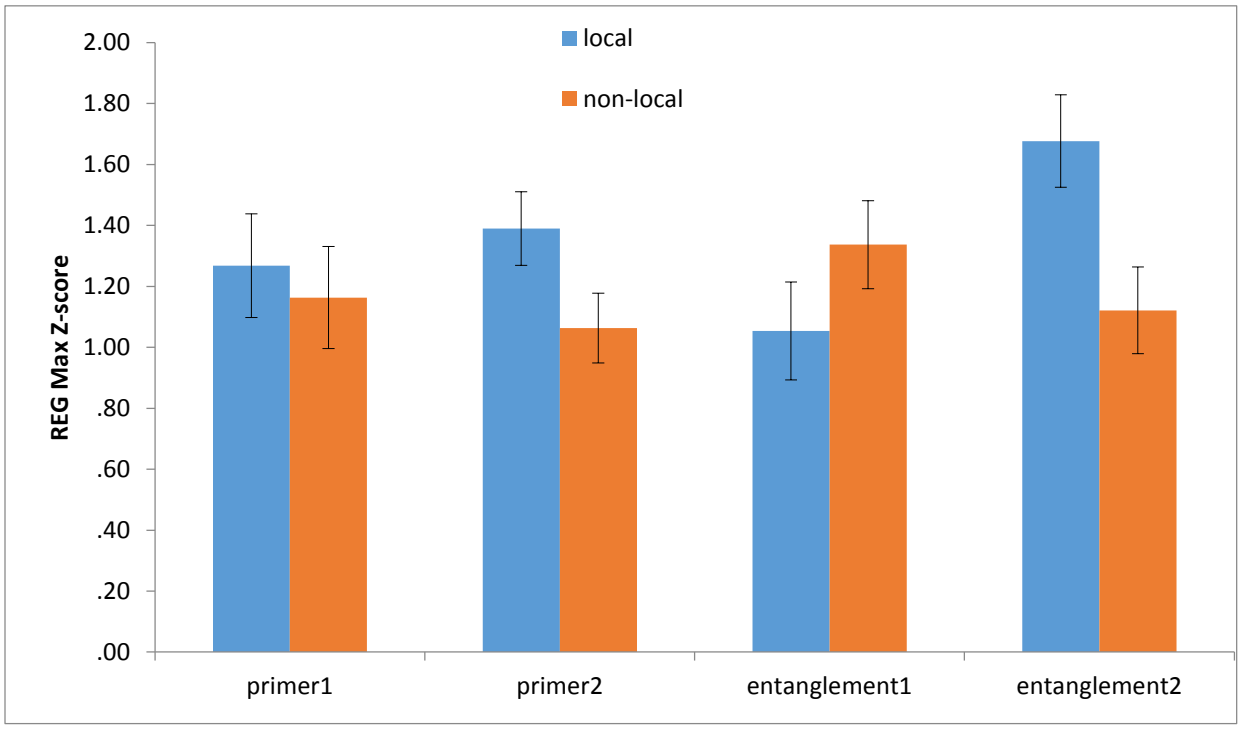

Figure 4.15 REG Max z-score values by location (local/non-local) during primer and entanglement conditions

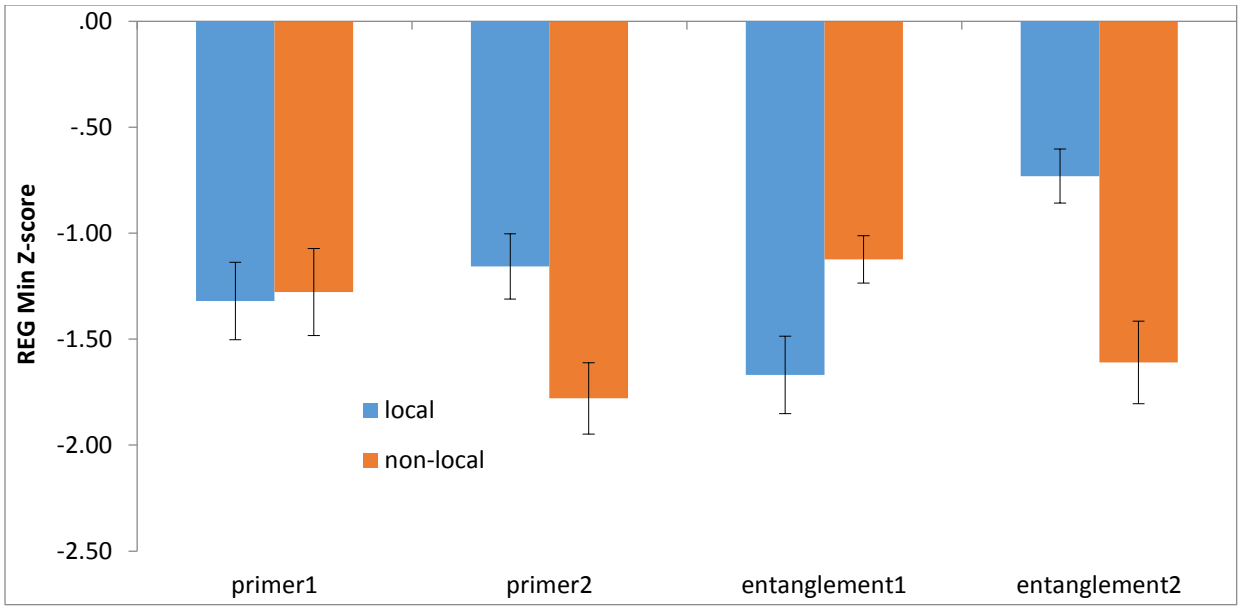

Figure 4.16 REG Min Z-score values by location (local/non-local) during primer and entanglement conditions

4.4 Discussion

Conventional assumptions of interactions between units, be them atoms or photons, assume an intrinsic locality by which some processes mediates the reaction between two spaces occupied by those units. Non-locality assumes there are no necessary processes that mediate the association and in fact the changes occur simultaneously as if the two loci where superimposed into the same space. For the traditional "excess correlation" between photons, the experimental shift in polarity in one direction of one of the pairs of photons is associated with the simultaneous shift in polarity of the other photon in the opposite direction.

In the present experiment random physical systems, the same equipment that was affected by intention also appeared to display excess correlation if the two loci shared the optimal magnetic field configuration. This occurred from the simultaneous application of rotating electromagnetic fields. Although no human participants were used in the study both REG's used within the

experiment underwent an alteration in random computation during primer and entanglement conditions. The shifts in random number generation for the two systems were in opposite direction. This might be considered analogous to the opposite polarity exhibited by paired, entangled photons.

If only 1 REG device was used within this particular experiment then one might conclude that a field effect was apparent. However having two REG measures undergoing the same EM field treatments resulted in a type of parity. The output of each REG fluctuated away from chance expectation throughout the duration of the experiment but in the opposite direction. The results also suggest this effect required only about 4 minutes to emerge, despite the weak complex EM configuration.

The most robust REG effects did occur during the 'entanglement' condition that has elicited significant shifts in non-local pH units, increased non-local photons from the injection of local proton donors, and increased shared sources of electroencephalographic power. Assuming (1) EM fields were used to facilitate entanglement, (2) that we are all immersed within the earth's EM field, and (3) that humans have a significant influence on the production of random event computation, then the effects of directed human intention could be able to affect non-local events if they shared 'excess correlation' or 'entanglement' features through naturally occurring and abundant geomagnetic energies.

5 Chapter 5 Discussion

The results of these experiments could suggest that the paradigm representing the classical mechanical approach of understanding Mind Matter Interaction and the role of consciousness within the universe should be modified. The general patterns, of which there were many relationships that can be gleaned from these multiple quantitative analyses, is that specific weak magnetic fields applied to the cerebrums of human beings during intention upon "random" processes can modify the direction of these processes. The "smallness" of the effect with respect to deviation from chance should not reduce its significance. From some perspectives the events that ultimately result in the collapse of a building or the failure of an electronic system aboard an aircraft begins with a single electron whose energies are well within those that were affected at the PN junctions in the experiments. As calculated by Persinger, Koren and Lafreniere (2008) the difference in energies near light velocity to produce the shift in radius from a wave to a particle, perhaps the analogue of the "collapse of the wave function, is in range of 10^{-20} J.

The data from the three separate experiments act both as a confirmatory analysis and as a novel report in understanding the role of "consciousness" within the universe. In the case of the former, the findings that human intention has the ability to significantly alter the production of random events computed from a REG device has been reported for as long as such measurements were made available. The role of 'excess correlation' between two non-local stimuli in remote but 'shared spaces' due to the facilitation of specific EM field applications may add to the potency of intention. It has already been demonstrated at different levels of discourse ranging from the spin of an electron to coupled QEEG readings of specific frequency bands in localized regions.

To the author's knowledge this thesis is the first to quantify the patterns of subject experiences experience as inferred by traits of absorption associated with both the multiple matrices of human brain activity and position (the location of the sensors). Although the multiple tables of associations may appear to be endless lists of numbers they were presented not as proofs but as a reservoir of data that might be mined at some future time for relevant relationships. Results from said analysis should allow investigators to obtain a more complete understanding of the many aspects of this trait when the TAS is implemented in clinical settings and as a diagnostic tool.

Aspects of the trait of absorption were able to identify and distinguish "high" and "low" hitters for specific Psi tasks during baseline as well as during exposures to specific physiologically-patterned EM field. This finding could suggest that aspects of this trait might induce a higher "signal-to-noise ratio" even without applied magnetic field enhancements for the subtle stimuli that contribute to these phenomena. The scale would therefore act as a strong predictor of Psi ability. The absorption could be enhanced or exposed under the appropriate stimulation.

The absorption related traits that were associated with effects on random variation within the no field and baseline conditions included: "Can summon vivid and suggestive images", "Can become absorbed in own thoughts and imaginings", and "Responsive to inductive stimuli". Experiences such as "Vivid Reminiscence" and "Can vividly re-experience the past" entered the delta baseline predictive models that predicted this "psi" ability. The vigorous expression of absorption was demonstrated to be enhanced after the application of specific electromagnetic field configurations, namely Burst-X. This pattern has been associated with opiate-like experiences that facilitate detachment.

While the absorption trait "Can summon vivid and suggestive images" was not significantly associated with QEEG measures, the other non-field absorption related predictors of psi ability exhibited associations with left occipital activation and increases in slower wave activity over the right temporal and left parahippocamal regions. This was evident for the "becoming self-absorbed" Content cluster 6 items. Decreased activity in frequencies associated with active thinking in regions of the brain associated with body boundary (the parietal lobe) as well as increased alpha activity in the left central regions (which has been associated with "images of words" in the absence of EM field exposure was also observed.

The vigor component of absorption in-and-of-itself as identified in this study might stem from the decreased frontal lobe inhibition which appears to be QEEG signatures of absorption. The QEEG profiles of psi related states and traits as specified by the TAS are associated with decreases in occurrence, length, and global field power (GFP) of common states and increases in uncommon states as suggested by the microstate predictors of these subjective measures. A decrease in GFP for class A microstates (the right frontal-left caudal diagonal parity) for example was the main predictor of high scorers and who report frequent ESP-like episodes. This was accompanied by gamma fluctuations (40 Hz) from the left frontal lobe to the right temporal lobe, a feature that is central to consciousness related phenomenon and a classic configuration for the relationship between intention and photon emission during imagination from the right temporal lobe. The argument of absorption as a *trait* as opposed to a *state* was supported given the significant Δt between the time of the baseline QEEG recordings and when the TAS was completed.

Discrepancies in REG data during (1) human intention, (2) human baseline, (3) no-human baseline and (4) no-human EM field conditions could provide information as to how reliable, consistent, and significant deviations in random physical systems are manifested. Discrepancies between EM field configurations also elicited unique results. In the case of the primer field (Lindagene) as described in Chapter 2, min z-scores were achieved significantly more quicker in the background (non-human) conditions in comparison to human conditions for 1,1 and 3,3 millisecond field parameters.

Human and background testing did differentiate the length of time necessary to obtain the min z-score value within the REG output. The min z-scores appeared within 10-25 seconds for both 1,1 and 3,3 field parameters during non-human testing and 50-150 seconds during human testing for both 1,1 and 3,3 field parameter conditions. The time it took for the min z-score value to appear within either human or background testing was not significantly different as a result of field parameter control. This is important because the min and max values indicate the boundary conditions of the output. The larger values indicated greater bias within the electron tunneling processes occurring within the device. This finding suggests that despite discrepancies in field presentations, field effects remained constant despite the facilitation of lower (1,1) or higher (3,3) order processes when analyzing REG data in the presence *or* absence of human proximity/intention.

This non-discrepancy in effects for both 1,1 and 3,3 millisecond EM field presentation on REG output is also important. Only 1,1 point duration and delay between point configurations were

employed in the excess correlation study. Robust field and REG effects were apparent. This is to be expected insofar as the EM fields used were configured and ordered such that the effects of the treatment could affect quantum processes associated with electrons. According to the calculations by Persinger and Koren, who employed the Hubble parameter applied to Planck's length, 1 ms durations are more consistent with the time for an electron to expand one Planck's Length while 3 ms is the time more typical of the proton. These predictions were supported by experimental data by Koren, Dotta and Persinger (2014) for photon reactions.

The concept of non-local random events demonstrating excess correlation through electromagnetic stimulation is intriguing. The earth's EM field has an average intensity of 50,000 nT (0.5 Gauss). Assuming there are random events that can be actively attended too and significantly influenced by focused human intention, then one might speculate – at least with regard to this data – that deviations in non-local or unfocused random events could correspond to the changes in the local or focused random events due to the conservation of energy derived from solutions from the 2^{nd} law of thermodynamics.

With an intrinsic energy of 10^{-20}J associated with cellular activity, membrane function, and the energy of a single action potential (assuming a net charge of 120 mV (1.2×10^{-1}V) which converts to a unit charge of 1.6×10^{-19} Amp-seconds) coupled with a total immersion within the earths electromagnetic field with an average intensity of 50,000 nT (.5 Gauss), there is a seemingly a possible and intricate relationship between forces, energies, and frequencies between the earths EM field and the resonant frequency of the human with regard to human influence and influence on the human. For example this quantum of energy divided by the

earth's average magnetic field of 10^{-5} T would be equivalent to a magnetic moment of 10^{-15} A-meter-squared. When multiplied by the typical amplitude shared by geomagnetic activity and changes in the gravitational constant G, that is 5 nT (Persinger and St-Pierre, 2013), the second order energy would be in the range of 10^{-24} J. This is sufficiently close to the frequency of the neutral hydrogen frequency line (1.42 GHz) to allow an expansion over non-traditional distances.

Assuming 10^{13} synapses within the human brain, the average calculated value within the cerebral cortices (Persinger, 2010) and each synapse interface reflected the resting membrane potential of about 0.1 V (100 mV), the "total" potential difference would be 10^{12} V and when spread across the cerebral cortices of 3 mm, would be equivalent to $3 \cdot 10^{14}$ $V \cdot m^{-1}$. Although this value would appear excessive it may not be coincidence that when divided by magnetic field strength from all of the energy within the final epoch of the universal volume ($1.5 \cdot 10^{-9}$ T), the solution is $2 \cdot 10^{23}$ $m \cdot s^{-1}$. This is the same coefficient and order of magnitude as the entanglement latency calculated by Persinger and Koren (2013) from the four dimensional structure of universal geometries.

Nunez postulated that these synapses are confined to a limited space, insofar as the circumference of the space to which these synapses are contained within – about 1.73 x 10^{-3} m^3. This aggregate plus the bulk velocity of 4.5 $m \cdot s^{-1}$ results in a resonant frequency of the human brain to be in the frequency range of about ~7Hz, a value proximal to that of the Schumann resonance- the intrinsic resonance of the earth itself (Nunez, 1995). The second harmonic of the Schumann resonance has been shown mathematically to be a potential interface for gravitational waves, one of the presumed correlates for entanglement.

A cerebral state operating in low alpha electroencephalographic band would result in an abundance of action potentials firing in a contained space and time which could be resonant with that of the Schumann resonance. This frequency (1/s= Hz) -with regard to the earth - is obtained by dividing the velocity by the circumference. Persinger has calculated, assuming the speed of light of 3×10^8 m/s and the circumference of 40,000 km (4×10^7 m) , the natural frequency of the earth to be 7.8 Hz (Persinger, 2012). This value is frequently described as the Schumann resonance (Cherry, 2002).

If this overlap in fundamental frequencies from both the earth and the energies emitted from that of select cerebral thinking processes do in fact converge or interact, one might speculate that energies, forces, and frequencies between these magnetic fields have an intricate relationship which may be the means to significantly altering random events in both local and non-local contexts. The energies would always be present. The strength would increase or decrease as the brain and the Schumann system drifted between as well as in and out of phase coupling.

If for example the billions of neurons and synapses within the human brain are activated coherently as a field. Influence of extra cellular space through subtle but measurable energies could have large consequences. Several experiments have demonstrated that the action potential of only one neuron can affect the activity of an overt complex behavior in mammals (Houweling & Brecht, 2007). The state-dependent organization of the entire cerebral manifold was shown by Yu-Cheng and colleagues to be modified by a single neuron.

The effects of field treatment on the Remote Behavioral Guessing measure provided interesting

differences in accuracy by condition. Accuracy during the primer field ("lindagene") appeared to be more accurate than the other field conditions. This primary field was composed of about 25 different physiologically-based patterns that were sufficient to affect the migration of neurons within the hippocampal formation in rats if they were exposed continuously to this configuration during prenatal development.

The measurable effects of the field can be observed in the spectral analysis of baseline and Lindagene conditions for human and background (non-human) testing conditions. In this case the analyses of the delta power when comparing the change in REG frequencies from baseline to primer field conditions for both human and background testing revealed how the participant might influence the REG during primer field application in comparison to baseline (no field) intention. Additional research could isolate more clearly how the EM fields affect REG fluctuations associated with electron tunneling during primer field conditions in comparison to no-field baseline REG output. Humans have the capacity to alter random physical systems but the appropriate and specific temporal configurations (albeit electromagnetic in nature) might also have an effect on random computation and may be the facilitating agent in such a process.

Is it not intuitive to assume that Eddington's solutions and convergences are correct? That is to say, why would there be the necessity of multiple perspectives of the same thing (the universe or reality) if they were not to change or have an affect on what is experienced. Eddington suggested that perhaps the very act of observation was all that was required. Indeed photon emissions have been demonstrated from an actively engaged cerebrum and have even been recorded from the retina while in the act of observation.

Would the universe not correspond to these energies then? Even the possibility that a multiverse collapses into and out of physical form and dictates or responds to the likelihood of probable sequences of events determined by previous and future events suggests that intention, the net sum of quanta of neuronal energy, becomes relevant. Perhaps ‘random’ does not exist at all. Perhaps “random” is the result of the limited temporal and spatial span of perception (and measurement). The interaction between cerebral intention and the functional space of the RNG may have occurred because they share similar spatial (1 um width), boundary interaction (electron tunnelling or gap junction electron jumps) and temporal (millisecond) levels of discourse.

6 Appendix

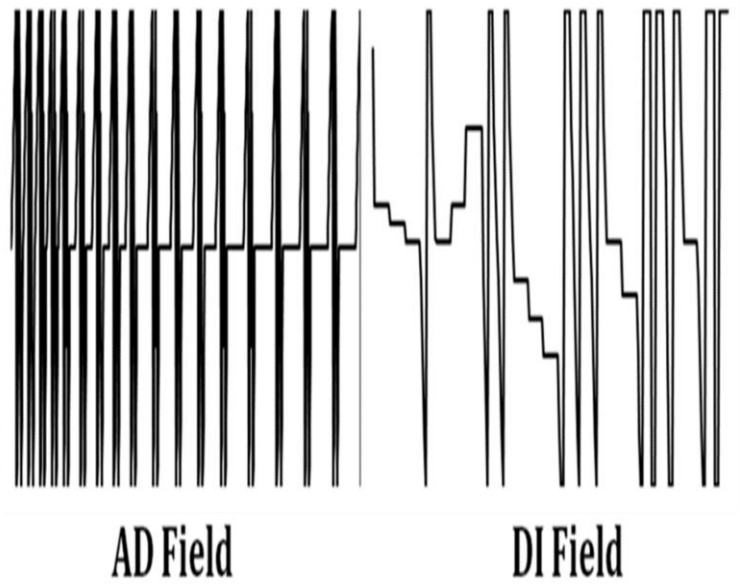

Figure 6.1 Visual Representation of Thomas Pulse (AD Field) and Burst-X (DI Field) field configurations

7 References:

Ahn, J., Weinacht, T.C., & Bucksbaum, P.H. (2000). Information storage and retrieval through quantum phase. *Science,* 287:462-466.

Aczel, A.D. (2002) Entanglement: The Greatest Mystery in Physics.

Atmansphacher, H., Bosch, H., Boller, E., Nelson, R.D., & Scheingraber, H. (1999). Deviations from Random Physical Randomness Due to Human Agent Intention?. *Chaos, Solitons & Fractals,* Vol. 10, No. 6, pp. 935-952.

Atmanspacher, H. (1989). The aspects of information production in the process of observation. *Foundations of physics*, 19, 533-577.

Baker-Price, L.A., & Persinger, M.A., (1996). Weak, but complex pulsed magnetic fields may reduce depression following traumatic brain injury. Perceptual and motor skills, 83(2), 491-498.

Bierman, D.J. (1996). Exploring Correlations Between Local Emotional and Global Emotional Events and the Behavior of a Random Number Generator. Journal of Scientific Exploration, Vol. 10, No. 3, pp. 363-373.

Belicki K., & Belicki D. (1986). Predisposition for nightmares: A study of hypnotic ability, vividness of imagery, and absorption. Journal of Clinical Psychology, 42: 714-718 [PubMed: 3760201].

Bosch, H., Steinkamp, F., & Boller, E. (2006). Examining Psykchokinesis: The Interaction of Human Intention With Random Number Generators- A Meta-Analysis. Psychological Bulletin, Vol. 132, No. 4, 497-523.

Braud, W. G. (2000). Wellness implications of retroactive intentional influence: Exploring and outrageous hypothesis. Alternative Therapies in Health and Medicine, 6, 37–48.

Burke, R.C., Gauthier, M.Y., Rouleau, N., & Persinger, M.A. (2013). Experimental Demonstration of Potential Entanglement of Brain Activity over 300 KM for Pairs of Subjects Sharing the Same Circular Rotating, Angular Accelerating Magnetic Fields: Verification by sLORETA, QEEG Measurements. Journal of Consciousness & Exploration Research, Vol. 4, Issue 1, pp.35-44.

Caswell, J.M., Collins, M.W.G., Vares, D.A.E., Juden-Kelly, L.M. (2013). Gravitational and Experimental Electromagnetic Contributions to Cerebral Effects Upon Deviations from Random Number Variations Generated by Electron Tunneling. *International Letters of Chemistry, Physics, and Astronomy*, 11, pp. 72-85.

Caswell, J.M., Vares, D.E.A., Juden-Kelly, L.M., & Persinger, M.A. (2014). Simulated Effects of Sudden Increases in Electromagnetic Activity on Deviations in Random Electron Tunneling Behaviour Associated with Cognitive Intention. *Journal of Consciousness Exploration & Research*, Vol. 5, Issue 2, pp. 85-102.

Challis G. C., & Stam, H.J. (1992). A longitudinal study of the development of anticipatory nausea and vomiting in cancer chemotherapy patients: The role of absorption and autonomic perception. *Health psychology*; 11: 181-189. [PubMed: 1618172].

Cherry, N. (2002). Schumman resonances, a plausible biophysical mechanism for the health effects of solar/geomagnetic activity. *Nat. Hazards*, 26, 279-331.

Crookes, W., Horsley, V., Bull, W. C., & Myers, A. T. (1885). Report on an alleged physical phenomenon. *Proceedings of the Society for Psychical Research*, 3, 460–463.

Dotta, B.T., Mulligan, B.P., Hunter, M.D., & Persinger, M.A. (2009). Evidence of Macroscopic Quantum Entanglement During Double Quantitative Electroencephalographic Measurements of Friends vs Strangers. *NeuroQuantology*, Vol. 7, Issue 4, pp. 548-551.

Dotta, B.T., Murugan, N.J., Karbowski, L.M., & Persinger, M.A. (2013). Excessive Correlated Shifts in PH within distal solutions sharing phase-uncoupled angular accelerating magnetic fields: Macro-entanglement and information transfer. *International Journal of Physical Sciences*, Vol. 8(36), pp. 1783-1787.

Dotta, B.T., & Persinger, M.A. (2011). Increased Photon Emissions from the Right But Not the Left Hemisphere While Imagining White Light in the Dark: The Potential Connection Between Consciousness and Cerebral Light. *Journal of Consciousness Exploration & Research*, Vol. 2, Issue 10, pp. 1463-1473.

Dunne, B.J., & Jahn, R.G. (1992). Experiments in Remote Human/Machine Interaction. *Journal of Scientific Exploration*, Vol. 6, No. 4, pp.311-332.

Dunne, B.J., Nelson, R.D., & Jahn, R.G. (1988). Operator-Related Anomalies in a Random Mechanical Cascade. *Journal of Scientific Exploration*, Vol. 2, No. 2, pp.155-179.

Feather, R. S., & Brier, R. (1968). The possible effect of the checker in precognition tests.*Journal of Parapsychology*, 32, 167–175.

Fickler, R., Lapkiewicz, R., Plick, W.N., Krenn, M., Schaeff, C., Ramelow, S., & Zeilinger, A. (2012). Quantum entanglement of high angular momenta. *Science*, 338:640-644.

Flor H., & Turk D.C. (1989). Psychophysiology of chronic pain: Do chronic pain patients exhibit symptom- specific psychophysiological responses? *Psychological Bulletin*, 105:215-259. [PubMed: 2648442].

Gloor, P. (1997). The temporal lobe and limbic system. New York: *Oxford University Press*.

Haan, N. (1963). Proposed model of ego functioning: Coping and defense mechanisms inrelationship to IQ change. *Psychological Monographs: General and Applied*, Vol. 77(8), 1-23.

Honorton, C., & Ferrari, D.C. (1989). "Future telling": A Meta-Analysis Of Forced-Choice Precogition Experiment, 1935-1987. *Journal of Parapsychology,* Vol. 53, December.

Hoffman, J., Krug, M., Ortegel, N., Gerard, L., Weber, M., Rosenfield, W., & Weinfurter, H. (2012). Heralded entanglement between widely separated atoms. *Science*, 337:72-75.

Houweling, A.R., & Brecht, M. (2007). Behavioural report of a single neuron stimulation in somatosnesory cortex. *Nature*, 450 (7172).

Jahn, R., Dunne, B., Nelson, R., Dobyns, Y., & Bradish, G.J. (1997). Correlations of random binary sequences with pre-stated operator intention: A review of a 12-year program. *Journal of Scientific Exploration*, 11(3), 345-367.

Julsgaard, B., Kozhekin, A., & Polzik, E.S. (2001). Experimental long-lived entanglement of two macroscopic objects. *Nature*. 413: 400-403.

Jun, B., & Kocher, P (1999). The Intel ® Random Number Generator. *Cryptography Research Inc. White paper.*

Kennedy, J.E., & Taddonio, J.L. (1976). Experimenter effects in parapsychological research. *Journal of Parapsychology,* 40(1), 33.

Maddocks, R.S., Matthews, S.,Walker, E.W., & Vincent,C.H. (1972). A compact and accurate generator for truly random binary digits," *J. Physics E,* vol. 5, no. 5, pp. 542–544, 1972.

McFadden, J. (2002). Synchronous firing and its influence on the brain's electromagnetic field: evidence for an electromagnetic theory of consciousness. *Journal of Consciousness Studies*, 9: 23-50.

McFadden, J. (2007). Conscious Electromagnetic (CEMI) Field Theory. *NeuroQuantology*, 2:262-270.

Ment, L.R., Vohr, B., Allen, W., Katz, K.H., Schneider, K.C., Westerveld, M., & Makuch, R.W. (2003). Change in cognitive function over time in very low-birth-weight infants, *Jama*, 289(6), 705-711.

Menzies V., Taylor, A.G., & Bourgiugnon C. (2008). Absorption: An individual difference to consider in Mind- Body interventions. *JHolist Nurs*, December 26(4): 297 302.doi:10.1177/0898010107307456.

Neff, D.F., Blanchard E.B., & Andrasik., F. (1983). The relationship between capacity for absorption and chronic headache patients' response to relaxation and biofeedback treatment. *Biofeedback and Self- Regulation*, 8:177-183. [PubMed: 6882814].

Nunez, P.L. (1995). Neocortical dynamics and human EEG rhythms. *Oxford University Press*, USA.

Parker, R.S., Rosenblum, A. (1996). IQ loss and emotional dysfunctions after mild head injury incurred in a motor vehicle accident. *Journal of clinicalpsychology*, 52(1), 32-43.

Persinger, M.A. (2010). 10-20 Joules as a Neurochemical Quantum in Medicine Chemistry: An Alternative Approach to Myriad Molecular Pathways?. Current Medicinal Chemistry, 17, 3094-3098.

Persinger, M.A. (2013). Billions of Human Brains Immersed Within a Share Geomagnetic Field: Quantitative Solutions and Implications for Future Adaptations. The Open Biology Journal, 6, pp. 8-13.

Persinger, M. A. (2012). Brain electromagnetic activity and lightning: potentially congruent scale-invariant quantitative properties. Frontiers in integrative neuroscience, 6.

Persinger, M.A., Koren, S.A., & Lafreniere, G.F. (2008). A NeuroQuantologic Approach to How Human Thought May Affect The Universe. NeuroQuantology, Vol. 6, Issue 3, pp. 262-271.

Persinger, M.A., Roll, W.G., Tiller, S.G., Koren, S.A., & Cook, C.M. (2002). Remote Viewing With The Artist Ingo Swann: Neuropsychological Profile, Electroencephalographic Correlates, Magnetic Resonance Imaging (MRI), And Possible Mechanisms. Perceptual and Motor Skills, 94, 927-949.

Persinger, M.A., & Saroka, K.S. (2012). Protracted parahippocampal activity associated with Sean Harribance. International journal of yoga, 5(2), 140.

Persinger, M.A. (2013). Support for Eddington's Number and his approach to astronomy: recent developments in the physics and chemistry of the human brain. International Letters of Chemistry, Physics and Astronomy, 8.

Pettinati, H.M., Horne, R.L., & Staats, J.M. (1985). Hypnotizability in patients with anorexia nervosa and bulimia. Archives of General Psychiatry, 42:1014-1016. [PubMed: 3862367].

Radin, D., & Nelson, R.D. (1989). Evidence for Consciousness-Related Anomalies in Random Physical systems. Foundations of Physics, Vol. 19, No. 12.

Radin, D.I., & Nelson, R.D., (2003). Meta-analysis of mind-matter experiments: 1959-2000. Healing, Intention and Energy-Medicine. London: Harcourt Health Sciences, 39-48.

Radin, D., Nelson, R., Dobyns, Y., & Houtkooper, J. (2006). Reexamining psychokinesis: comment on Bösch, Steinkamp, and Boller (2006).

Radin, D., Taft, R., & Yount, G. (2004). Effects of Healing Intention on Cultured Cells and Truly Random Events. The Journal Of Alternative And Complimentary Medicine, Vol. 10, No. 1, pp. 103-112.

Roche, S.M., & McConkey, K.M. (1990). Absorption: Nature, assessment, and correlates. Journal of Personality and Social Psychology, 59: 91-101.

Rose, D. (2006). Consciousness: philosophical, psychological and neural theories. Oxford: Oxford University Press.

Rosenthal, R. (1979). The file drawer problem and tolerance for null results. Psychological Bulletin, Vol 86(3), 638-641.

Saxon, J., & Wickramasekera, I. (1994). Discriminating patients with organic disease from somatizers among patients with chest pain using factors from the high risk model threat perception; Paper presented at the meeting of the Society for Experimental and Clinical Hypnosis; San Francisco, CA.Oct.

Shea J.D., Burton R., & Girgis, A. (1993). Negative affect, absorption, and immunity. Physiology & Behavior, 53:449-457. [PubMed: 8451309].

Smith, W.B., (1942). Dice Rolling Device. *United States Patent Office*, 2,269, 742, serial No. 397, 043.

Spekkens, R.W., & Rudolph, T. (2002). Quantum protocol for cheat-sensitive weak coin flipping. *Phys. Rev. Lett*, vol 89, 227901.

Storm, L. (2006). Meta-analysis in parapsychology: 11. Psi domains other than ganzfeld." *Australian Journal of Parapsychology*, 6(2), 135.

Tellegen, A., & Atkinson, G. (1974). Openness to absorbing and self-altering experiences ("absorption"), a trait related to hypnotic susceptibility. *Journal of abnormal psychology*, 83(3), 268.

Tellegen, A. (1992). Note on structure and meaning of the MPQ Absorption Scale. Unpublished manuscript, *University of Minnesota*, August.

Tellegen, A. (1982). Content categories: Absorption items (Revised). Unpublished manuscript, *University of Minnesota*, October 10..

Utts, J. (1991). Replication and Meta-Analysis in Parapsychology. *Statistical Science*, Vol. 6, No. 4, pp. 363-378.

Venkatasubramanian, G., Jayakumar, P.N., Nagendra H.R., Nagaraja, D., Deepthat, R., & Gangadhar, B.N. (2008). Investigating paranormal phenomena: Functional brain imagning of telepathy. *International journal of yoga*, 1:66-71.

Vincent, C.H. (1970). The generation of truly random binary numbers. *J. Physics E*, vol. 3, no. 6, pp. 594–598.

West, D. J., & Fisk, G. W. (1953). A dual ESP experiment with clock cards. Journal of the Society for Psychical Research, 37, 185–196.

Wickramasekera, I. (2000). On the interaction of two orthogonal risk factors, (1) hypnotic ability and (2) negative affect (threat perception) for psychophysiological dysregulation (sympathetic and parasympathetic) in somatization disorders. In: DePascalis, V., Gheoghiu, V.A., Sheehan, P.W.,Kirsch, I., editors. Suggestion and suggestibility- theory and research. Munich, Germany: hypnosis International Monograph, P. 245- 252.

Wickramasekera, I., & Pope A.T. (1990). Absorption: Nature, assessment, an correlates. Journal of Personality and Social Psychology, 59: 91-101.

Wickramasekera, I. (1995). Somatization-concept, data, and predictions from the high risk model of threat perception. Journal of Nervous and Mental Disease, 183: 15-23. [PubMed: 7807064].

Wickramasekera, I. (2003). The high risk model of threat perception and the trojan horse role induction: Somatization and psychophysiological disease. Handbook of mind-body medicine for primary care, P. 19-42.

Wickramasekera, I. (1988). What kinds of people are at high risk to develop chronic stress-related symptoms?. In: Wickramasekera, I.E., editor. Clinical behavioral medicine: Some concepts and procedures, New York: Plenum. P.5-14.

Wiseman, R., & Greening, E. (2002). The Mind Machine: A mass participation experiment into the possible existence of extrasensory perception. British Journal of Psychology.

Zachariae, R., Paulsen, K., Mehlson, M., Jensen, A.B., Johansson, A., & Von der Masse, H. (2007) Anticipatory nausea : The role of individual differences related to sensory perception and automatic reactivity. Annals of Behavioral Medicine, 33(1): 69-79. [PubMed: 17291172].